NUREG/CR-0461

INSPECTION OF NUCLEAR REACTOR WELDING BY ACOUSTIC EMISSION

Final Report

November 1974 through November 1977

D.W. Prine
T.A. Mathieson

GARD, Inc.

Prepared for

U.S. Nuclear Regulatory Commission

R

Available from
National Technical Information Service
Springfield, Virginia 22161
Price: Printed Copy $6.50 ; Microfiche $3.00

The price of this document for requesters outside of the North American Continent can be obtained from the National Technical Information Service.

NUREG/CR-0461

INSPECTION OF NUCLEAR REACTOR WELDING BY ACOUSTIC EMISSION

Final Report
November 1974 through November 1977

D.W. Prine
T.A. Mathieson

Manuscript Completed: November 1977
Date Published: November 1978

GARD, Inc.
7449 Natchez Avenue
Niles, IL 60648

Prepared for the
Division of Reactor Safety Research
U.S. Nuclear Regulatory Commission
Under Contract No. AT (49-24)-0187

ABSTRACT

This report presents results for the first three years of a program aimed at proving feasibility and applying the in-process acoustic emission (AE) monitoring of welds to the NDE of Nuclear power component welds. The method has been tested under both controlled laboratory conditions and in nuclear fabrication shops. Prototype single and two channel monitors have been built and production tested. Over 13,000 feet of weld passes have been monitored with excellent correlation of AE to conventional NDE and metallography. AE has been proven to be a reliable and practical NDE tool for detection and location of weld flaws. Current efforts are aimed at improving the method to provide flaw characterization as to type and size.

This report presents in detail the analysis of a large bank of laboratory controlled weld data. This work is providing; flaw detection probabilities for various flaw types, AE flaw detection mechanisms, and candidate AE signal parameters for flaw size and type discrimination.

CONTENTS

FOREWORD

The work described in this report was performed by the GATX Corporation, GARD, INC., 7449 North Natchez Avenue, Niles, IL 60648 for the Nuclear Regulatory Commission under Contract AT(49-24)-0187. The NRC Technical Representative was Dr. J. Muscara.

The work was performed at GARD in the Electronic Systems Department, (J. A. Ferro, Manager) under W. L. Lichodziejewski, Manager of NDT and Diagnostics by D. W. Prine, Project Engineer and Principal Investigator with the assistance of R. N. Clark, NDT Engineer, and T. A. Mathieson, NDT Engineer.

The authors gratefully acknowledge the assistance of E. P. Loch, Manager of Materials & Processes Engineering and S. W. Wismer, Sr. Metallurgical Engineer, Westinghouse Electric Corporation, Water Reactors Division, Tampa, Fla. in coordinating the pressure vessel production testing. This report is the final report for the first three years and presents data developed since March 1, 1977 through September 30, 1977 in detail as well as summaries of all results obtained from November, 1974 to March, 1977.

Section 1

OBJECTIVE

The overall objective of this work is to provide improved detection and characterization of flaws by nondestructive testing during the fabrication of nuclear piping and pressure vessel weldments using acoustic emission monitoring during the welding process.

To accomplish this end, the following specific goals were set within a three year program:

- Show feasibility of in-process acoustic emission monitoring on nuclear piping and pressure vessel welds.
- Fabricate piping and pressure vessel monitoring equipment and evaluate under nuclear fabrication shop conditions.
- Provide data to be used as a basis for development of a case for NRC and ASME code acceptance of in-process acoustic emission monitoring of welds in nuclear components.

This report covers all work done towards achieving the above listed goals. Topics covered in detail in previous reports are presented in summary form. Work completed during this report period is presented in detail.

Section II

INTRODUCTION

Acoustic Emission (AE) is the acoustic energy generated in a material under stress. Acoustic Emission results from mechanisms such as plastic deformation and flaw propagation. In welding, stress is generated by the shrinking of the weld as it solidifies and cools. If welding conditions are improper, flaws such as cracks may form during this process and acoustic emission will result. The detection and utilization of these acoustic signals is the basis for a powerful NDE tool.

GARD began a study of acoustic emission weld monitoring under GATX Corporate sponsorship in 1971 with the goal of improved NDE of welds in the manufacture of railroad tank cars. Real time in-process inspection of these welds was desirable for several reasons. A real time in-process inspection tool could be used to warn welders that welding conditions are improper thus allowing the welder to make appropriate adjustments and reduce the overall flaw output and resulting repair costs. Real time in-process inspection allows the flaws to be repaired on the production floor which minimizes material handling and eliminates re-radiography of repaired sections.

The in-process inspection and repair of welds is particularly desirable in the welding of thick sections where many weld passes are required. The flaws may be detected and the repair facilitated before the flaw is buried deep within the weld.

The primary problem encountered when applying acoustic emission to in-process weld inspection is that the AE signals are random and noise-like. There are many sources of similar noises present in any typical production welding situation, therefore, one must develop techniques to suppress the background noises from such things as the welding arc, slag cracking, and mechanical noises (grinding, chipping, and part manipulation) and allow the AE signals from weld flaws to be detected. GARD under GATX Corporate sponsorship developed signal processing techniques and incorporated them in systems applicable to railroad tank car fabrication which primarily consists of submerged arc welding (SAW) of mild carbon steel.

In November of 1974 GARD, under NRC sponsorship, commenced a three year program aimed at proving feasibility and applying the in-process AE monitoring of welds to the wider range of materials and welding processes encountered in fabrication of nuclear power plant components. The basic program plan has followed a three step procedure for both piping and pressure vessel type welds.

Under this plan:

- First, a series of calibration welds with intentional flaws are monitored and the AE signals stored on magnetic tape using the GARD laboratory AE system. The results of these tests are analyzed to provide information as to feasibility and optimal AE signal processing parameters for the weld methods and materials utilized.
- Second, the laboratory system is adjusted to the settings indicated by the above results and the system is tested in a series of actual production welds to test the validity of the above conclusions and to provide any additional inputs needed on special production oriented problems.
- Third, stand-alone AE monitors are fabricated and evaluted in actual production facilities. The results of these tests are compared with normal production NDE to show the effectiveness and practicality of using AE for in-process weld inspection.

A summary in chronological order of the welding that was AE monitored during this program is shown in Table I. A total of twelve tests were run covering the four most commonly used weld methods and the four commonest materials in nuclear fabrication. The total number of welds monitored is approximately 200 while the total footage of weld passes exceeds 13,400 feet.

The three step process produced, as planned, two AE monitors which were successfully evaluated in nuclear piping and pressure vessel facilities. These evaluations conclusively showed that in process AE can be successfully

TARLE I

SUMMERY OF AE WELD MONITORING FOR PHASES I, II, III

	Test	Location	Date	Number of Welds	Feet of Weld Pass	Material	Weld Method
1	Piping Lab.	Southwest Fab., Houston, Texas	02-75	20	250	A312T304/A106	1, 2, 3, 4
2	Piping Prod. # 1	Southwest Fab. Houston, Texas	05-75	18	400	A312T304/A106	1, 2, 3, 4
3	Piping Prod. # 2	ITT Grinnell Kernersville, N.C.	06-75	10	340	A106	1, 3, 4
4	Pressure Vessel Calibration # 1	B&W Barberton, Ohio	11-75	1	500	A508	3
5	Pressure Vessel Calibration # 2	CE Chattanooga, Tn.	02-76	1	260	A533	3
6	Additional Piping Lab. Tests	M&O Products San Luis Obispo, Ca.	12-76	30	290	A106	1, 2, 4
7	Pipe Shop Evaluation	G+W Plant # 1 Cicero, Il.	12-76/ 02-77	80	5800	A106	3
8	Pressure Vessel Production # 1	B&W Mt. Vernon, Ind.	01-77	1	680	A508	3
9	Pressure Vessel Production # 2	Westinghouse Tampa, Fla.	02-77	1	1800	A533	4
10	Pressure Vessel Production # 3	Westinghouse Tampa, Fla.	05-77	3	2000	A533	3
11	Additional Piping Lab. Tests	M&O Products San Luis Obispo, Ca.	06-77	19	250	A312T304/A106	1, 2
12	Additional Pressure Vessel Lab. Tests	GARD, INC. Niles, Il.	08-77	15	900	A533	3

Weld Methods: 1-GTAW, 2-GMAW, 3-SAW, 4-MMAW

utilized in a typical nuclear production shop to detect discontinuities in welds in a variety of materials and with various welding processes common to nuclear fabrication.

In addition to detecting flaws, an NDT method should provide information to allow some degree of characterization of the flaws as to type and size since these criteria are necessary to allow evaluation of the flaw to be made as to potential severity and hence allow a decision to be made on whether the particular flaw necessitates repair.

This type of information on AE can only be developed as a result of carefully controlled experimentation where known flaws are induced in welds and careful confirmation by both NDE and metallography is applied. Because of the random nature of both the flaws and the resulting AE a sufficiently large number of each flaw type in a range of sizes must be produced and analyzed to provide reasonable statistical accuracy.

In an effort to provide this vital information an extensive series of test welds were generated. The welds covered processes and materials typical of both nuclear piping and pressure vessel welds. The acoustic emission signals from these welds were recorded on an improved wide band magnetic tape system and were also stored in digital form on magnetic disc by means of GARD's on-line acoustic emission analysis computer program. The welds were radiographed and in addition ultrasonic testing, dye penetrant, and metallographic testing were used to confirm flaw data. The AE data was analyzed with the aid of a computer and correlated with conventional NDE and metallography to provide:

1. AE detection probabilities for the various flaw types which include, cracks, slag inclusions, porosity, incomplete penetration, lack of fusion, and tungsten inclusions.

2. AE flaw signal characteristics that will allow flaws to be identified as to type.

3. AE flaw signal characteristics related to flaw size.

In addition, these tests shed some light on some of the mechanisms by which AE detects some flaws.

In addition to greatly increasing our understanding of the basic physics of acoustic emission flaw detection in welds, analysis of this large bank of controlled flaw data and understanding the resulting implications is the first step in reaching the future goal of a "smart" AE monitor that not only can detect flaws during welding but in addition supply some degree of flaw characterization.

Section III

SUMMARY, CONCLUSIONS AND RECOMMENDATIONS

3.1 Summary

The feasibility of utilizing in-process acoustic emission monitoring to detect flaws in nuclear reactor piping and pressure vessel welds has been proven on over 13,400 feet of weld passes in the four most commonly used nuclear fabrication materials and utilizing the four most commonly used weld methods in both laboratory and shop environments.

Two production AE monitors were fabricated, one a simple single channel system for use primarily on low heat input welding typical of most nuclear pipe fabrication, and two, a sophisticated two channel system capable of time of arrival AE source location measurements that incorporates a customized dedicated microcomputer to control AE calibration, data storage, and display functions. The latter system was designed for use on higher heat input welds such as submerged arc welding of nuclear pressure vessels. Both monitors utilize GARD-developed AE signal processing circuitry to detect flaw signals and suppress the background noise inherent in typical welding processes.

Both monitors were successfully tested in actual nuclear fabrication facilities. Good correlation was achieved between in-process AE and production radiography, dye penetrant and visual inspection in these tests. Furthermore, the practicality of utilizing AE in actual shop environments was amply demonstrated.

A series of carefully documented laboratory test welds consisting of over 64 welds comprising approximately 420 passes containing artificially induced as well as natural flaws in six categories (cracks, slag inclusions, tungsten inclusions, incomplete penetration, lack of fusion, and porosity) in a range of sizes has been fabricated and AE monitored. The welds contained approximately 180 flaws of both planned and natural types. The AE data is stored in raw analog form on magnetic tape with a bandwidth of from .1 to 1 MHz and in preprocessed digital form on flexible diskettes. Data on these welds includes GARD computer-generated printouts for each weld giving:

- Total elapsed time
- Time between events
- Ringdown count for each event in the weld
- Relative peak value of intensity in each of eight frequency bands from .1 to 1 MHz for each event
- Condition of four signal processing bits in the monitor alarm circuits

In addition, the computer can and did generate a variety of plots and histograms of various AE signal parameters, and performed some statistical analysis on the data.

Such an analysis would not have been practical without the availability of the computer-aided analysis. Even with this powerful tool the analysis of the lab test welds has turned out to be a far greater task than originally anticipated. Two major factors contributing to this increased analysis complexity are the presence of more than one flaw type in a given location in the test welds and the presence of an appreciable number of natural flaws that were not originally planned. Flaw confirmation is also a difficult process, particularly for those flaws that are either not detectable by careful radiography or do not show up clearly on the radiographs. Metallography applied to these areas is at best a guessing game and metallographic sectioning and polishing of the pressure vessel welds (2" thick A533) is a very expensive and time-consuming process. Within these constraints, the data so far has yielded considerable information as to

- AE Flaw detection probabilities for the various flaw types
- AE signal correlation with flaw size
- AE signal characteristics which may allow flaw type to be determined
- Basic AE flaw detection mechanisms

These experiments and the resulting massive AE data bank are not only contributing greatly to the documentation necessary to gain acceptance of the in-process AE method but are also paving the way for the development of a "smart" AE monitor that will indicate flaw size and type for nuclear component welding.

3.2 Conclusions

The shop confirmation tests included a total of six tests. Four of these tests utilized the GARD laboratory system in two each nuclear pressure vessel and piping production facilities. The remaining two tests utilized the production monitors. The piping production tests which were run with the lab system covered a total of 740 feet of weld passes in both stainless and carbon nuclear grade steel piping. A total of 11 AE indications for these welds were observed and all 11 indications correlated with either code radiography, dye penetrant, or visual inspection. No AE events occurred which were not correlated nor were any flaws missed by AE in this series of tests. Flaws detected by AE included both cracks and slag inclusions.

An extended evaluation of the single channel production piping monitor on some 5800 feet of weld passes on submerged arc welding of longitudinal welds in nuclear grade carbon steel piping produced the following overall results. AE detected 61% of the X-ray indications with only a 3.9% over call (AE detected and X-ray didn't). AE was correct in indicating an X-ray detectable indication 70% of the time. On the basis of individual flaw types, AE detected 100% of the cracks, 58% of the porosity and 63% of the slag inclusions. Production radiography was the only means of flaw confirmation for these tests. Also, production flow arrangements made monitoring of the I.D. or root portions of the weld impractical. Within these limitations AE performed very well. Gulf & Western personnel, in whose facility the evaluation was run, are currently making arrangements to utilize the AE monitor to indicate end cracks in these welds and to facilitate immediate production floor repairs of this flaw.

Like the piping shop tests the pressure vessel shop test consisted of 3 tests, two with the laboratory system and one with the two channel production AE monitor. The first test with the laboratory system consisted of monitoring the OD weld on a reactor vessel inlet nozzle with a three channel version of the laboratory monitor. The weld in A508 pressure vessel steel, approximately 12 inches thick, produced only one AE indication. This indication correlated visually with a slag entrapment on a top cap pass of the weld which will be removed by final machining of the weld. Due to production delays, radiography has not been completed on this weld as of this date. This test was the first opportunity to demonstrate in-process AE monitoring in a nuclear pressure vessel shop. The demonstration was very positively received and definitely impressed the manufacturer with the potential of on-line AE inspection for nuclear pressure vessel welds.

The second PV test monitored with the GARD lab system was not strictly a production test involving an actual nuclear power plant component. It was a half bead temper repair weld on a test vessel that was part of the NRC/ORNL HSST program. The weld was accomplished with manual stick welding and took 21 days to complete with welding proceeding 24 hours a day. The weld was very quiet acoustically and produced only a few scattered AE indications. The more severe of these led to the grinding away of a substantial portion of one of the upper weld layers which visually confirmed the presence of scattered porosity.

Radiography and ultrasonic testing on the finished weld confirmed additional areas of porosity, however they were judged code-acceptable. One additional area of visual porosity was uncovered upon grinding away the backing bar and was ground out and repaired. AE had also produced indications in this region, however they were not as severe as the upper layer indications previously discussed. Again, AE and conventional NDE were in agreement on this weld.

The production pressure vessel monitor was successfully tested on a series of three longitudinal seams in nuclear steam generator shells. In approximately 1500 feet of weld passes the monitor detected and properly

located a total of six indications that were all visually confirmed. The indications were in the runoff pad on one weld and in the lower six passes on the second weld. The lower passes are ground out and rewelded in normal production and so are not available to final radiography.

As of this writing production radiography has been performed on the first seam only. It has confirmed the AE findings that the body of the weld was free from flaws.

A total of six laboratory tests have been run during this three year program. The first three (one on piping type welds and two on pressure vessel welds) were used for initial calibration and proof of feasibility purposes. A limited number of flaws was generated in three categories; cracks, slag inclusions, and porosity. All of the planned flaws of the first two types were detected along with several natural slag inclusions. Agreement of NDE and metallography with AE was 100% on cracks and slag inclusions; porosity was not detected by AE.

The latter three laboratory tests consisted of a very large bank of flaws (approximately 180) in both piping and pressure vessel welds. Six flaw types were generated in a wide range of sizes. Analysis of this data has so far shown that the probabilities of AE detection for cracks and slag inclusions are 100%. Incomplete penetration was detected 100% in submerged arc welds and about 75% in gas shielded welds. Metallographic sectioning has shown that in the sub arc welds incomplete penetration had slag entrapment associated with it, which probably accounts for the improved detection probability for this type of welding. Porosity in submerged arc welds has shown an 80% detection probability. However, the 80% that was detected had associated slag entrapment while the remaining undetected porosity didn't. This mechanism of detection is further borne out in the gas shielded welds where slag is eliminated. Here, the detection probability for porosity is under 5%. Lack of fusion was not detected by acoustic emission. The detectability of tungsten inclusions by AE was very low. Some very low level AE is associated with the production of tungsten inclusions, however current AE alarm logic will not reliably detect this flaw.

The AE signals from cracks and incomplete penetrations show a general correlation with size when one looks at either number of AE alarms plotted vs crack size or average ring down count activity associated with the flaw plotted vs crack size. The variability becomes greatest for large flaw sizes (< 2").

Slag inclusion size is roughly related to the number of AE events during which the AE alarm is activated.

In the area of flaw identification, cracks and slag inclusions may be differentiated from each other on the basis of the delay between when the weld head passes over the flaw and when the AE activity occurs. In general, the activity in the first pass with a slag inclusion occurs immediately while crack activity is delayed from 10 to 30 seconds after passage over the flaw. Also the duration of the AE activity for cracks is shorter by roughly a factor of one half of the activity for a slag inclusion. Both cracks and slag show marked increase in high frequency activity, however as of yet, no clear distinction on the basis of frequency spectrum has been discovered. There is some indication that a marked increase in high frequency occurs just prior to the high energy activity that accompanies a crack. This activity is associated with low ringdown count AE events and may correspond to the AE detection of some type of precursor activity for cracks. The effect is consistent in that it is associated with every case of confirmed crack. This high frequency low energy activity also occurs in other areas of the weld where no flaws have been confirmed. The possibility exists that this activity could be associated with some sort of microscopic process that under certain conditions leads to crack formation.

Incomplete penetration appears to act very much like slag (a fact that may be accounted for in the sub arc welds by the presence of trapped slag in the incomplete penetration flaws). There is some increase in low frequency AE activity also associated with incomplete penetration.

3.3 Recommendations

The feasibility of utilizing in-process AE to detect flaws in nuclear component welds has been amply proven in this three year program. Furthermore, the shop tests have shown that the method is practical to apply under typical nuclear fabrication environmental conditions and that it may be implemented without undue interference to normal production processes. Extensive laboratory testing has explained some of the detection mechanisms for various flaw types and has shown that two of the most serious flaw types have very high AE detection probabilities (cracks and incomplete penetration). In addition, the third high AE detection probability flaw (slag inclusion) is a commonly occurring flaw in submerged arc welding. Some indication of size and type discrimination are evident also.

Analysis of this large data bank in considerably greater detail than was possible within the current scope is very desirable. This detailed analysis may provide excellent additional basis for development of a code acceptance case. In addition, current status definitely indicates the possibility of a "smart" AE monitor which not only would detect but provide flaw size and type information. The development of this class of AE monitor will greatly extend current NDE capabilities and be a large step toward greater nuclear component safety along with considerable economic savings in the area of repair costs. Therefore, we recommend that future efforts be concentrated in the two following areas:

1. More detailed analysis of the existing AE data bank to provide better understanding of the flaw size and type discrimination characteristics and to provide additional evidence of the effectiveness of in-process AE weld monitoring.

2. Development of an AE monitor that not only detects flaws during welding but provides information on size and type of flaw.

Section IV

LABORATORY STUDY OF IN-PROCESS WELD MONITORING

4.1 Introduction

The "laboratory" tests were conducted to provide as clear a data base as possible for a series of analyses which would answer three questions about the inspection of welds using acoustic emission. First, what is the probability that acoustic emission monitoring will detect a flaw of given type with a minimum number of false alarms? Second, if a flaw type can be detected with any degree of reliability, can the size or severity of the flaw be related to any parameter of the acoustic emission? Third, are there any parameters of the acoustic emission from welds that can be used to differentiate among detectable flaw types?

To answer these questions, a series of welds was fabricated under carefully controlled conditions designed to create a broad sampling of weld defects. The acoustic emissions from these welds were monitored and recorded. The recorded emissions were then processed using a GARD-designed microprocessor-based analysis system (Figure 4-1). This system is composed of a preprocessor, a microcomputer, and a floppy disc mass storage device. The preprocessor (Figure 4-2) is a GARD-modified Dunegan-Endevco totalizer system which monitors amplified acoustic emission, converts it to ringdown counts, performs hard-wired logic on the magnitude and timing of the acoustic emission, samples the voltages being held in peak detectors tied to the outputs of eight frequency filter circuits, and presents the results to the microcomputer in a digital format. The microcomputer normally processes, stores, and displays the results of previous acoustic emission events and is stopped, or "interrupted", by the preprocessor when new incoming data from an acoustic emission event is ready to be transferred. The microcomputer then preserves its state, accepts the data, distributes it to the various storage and analysis areas, and then resumes its normal operation. This "interrupt" method of data acquisition is the most efficient means of recording digitally-processed acoustic emission events because it records the data only when there is data to be recorded.

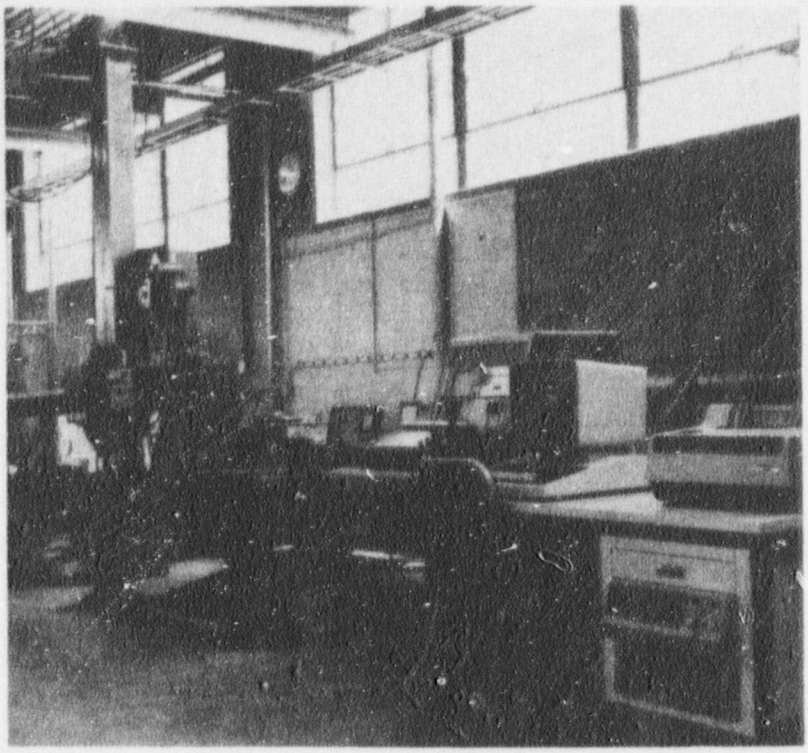

Figure 4-1. MICROPROCESSOR-BASED ANALYZER SYSTEM

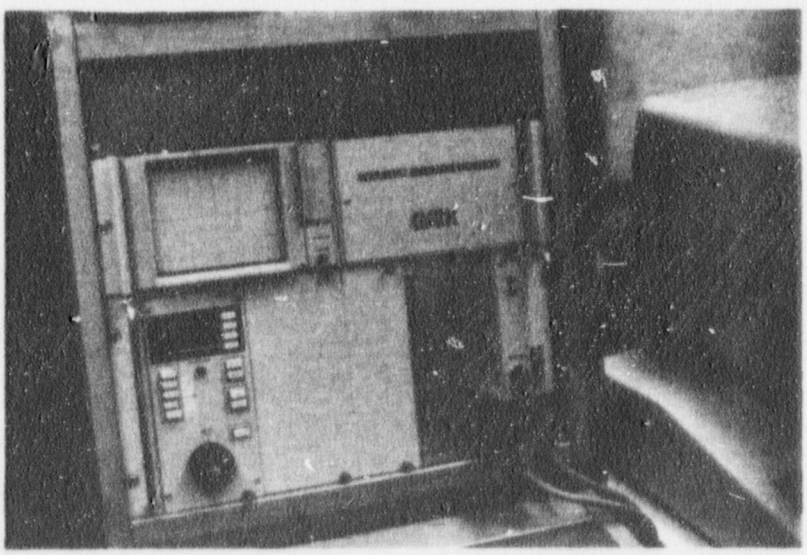

Figure 4-2. SYSTEM PREPROCESSOR

Information can thereby be efficiently and densely packaged during a weld in which the acoustic emission occurs only a small percentage of the time. This advantage is balanced by the disadvantage that if the "interrupt" is keyed to respond to the presence of one type of data (as ours is keyed to interrupt on the stabilization of a processed ringdown count at a selected gain), if that datum is not present whereas others are (such as frequency band activity in our system), important information may be missed. We have noted in the analysis a few instances in which this has happened, but no serious discrepencies or questions have arisen because of it. A simple change in the programming of the microcomputer will be required to allow a detailed look at these "blind" areas in the present analysis, but such a reanalysis is beyond the scope of the present project.

When the data is transferred from the preprocessor, it is organized into a format for storage to disc. This format is a collection of twelve computer words or "bytes" arranged in the following way. The first two bytes stored to or read from disc represent the number of computer-generated display sweeps which has elapsed since the previous acoustic emission event. Approximately 47 such sweeps occur per second. This provides the timing for all time-based records and analyses. The time-base resolution is 21 milliseconds. The next two bytes are a combined input composed of a 12-bit representation of the ringdown count and 4 bits representing the status of four flags used by the preprocessor logic. These flags and their significance are summarized in Table 4-1. Each of the final eight bytes in the disc format is an 8-bit representation of the voltage sensed in one of the eight frequency bands analysed. The ordering of these bytes in the format is 920 KHz, 675 KHz, 500 KHz, 370 KHz, 270 KHz, 200 KHz, 150 KHz, and 110 KHz.

Once the data has been accepted and stored by the microcomputer, a number of analyses can be performed. Most of these analysis procedures provide graphed summaries of acoustic energy distributions, accumulated activity in the monitored frequency bands, or time-based plots of these parameters. An elementary statistics and tabulation package has been

FLAG	SIGNIFICANCE
Counts	Set when ringdown count is greater than 100. Otherwise clear.
Overflow	Set when ringdown count is greater than 1000. Otherwise clear.
Frequency	Set when flaw frequency criterion is satisfied. Otherwise clear.*
Alarm	Set as a result of logical processing of above three flags and timing factors associated with emission. Otherwise clear.

* In these analyses, this circuit was disabled permanently setting the flag high.

Table 4-1. PREPROCESSOR FLAG DESCRIPTION

added recently to aid in trend analysis as part of a search for characteristic patterns of flaw type. The present capabilities of the acoustic emission analysis system are summarized in Table 4-2.

Preliminary analyses of the laboratory weld data base indicated that time-based records of alarm flag activity would be sufficient to determine the flaw detectability statistics and would aid in the investigations of flaw size indicators in the acoustic signal. Further analysis of flaw size indication would also be aided by tabulated summaries of event-by-event activity during the time the flaw was acoustically active. Finally, characteristic flaw type patterns could be sought via a trend analysis using lumped averages of acoustic emission parameters for welds in which the flaw was extensive, or by using time-distributed averages of acoustic emission parameters for welds in which the flawed area was very small in relation to the weld. Thus, of all the capabilities summarized in Table 4-2, only four have been used extensively to analyze the weld data. They are:

1. Time-based analysis of all events occurring when alarm flag is high.
2. Tabular summary of acoustic emission event parameters.
3. Lumped averages of acoustic emission event parameters.
4. Time distributed averages of acoustic emission event parameters.

The data base used in this analysis is composed of 70 welds or beads, representing a total of 427 weld passes monitored. The weld processes monitored for this analysis were gas-metal arc (GMA), gas-tungsten arc (GTA), and submerged arc (SA). The GTA and GMA welds were monitored as fabricated by our subcontractor in California. Acoustic emission from these welds was recorded by videotape only. The submerged arc welds were monitored during fabrication at the GARD weld facility in Niles, Illinois. Acoustic emission from these welds was processed and stored on disc by the analysis system during fabrication in addition to being recorded on videotape.

Energy-related

Accumulative ringdown count distribution for all events
Accumulative ringdown count distribution when preprocessor alarm is set
Accumulative ringdown count distribution when preprocessor counts is set
Accumulative ringdown count distribution when preprocessor overflow is set
Accumulative ringdown count distribution when preprocessor frequency is set

Frequency-related

Accumulative activity for eight frequency bands:

110 kHz	150 kHz
200 kHz	270 kHz
370 kHz	500 kHz
675 kHz	920 kHz

Time-related

Events satifying selected ringdown count and preprocessor flag criteria
Activity for any one of above frequency bands

Statistical

Tabulation of time of occurrence, interval time, ringdown count, frequency band activity, and preprocessor flag status for acoustic emission events satisfying selected energy and time criteria

Averaging of ringdown counts and frequency band activity for acoustic emission events satisfying selected energy and time criteria

Normalization of frequency band activity to the activity in a selected band

Table 4-2. PRESENT CAPABILITIES OF THE ANALYZER SYSTEM

The GMA welding process was used exclusively to join 6" lengths of ½" ASTM A106 carbon steel of the type used in nuclear grade pipe and the SA process was used for the joining of 36" lengths of 2" ASTM A533 Grade B carbon steel of the type used in the reactor pressure vessels. GTA welding process was used for creating tungsten inclusions and porous flaws.

The induction of six flaw types was attempted for this data base. They were cracks, slag inclusions, tungsten inclusions, incomplete penetration, lack of fusion, and porosity (spherical or tailed). For each of the flaw types a gradation of at least three degrees of flaw intensity or magnitude was attempted, and in all cases at least two were achieved. Table 4-3 presents a summary of the data matrix of the 154 flaws used in these analyses. Our total data base contains more flawed welds than have been analyzed for this report. These unanalyzed welds were done on pipe and the radiography performed was not adequate to confirm or deny the presence of the intended flaw. This group of data represents 14 welds or beads and a total of 20 passes in which 29 flaws were attempted. Since preliminary computer-aided analysis does not show any significant differences in acoustic emission due to the geometry of the weldment, we felt justified in leaving this data for later treatment.

The confirmation of the presence of the intended flaw in the weld was accomplished adequately in most cases by radiographic examination. In particular, the presence and extent of slag inclusions, incomplete penetration, lack of fusion, tungsten inclusions, and porosity could be done entirely by radiography. Approximately three quarters of the intended cracks could be confirmed radiographically (especially the larger network types) and ultrasonic inspection or metallographic sectioning was required for confirming the presence of the others. As will be elaborated in the discussions below, in a number of cases an incomplete penetration or slag inclusion not readily apparent on the radiograph would be detected by the acoustic emission record and subsequently confirmed by metallographic sectioning.

FLAW TYPE	NUMBER OF WELDS	NUMBER OF FLAWS
CRACKS		
Piping welds	6	14
Vessel welds	6	20
POROSITY		
Piping welds	16	15
Vessel welds	2	13
INCOMPLETE PENETRATION		
Piping welds	8	8
Vessel welds	14	21
LACK OF FUSION		
Piping welds	6	22
TUNGSTEN INCLUSIONS		
Piping welds	6	4
SLAG INCLUSIONS		
Vessel welds	6	37
TOTAL	70	154

Table 4-3. SUMMARY OF "LABORATORY" WELDS

4.2 Detection Probability

The first type of information to be extracted from the analysis is that of the probability of detection of the various flaw types using the different weld processes. The criteria of detectability used was the ability of the preprocessor to detect the flaw-related activity and thereby set the alarm flag. This criteria involved little computer-aided processing, but by storing preprocessor flag status as part of its data acquisition, the computer could speed up the analysis by rapidly recalling and displaying in proper time context the alarm flag status. A summary of the following discussions is presented in Table 4-9.

Cracks

Crack flaws were generated in A106 steel joined by the GMA process by contamination with A304 stainless steel rod or copper wire. Six such welds were made, representing 24 passes in which 7 cracks were attempted (3 by stainless steel contamination, 4 by copper contamination). Radiography showed these welds to have a number of indications for porosity, but careful examination detected indications for the intended flaws plus a few unintended cracks. Table 4-4 summarizes the confirmations and Figures 4-3a through 4-3g are the computer generated time-base plots of alarm flag activity. All these plots except (c) represent a duration of 2 minutes. Plot 4-3c represents 4 minutes. In each case, alarms occur at or shortly after the time of intended flaw inducement. In addition, alarms appear to occur for the unintended cracks also (Figures 4-3c, e, and g). Note the delay between the creation of the flaw and its detection. In root passes it is less than 15 seconds, averaging about 10 seconds. In higher passes, it varies from 10 to 45 seconds, averaging about 30 seconds. This is due to the material being hotter in subsequent passes and taking longer to cool down to a point sufficient to stress the flaw. These results are derived from data retrieved at a gain 15 db higher than usual for acoustic monitoring during welding. This was due to the weld set-up for this

FLAW TYPE	SIZE	MATERIAL	PROCESS	CONFIRMATION	BOOK	PAGE	SPMN	GAIN
CRACK(2)	0.25"	A106	GMA	X-RAY	693	7	38	70
CRACK(5)	0.12"	A106	GMA	X-RAY	693	7	39	75
CRACK	0.25"	A106	GMA	X-RAY	693	8	40	70
CRACK(2)	0.12"	A106	GMA	X-RAY	693	8	41	70
CRACK	0.06"	A106	GMA	X-RAY	693	8	42	70
CRACK(3)	0.12"	A106	GMA	X-RAY	693	8	43	70
CRACK	0.50"	A533B	SA	X-RAY, UTS	693	10	W1R2	40
CRACK	0.50"	A533B	SA	UTS	693	11	W1R3	40
CRACK	0.50"	A533B	SA	UTS	693	11	W1R4	40
CRACK	0.50"	A533B	SA	UNCONFIRMED	693	11	W1R5	40
CRACK	0.50"	A533B	SA	UTS	693	12	W1T4	40
CRACK	0.50"	A533B	SA	UTS	693	12	W1T5	40
CRACK	0.50"	A533B	SA	X-RAY, UTS	693	12	W1T6	40
CRACK	2.00"	A533B	SA	X-RAY	693	11	W3R4	40
CRACK	2.00"	A533B	SA	X-RAY	693	11	W3R5	65
CRACK	2.00"	A533B	SA	X-RAY	693	12	W3T5	65
CRACK	1.00"	A533B	SA	UNCONFIRMED	693	21	W5T5	65
CRACK	0.75"	A533B	SA	X-RAY, SCT	693	23	W5R4	65
CRACK	1.00"	A533B	SA	X-RAY	693	23	W5R5	65
CRACK	1.75"	A533B	SA	X-RAY	693	23	W5R6	65
CRACK	0.50"	A533B	SA	X-RAY	693	22	W6T5	65
CRACK	0.75"	A533B	SA	X-RAY	693	22	W6T7	65
CRACK	1.75"	A533B	SA	X-RAY	693	24	W6R3	65
CRACK	1.50"	A533B	SA	X-RAY	693	25	W8R4	65
CRACK	2.50"	A533B	SA	X-RAY	693	25	W8R5	65
CRACK	2.50"	A533B	SA	X-RAY	693	25	W8T2	65
CRACK	2.00"	A533B	SA	X-RAY	693	26	W8T4	65
CRACK (N)	?	A533B	SA	SCT	693	13	W13RR	65
CRACK (N)	?	A533B	SA	UNCONFIRMED	693	13	W13T2	65
CRACK (N)	?	A533B	SA	UNCONFIRMED	693	13	W13T3	65
CRACK (N)	?	A533B	SA	UNCONFIRMED	693	13	W13T7	65

Table 4-4. INVENTORY OF WELDS FLAWED BY CRACKING

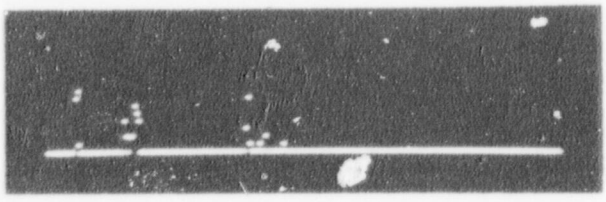

(a) Specimen 38 root pass

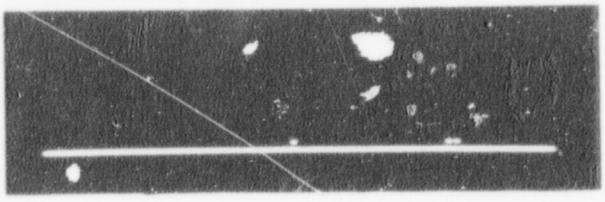

(b) Specimen 38 cover pass 3

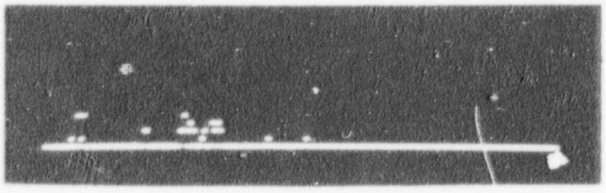

(c) Specimen 39 cover pass 2

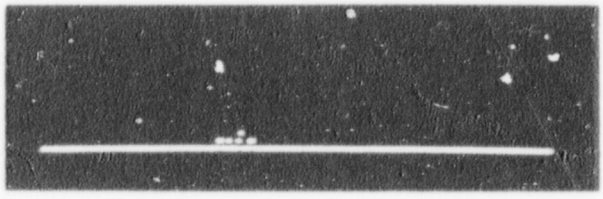

(d) Specimen 40 cover pass 1

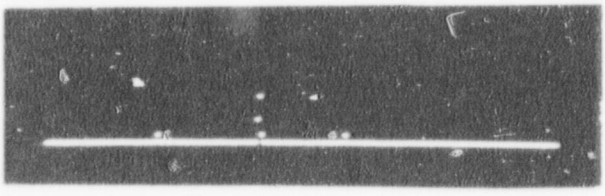

(e) Specimen 41 root pass

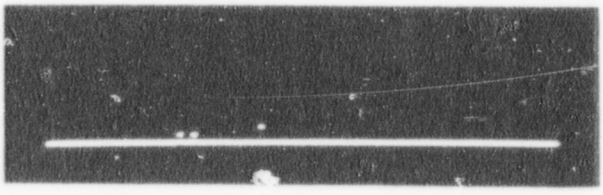

(f) Specimen 42 root pass

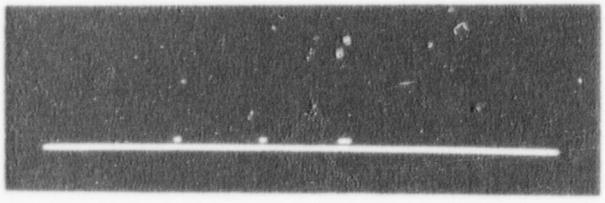

(g) Specimen 43 root pass

Figure 4-3. DETECTION OF CRACKS DURING WELDING OF A106 PIPING-TYPE STEEL USING GMA PROCESS

material, which gave a less efficient transducer coupling. The conclusion of this analysis is that 100% of the cracks occurring in A106 steel welds using the GMA process can be detected.

Crack flaws were generated in A533B steel plate joined by the submerged arc process by contamination with A304 stainless steel rod or copper tubing. Six such welds were made, representing 117 passes in which 21 cracks were attempted (7 by stainless steel contamination, 14 by copper contamination. Of these 21 flaws, 20 have been confirmed by radiography, ultrasonic inspection, or metallographic sectioning. Table 4-4 summarizes the confirmations and Figures 4-4 through 4-8 are the computer generated time-base plots of alarm flag activity for these welds. All these plots represent a time base of 4 minutes. In each case, alarms occur 10 to 30 seconds after the time of intended flaw creation. The conclusions of this analysis is that 100% of the cracks occurring in A533B steel welds using the submerged arc process are detected by acoustic emission.

Slag Inclusions

Slag inclusions were generated in A533B steel joined using the submerged arc process. Six such welds were made representing 128 passes in which 28 flaws were attempted. Radiography confirmed these flaws in approximately the intended locations and sizes (Table 4-5). It also showed that some intended single large inclusions broke up into several smaller inclusions and that some inclusions thought to be burned out during the first flaw attempts did remain in the weld. The first two "slag flaw" welds (welds 2 and 4) were largely an attempt to settle on a reliable technique for generating slag inclusions. The computer-generated time-base record (Figures 4-9 and 4-10) reflects the alarm flag activity for those passes of these welds in which the attempt was successful. The slag inclusion generating technique settled on was that of leaving slag from the root pass stuck in the root at the intended flaw site in the intended flaw lengths. Once the technique was developed, the records (Figures 4-11 through 4-14) for the last four "slag flaw" welds (Welds 9-12) gave a more accurate picture of slag inclusion

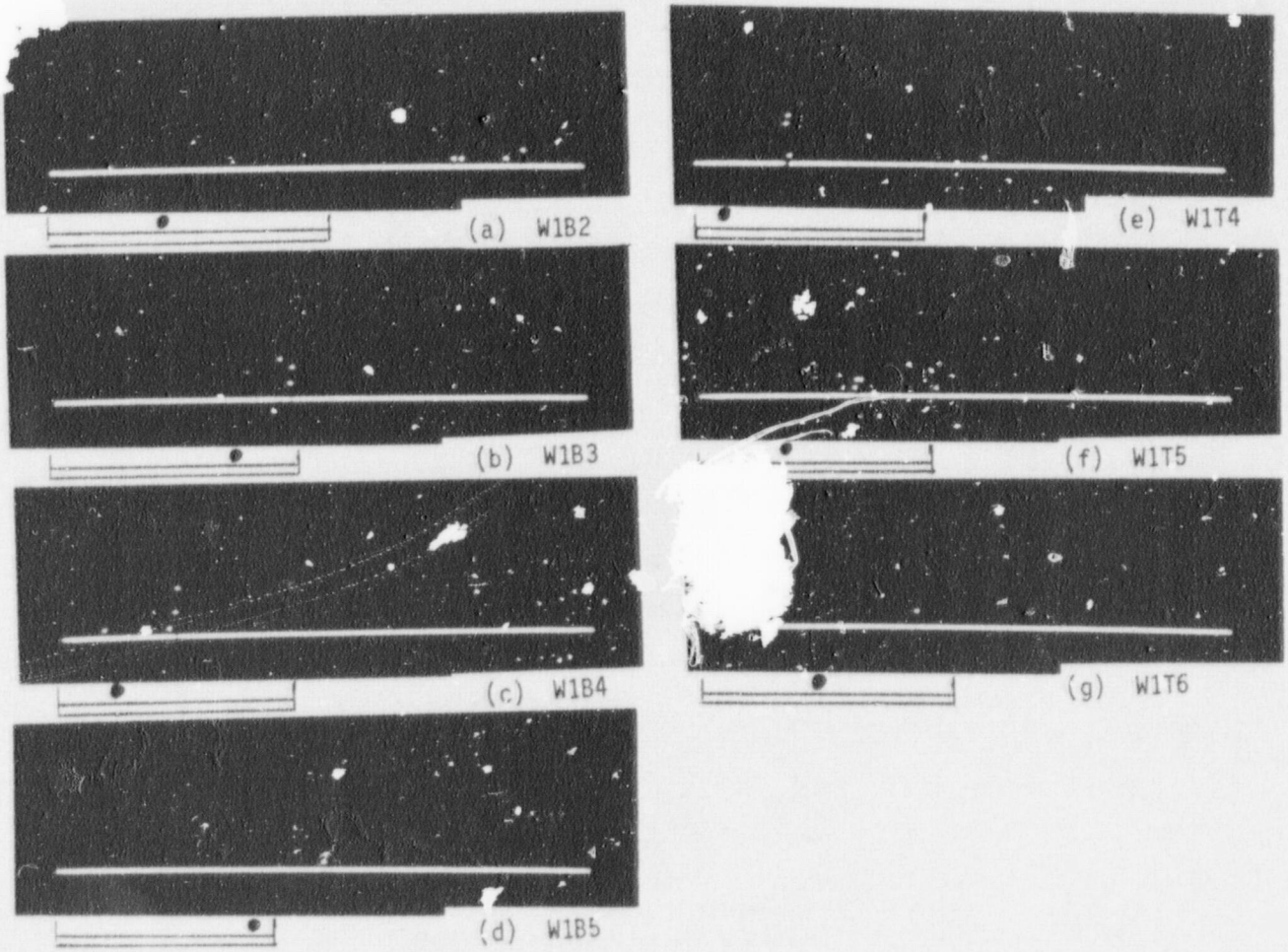

Figure 4-4. DETECTION OF 0.5" CRACKS DURING SUBMERGED ARC WELDING OF A533B PRESSURE VESSEL STEEL

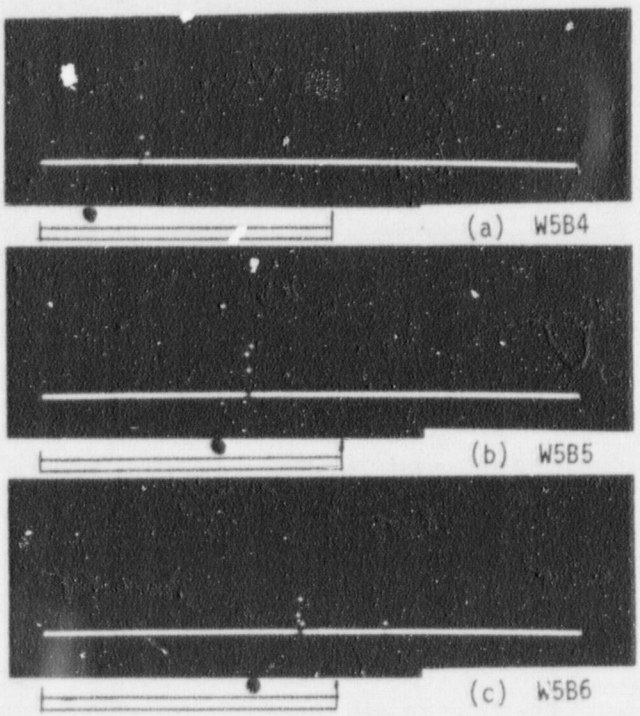

Figure 4-5. DETECTION OF 1.0" CRACKS DURING SUBMERGED ARC WELDING OF A533B STEEL

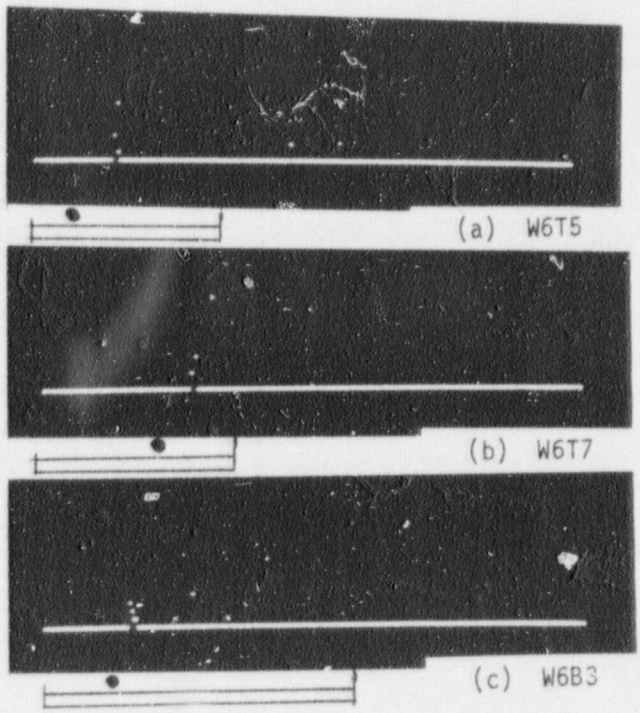

Figure 4-6. DETECTION OF 1.0" CRACKS DURING SUBMERGED ARC WELDING OF A533B STEEL

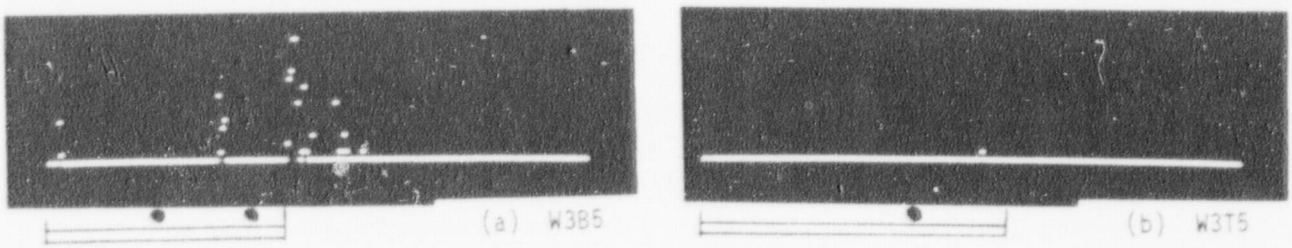

Figure 4-7. DETECTION OF 2.0" CRACKS DURING SUBMERGED ARC WELDING OF A533B PRESSURE VESSEL STEEL

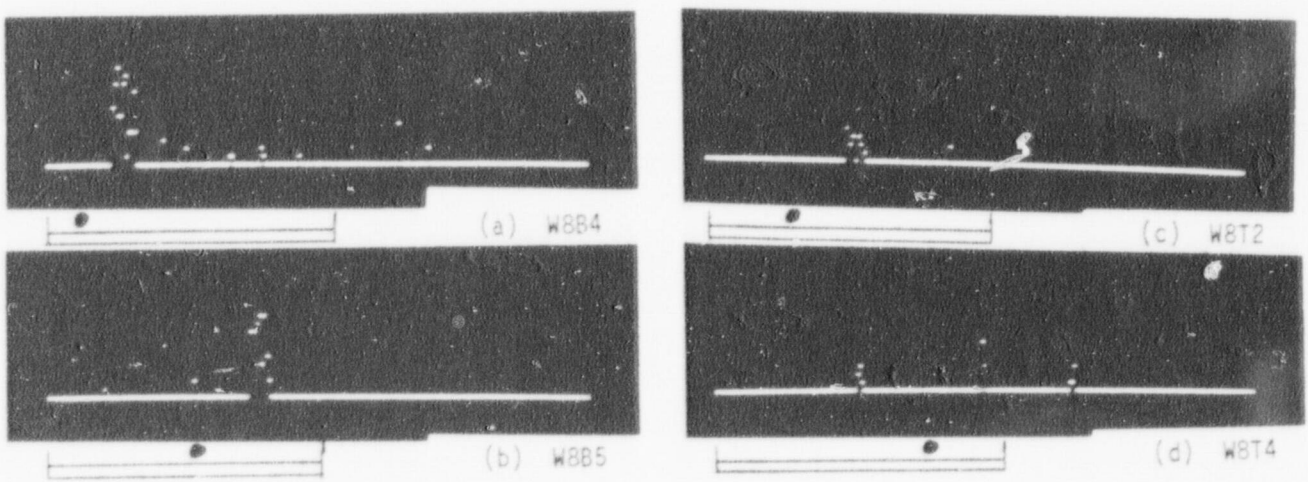

Figure 4-8. DETECTION OF 2.0" CRACKS DURING SUBMERGED ARC WELDING OF A533B PRESSURE VESSEL STEEL

FLAW TYPE	SIZE	MATERIAL	PROCESS	CONFIRMATION	BOOK	PAGE	SPMN	GAIN
SLAG	1.00"	A533B	SA	X-RAY	693	14	W2T4	65
SLAG	2.00"	A533B	SA	X-RAY	693	14	W2T5	65
SLAG	1.50"	A533B	SA	X-RAY	693	14	W2T6	65
SLAG	1.00"	A533B	SA	X-RAY	693	17	W2B6	65
SLAG	1.50"	A533B	SA	X-RAY	693	17	W2B6	65
SLAG	1.00"	A533B	SA	X-RAY	693	17	W2B6	65
SLAG (N)	2.00"	A533B	SA	X-RAY	693	17	W2B6	65
SLAG (N)	0.50"	A533B	SA	X-RAY	693	17	W2B6	65
SLAG (N)	1.00"	A533B	SA	X-RAY	693	17	W2B7	65
SLAG	1.50"	A533B	SA	X-RAY	693	15	W4T7	65
SLAG	1.00"	A533B	SA	X-RAY	693	15	W4T7	65
SLAG	8.00"	A533B	SA	X-RAY	693	15	W4T10	65
SLAG	2.00"	A533B	SA	X-RAY	693	16	W4T14	65
SLAG	2.00"	A533B	SA	X-RAY	693	16	W4B1	65
SLAG	1.00"	A533B	SA	X-RAY	693	16	W4B4	65
SLAG	1.50"	A533B	SA	X-RAY	693	16	W4B4	65
SLAG (N)	9.00"	A533B	SA	X-RAY	693	17	W4B9	63
SLAG (N)	2.00"	A533B	SA	X-RAY	693	17	W4B9	65
SLAG	[illegible].00"	A533B	SA	X-RAY	693	28	W9B1	65
SLAG	2.00"	A533B	SA	X-RAY	693	28	W9B1	65
SLAG	2.00"	A533B	SA	X-RAY	693	28	W9T1	65
SLAG	2.50"	A533B	SA	X-RAY	693	28	W9T1	65
SLAG	1.00"	A533B	SA	X-RAY	693	19	W10T1	65
SLAG	1.00"	A533B	SA	X-RAY	693	19	W10T1	65
SLAG	0.50"	A533B	SA	X-RAY	693	19	W10T1	65
SLAG	2.00"	A533B	SA	X-RAY	693	19	W10T1	65
SLAG	1.50"	A533B	SA	X-RAY	693	19	W10T1	65
SLAG	0.50"	A533B	SA	X-RAY	693	19	W10T1	65
SLAG	0.50"	A533B	SA	X-RAY	693	18	W11B1	65
SLAG	0.25"	A533B	SA	X-RAY	693	18	W11B1	65
SLAG	0.50"	A533B	SA	X-RAY	693	18	W11B1	65
SLAG	1.50"	A533B	SA	X-RAY	693	18	W11B1	65
SLAG	2.00"	A533B	SA	X-RAY	693	18	W11B1	65
SLAG (N)	2.00"	A533B	SA	X-RAY	693	18	W11B1	65
SLAG	3.00"	A533B	SA	X-RAY	693	20	W12T1	65
SLAG	3.00"	A533B	SA	X-RAY	693	20	W12T1	65
SLAG	3.00"	A533B	SA	X-RAY	693	20	W12T1	65

Table 4-5. INVENTORY OF WELDS FLAWED BY SLAG INCLUSIONS

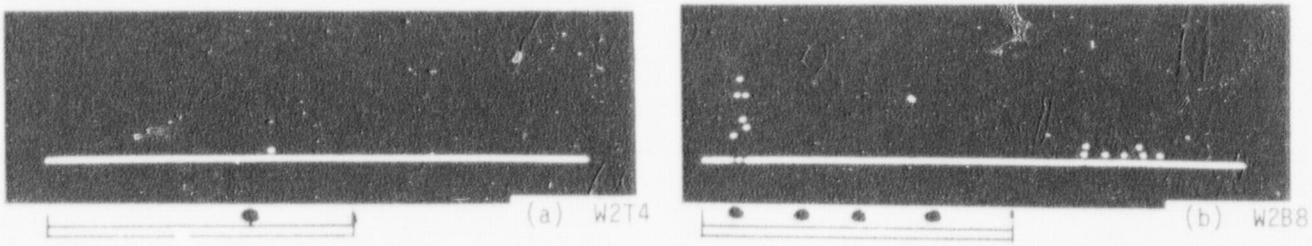

Figure 4-9. DETECTION OF 0.5" SLAG INCLUSIONS DURING SUBMERGED ARC WELDING OF A533B PRESSURE VESSEL STEEL

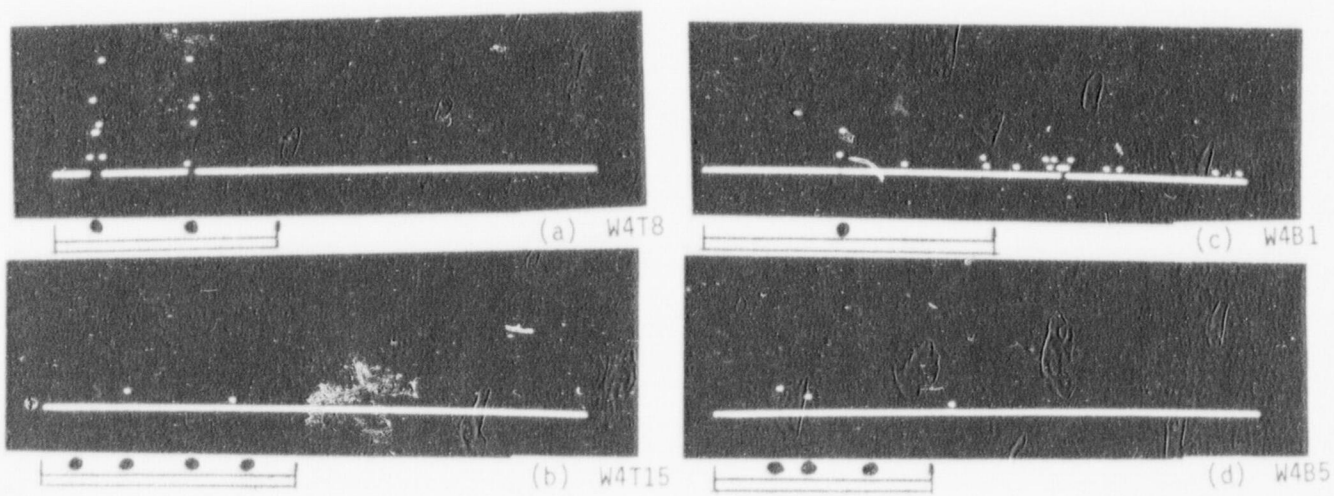

Figure 4-10. DETECTION OF 1.0" SLAG INCLUSIONS DURING SUBMERGED ARC WELDING OF A533B PRESSURE VESSEL STEEL

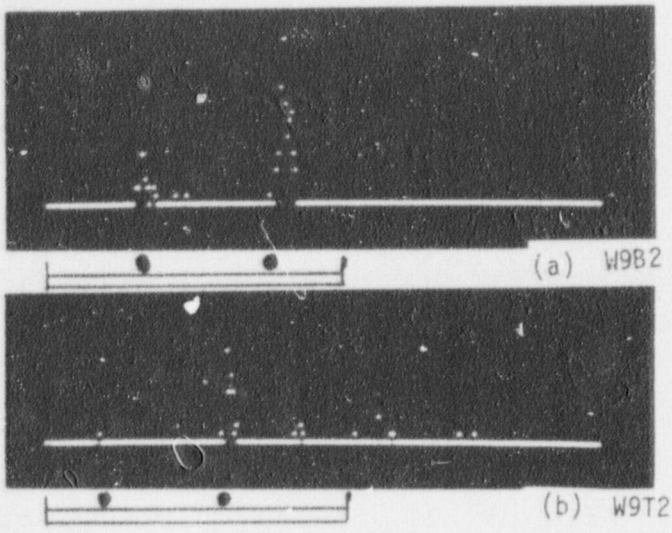

Figure 4-11. DETECTION OF 1.0" SLAG INCLUSIONS DURING SUBMERGED ARC WELDING OF A533B STEEL

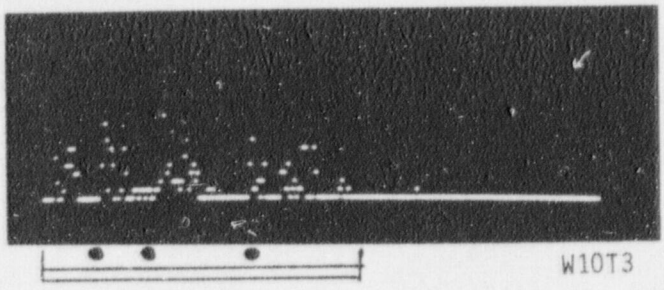

Figure 4-12. DETECTION OF 1.5" SLAG INCLUSIONS DURING SUBMERGED ARC WELDING OF A533B STEEL

Figure 4-13. DETECTION OF 2.0" SLAG INCLUSIONS DURING SUBMERGED ARC WELDING OF A533B STEEL

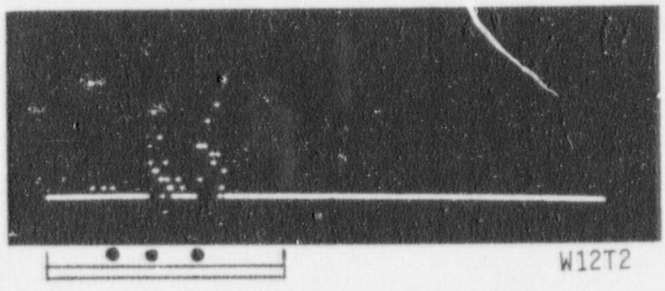

Figure 4-14. DETECTION OF 2.0" SLAG INCLUSIONS DURING SUBMERGED ARC WELDING OF A533B STEEL

detection probability. A point to note in these records is that whereas the acoustic emission from a crack generally occurs between 10 to 30 seconds after the crack has been induced, the acoustic emission from a slag inclusion seems to occur, and to be confined to, the time that the inclusion is being made. The conclusion of the analysis is that slag inclusions in submerged arc welding of A533B steel is 100% detectable by acoustic emission.

In addition to the intended slag inclusions, a number of "natural" or unintended s g inclusions were created in these welds and detected by AE. These cases will be more fully discussed later, but they generally occurred as slag was trapped in pores in welds intended to be flawed with porosity or as slag was trapped in incomplete penetration in most of the SA welds. In fact, it is questionable whether a real distinction can be made between slag inclusions and incomplete penetration or large pore porosity in submerged arc welds.

Incomplete Penetration

Incomplete penetration was generated in A106 steel joined by the GMA process. Eight such welds were made, representing 33 passes and 8 flaws of varying severity. Flaw severity was regulated by adjusting the weld gap (Figure 4-15) from nothing for the greatest flaw to nearly the recommended interval for the minimal flaw. Radiography and dye penetrant confirmed the presence and severity of the flaws (Table 4-6) and Figure 4-16 shows the computer-generated time records of alarm flag activity for the welds in which the flaw was detected. Six of the eight flaws gave an indication of some type during the weld, and these were generally the worst cases of incomplete penetration. The conclusions of this analysis are that 100% of moderate to severe incomplete penetration is detectable by acoustic emission, but that slight forms are not readily detectable at the gains used. The overall detectability of incomplete penetration in GMA welding was found to be 75%.

Incomplete penetration was also attempted in a weld of A533B steel using submerged arc process. The flaws were generated by jogging the weld

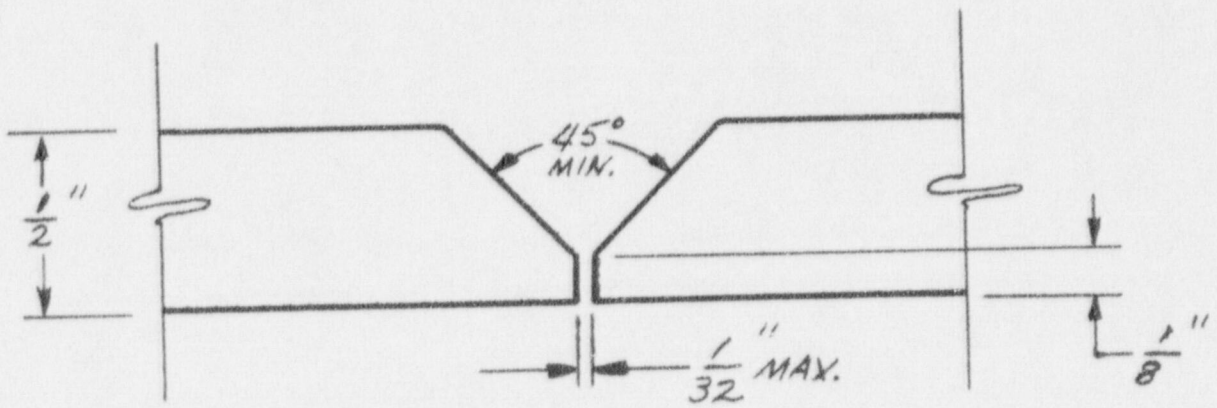

Figure 4-15. PROPER GAP INTERVAL TO MINIMIZE INCOMPLETE PENETRATION IN GMA WELDS

FLAW TYPE	SIZE	MATERIAL	PROCESS	CONFIRMATION	BOOK	PAGE	SPMN	GAIN
IP	?	A106	GMA	UNCONFIRMED	684	1	1	78ND
IP	MIN.	A106	GMA	X-RAY	684	1	2	65ND
IP	MIN.	A106	GMA	X-RAY	684	1	3	65ND
IP	MOD.	A106	GMA	X-RAY	684	1	4	65ND
IP	MOD.	A106	GMA	X-RAY	684	2	5	65ND
IP	MOD.	A106	GMA	X-RAY	684	4	14	65
IP	INT.	A106	GMA	X-RAY	684	4	15	60
IP	INT.	A106	GMA	X-RAY	684	5	16	60
IP	MOD.	A106	GMA	X-RAY	684	5	17	60
IP (N)	3.0"	A533B	SA	X-RAY	693	17	W2BR	65
IP (N)	3.0"	A533B	SA	X-RAY	693	17	W2BR	65
IP (N)	3.0"	A533B	SA	X-RAY	693	17	W2BR	65
IP (N)	1.0"	A533B	SA	X-RAY	693	11	W3BR	65
IP (N)	2.0"	A533B	SA	X-RAY	693	11	W3BR	65
IP (N)	2.0"	A533B	SA	X-RAY	693	11	W3BR	65
IP (N)	14.0"	A533B	SA	X-RAY	693	16	W4BR	65
IP (N)	21.0"	A533B	SA	X-RAY	693	23	W5BR	65
IP (N)	6.0"	A533B	SA	X-RAY	693	23	W5BR	65
IP (N)	36.0"	A533B	SA	X-RAY	693	24	W6BR	65
IP (N)	24.0"	A533B	SA	X-RAY	693	30	W7BR	65
IP (N)	5.0"	A533B	SA	X-RAY	693	25	W8TR	65
IP (N)	6.0"	A533B	SA	X-RAY	693	25	W8TR	65
IP (N)	36.0"	A533B	SA	X-RAY	693	28	W9TR	65
IP (N)	36.0"	A533B	SA	X-RAY	693	20	W12BR	65
IP (N)	13.0"	A533B	SA	UTS	693	13	W13BR	65
IP (N)	13.0"	A533B	SA	UTS	693	13	W13BR	65
IP (N)	6.0"	A533B	SA	X-RAY	693	32	W14TR	65
IP	25.0"	A533B	SA	X-RAY	693	27	W15BR	65
IP	2.0"	A533B	SA	X-RAY	693	27	W15BR	65
IP	5.0"	A533B	SA	X-RAY	693	27	W15BR	65

Table 4-6. INVENTORY OF WELDS FLAWED BY INCOMPLETE PENETRATION

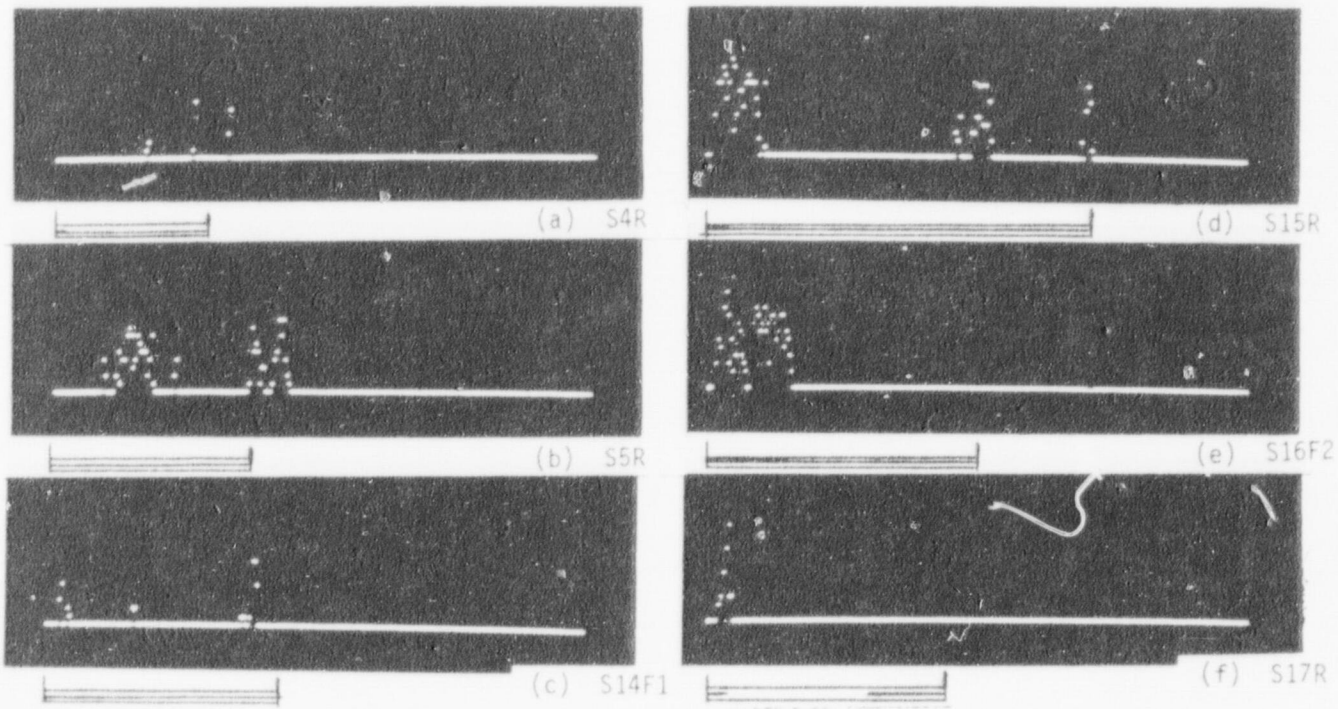

Figure 4-16. DETECTION OF INCOMPLETE PENETRATION DURING GMA WELDING OF A106 PIPING-TYPE STEEL

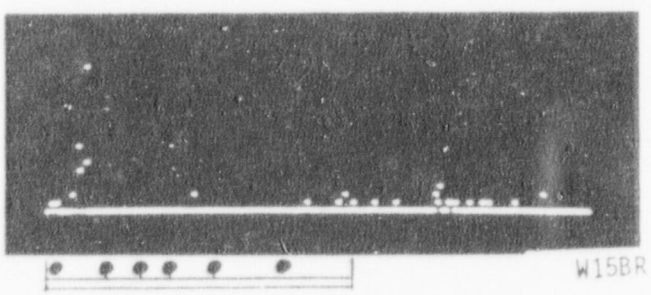

Figure 4-17. DETECTION OF INCOMPLETE PENETRATION DURING SUBMERGED ARC WELDING OF A533B PRESSURE VESSEL STEEL

head at six places in the back root pass and two different sizes of flaws were attempted. Radiography showed three indications, each a different length (Table 4-6). Figure 4-17 shows the computer-generated time record of alarm activity for this pass and indicates a detectability of 100% for incomplete penetration in A533B submerged arc welds. In addition, unintended incomplete penetration occurred in other welds due to misalignment of the V-groove from sloppy cutting. In those roots in which incomplete penetration is indicated radiographically, acoustic emission detected its presence, whereas the root which shows no radiographic incomplete penetration (Weld 11) is relatively quiet until late slag noise begins to build up near the weld's end.

Lack of Fusion

Lack of fusion was generated in A106 steel joined by the GMA process by reducing weld current. Six such welds were made representing 40 passes in which 22 flaws were attempted. Radiography confirmed the presence and severity of the flaws (Table 4-7), but the detectability of this type of flaw by acoustic emission was found to be nil. Computer-generated plots of ringdown count distribution show a variation in acoustic energy proportional to the radiographically indicated flaw severity (Figure 4-18) suggesting that an increase in monitor gain would increase detectability of lack of fusion. However, this higher sensitivity would probably greatly increase false alarms for current signal processing conditions. The distribution for specimen 11 is not shown as poor transducer coupling made the results invalid.

Porosity

Porosity was generated in beads layed on A106 steel using the GTA process by removing shield gas. Sixteen such beads were made in which fifteen flaws were attempted (one bead was a pass over a previously flawed bead). Radiography confirmed the presence of 12 attempted flaws (Table 4-8). Out of 8 attempts to induce spherical porosity, 7 succeeded but each attempt also added tailed porosity. Out of 7 attempts to induce tailed porosity, 5

FLAW TYPE	SIZE	MATERIAL	PROCESS	CONFIRMATION	BOOK	PAGE	SPMN	GAIN
LOF (N)	6.00"	A106	GMA	X-RAY	684	2	6	65ND
LOF	6.00"	A106	GMA	X-RAY	684	3	8	65
LOF	6.00"	A106	GMA	X-RAY	684	3	9	65
LOF	6.00"	A106	GMA	X-RAY	684	3	10	60
LOF	6.00"	A106	GMA	X-RAY	684	3	10	60
LOF	6.00"	A106	GMA	X-RAY	684	3	10	60
LOF	6.00"	A106	GMA	X-RAY	684	3	10	60
LOF	6.00"	A106	GMA	X-RAY	684	3	10	60
LOF	6.00"	A106	GMA	X-RAY	684	3	10	60
LOF	6.00"	A106	GMA	X-RAY	684	3	10	60
LOF	6.00"	A106	GMA	X-RAY	684	3	10	60
LOF	6.00"	A106	GMA	X-RAY	684	3	10	60
LOF	6.00"	A106	GMA	X-RAY	684	3	11	60
LOF	6.00"	A106	GMA	X-RAY	684	3	11	60
LOF	6.00"	A106	GMA	X-RAY	684	3	11	60
LOF	6.00"	A106	GMA	X-RAY	684	3	11	60
LOF	6.00"	A106	GMA	X-RAY	684	3	11	60
LOF	6.00"	A106	GMA	X-RAY	684	3	11	60
LOF	6.00"	A106	GMA	X-RAY	684	3	11	60
LOF	6.00"	A106	GMA	X-RAY	684	3	11	65
LOF	6.00"	A106	GMA	X-RAY	684	3	11	65
LOF	6.00"	A106	GMA	X-RAY	684	4	12	65
LOF	6.00"	A106	GMA	X-RAY	684	4	13	65

Table 4-7. INVENTORY OF WELDS FLAWED BY LACK OF FUSION

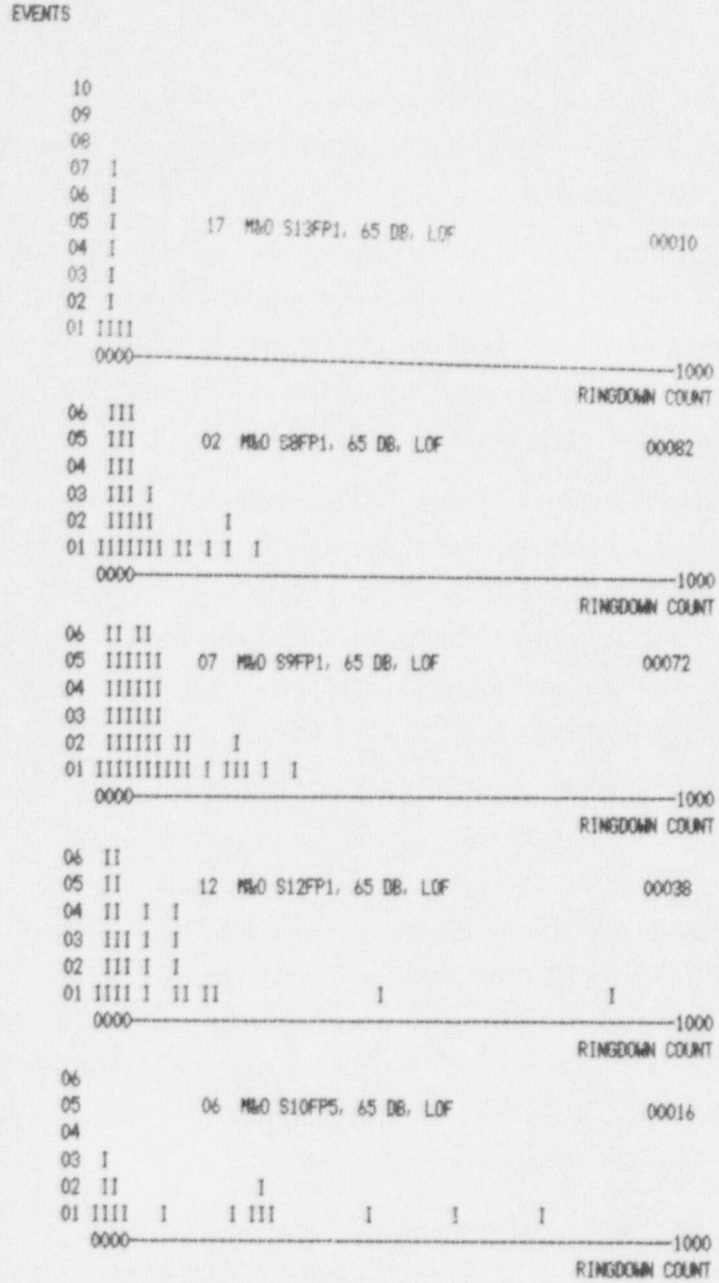

Figure 4-18. RINGDOWN COUNT DISTRIBUTIONS IN WELDS FLAWED BY LACK OF FUSION. ARRANGED FROM TOP IN ORDER OF RADIOGRAPHICALLY-DETECTABLE FLAW SEVERITY

FLAW TYPE	SIZE	MATERIAL	PROCESS	CONFIRMATION	BOOK	PAGE	SPMN	GAIN
T POR	H. D.	A106	GTA	X-RAY	684	5	18	75
T POR	H. D.	A106	GTA	X-RAY	684	5	18	75
T POR	H. D.	A106	GTA	X-RAY	684	5	18	75
T POR	H. D.	A106	GTA	X-RAY	684	5	19	75
T POR	H. D.	A106	GTA	X-RAY	684	6	19	75
T POR	----	A106	GTA	UNCONFIRMED	684	6	19	75
T POR	----	A106	GTA	UNCONFIRMED	684	6	19	75
T POR	L. D.	A106	GTA	X-RAY	684	6	20	75
T POR	L. D.	A106	GTA	X-RAY	684	6	20	75
T POR	L. D.	A106	GTA	X-RAY	684	6	21	75
T POR	L. D.	A106	GTA	X-RAY	684	6	22	75
T POR	L. D.	A106	GTA	X-RAY	684	6	22	75
T POR	H. D.	A106	GTA	X-RAY	684	7	23	75
T POR	H. D.	A106	GTA	X-RAY	684	7	23	75
S POR	L. D.	A106	GTA	X-RAY	684	6	20	75
S POR	H. D.	A106	GTA	X-RAY	684	6	20	75
S POR	----	A106	GTA	UNCONFIRMED	684	6	21	75
S POR	L. D.	A106	GTA	X-RAY	684	6	21	75
S POR	L. D.	A106	GTA	X-RAY	684	6	22	75
S POR	H. D.	A106	GTA	X-RAY	684	6	22	75
S POR	H. D.	A106	GTA	X-RAY	684	7	23	75
S POR	H. D.	A106	GTA	X-RAY	684	7	23	75
PORO	L. D.	A533B	SA	X-RAY	693	30	W7T4	65
PORO	L. D.	A533B	SA	X-RAY	693	30	W7T5	65
PORO	L. D.	A533B	SA	X-RAY	693	30	W7T5	65
PORO	L. D.	A533B	SA	UNCONFIRMED	693	30	W7T6	65
PORO	L. D.	A533B	SA	UNCONFIRMED	693	30	W7B3	65
PORO	L. D.	A533B	SA	X-RAY	693	30	W7B4	65
PORO	L. D.	A533B	SA	X-RAY	693	30	W7B5	65
PORO	L. D.	A533B	SA	X-RAY	693	30	W7B6	65
PORO	H. D.	A533B	SA	X-RAY	693	31	W14B5	65
PORO	H. D.	A533B	SA	X-RAY	693	31	W14B6	65
PORO	H. D.	A533B	SA	X-RAY	693	31	W14B7	65
PORO (N)	H. D.	A533B	SA	X-RAY	693	31	W14B10	65
PORO	H. D.	A533B	SA	X-RAY	693	32	W14T3	65
PORO	H. D.	A533B	SA	X-RAY	693	32	W14T3	65
PORO	H. D.	A533B	SA	X-RAY	693	32	W14T4	65
PORO	H. D.	A533B	SA	X-RAY	693	32	W14T4	65

Table 4-8. INVENTORY OF WELDS FLAWED BY POROSITY

FLAW TYPE	FLAW DETECTION PROBABILITY	
	Piping welds	Vessel welds
CRACKS	100%	100%
POROSITY	5%	80% *
INCOMPLETE PENETRATION	75%	100% *
LACK OF FUSION	0%	--
TUNGSTEN INCLUSIONS	0%	--
SLAG INCLUSIONS	--	100%

* enhanced by slag trapping

Table 4-9. FLAW DETECTABILITY FOR "LABORATORY" WELDS

succeeded. Detectability of porosity by acoustic emission in these welds was found to be nil. However, a preliminary look at the activity associated with porosity generation on pipe did show possible detection of two porosities. Radiographic confirmation of these welds was unsatisfactory, and they will have to be reshot before making any statement whether porosity was truly detected. A tentative detectability of porosity may be set at less than 5% for GTA welds.

Porosity was also generated in A533B steel joined by the submerged arc process. Two such welds were made, representing 34 passes in which 15 flaws were attempted. Generation of porosity was accomplished by reducing the amount of flux covering the molten pool. Variations in the flux covering were used to vary flaw density. Visual inspection at the time of welding confirmed all 15 flaws, but radiography confirmed only 13 of the attempted flaws (Table 4-8). Acoustic emission detected 12 flaws (Figures 4-20 and 4-21) giving a detectability of 80% for porosity in SA welding. This rate is at great variance to the rate found for GTA welds, and as will be discussed later, is largely due to slag entrapment during pore generation.

4.3 Size Indications

The next type of information to be extracted from the analysis is that resulting from a search for a parameter or group of parameters of the acoustic emission which can be related to flaw severity or magnitude. Since it has been shown above that cracks, incomplete penetration, and slag inclusions are the flaws with highest detection probability, the analysis will concentrate on these. Acoustic emission is a result of flaw propagation or growth. The materials studied in this program are markedly inhomogeneous on both maroscopic and microscopic scales. As a result of this inhomogeneity, flaw growth in these materials tends to proceed as a series of discrete discontinuous jumps as the flaw edge successively encounters nonuniform regions of stress.

Thus, it might be expected that the time density of acoustic emission associated with a flaw can be related to the amount of flaw growth. If the number of discrete flaw edge jumps is proportional to the flaw magnitude, this event density can be used as an indication of flaw size. In addition,

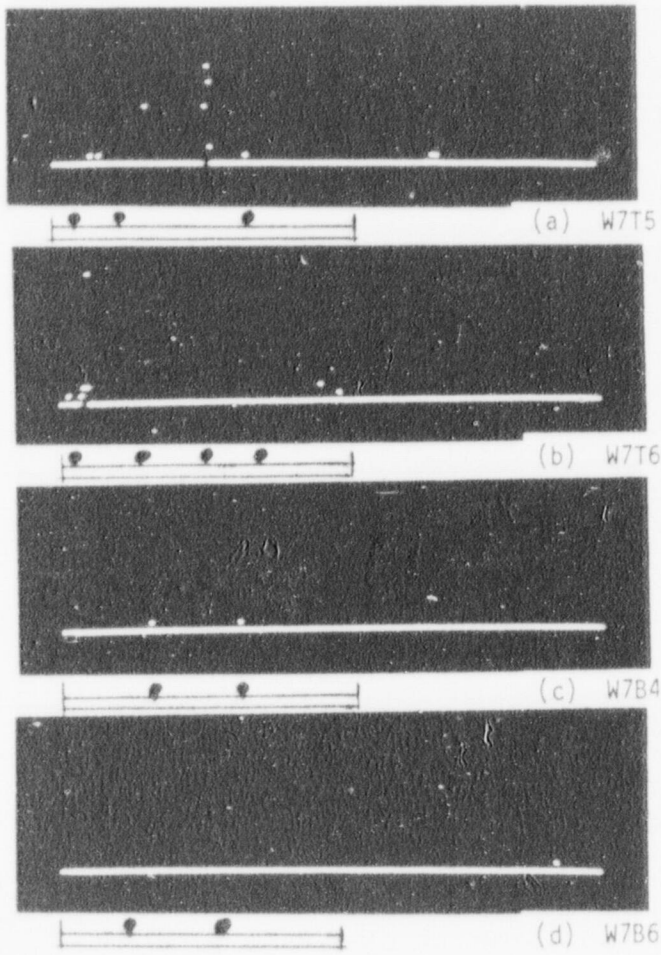

Figure 4-19. ALARM ACTIVITY ASSOCIATED WITH INTENDED POROSITY FLAWS DURING SUBMERGED ARC WELD 7 JOINING VESSEL-TYPE A533B STEEL

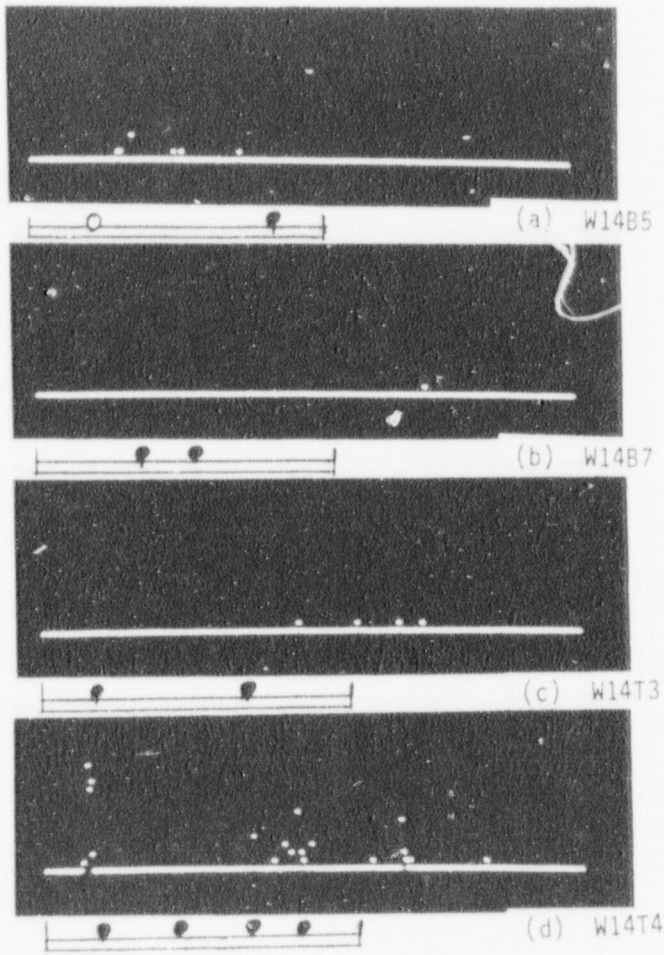

Figure 4-20. ALARM ACTIVITY ASSOCIATED WITH INTENDED POROSITY FLAWS DURING SUBMERGED ARC WELD 14 JOINING VESSEL-TYPE A533B STEEL

it might be expected that the size or severity of a flaw may be related to the energy released during each propagation event. As the energy of the region surrounding the flaw edge increases, the energy released to propagate the edge and to create the acoustic emission may increase. Since ringdown count is related to the acoustic wave energy, it may also be a useful indication of the propagation energy and thus, of the extent of propagation.

To analyze size relations, radiographic indications were used to establish flaw size. The computer analysis system provided 1) tabulations of the number of alarms occurring in conjunction with each flaw, 2) counts of the number of acoustic events having ringdown counts within a selected interval, and 3) averages of ringdown counts from selected time intervals during the weld.

Cracks

Figure 4-22 shows the time-based alarm activity of cracks in submerged arc welds presented in order of increasing size as indicated by radiography (weld 1 cracks have not been radiographically confirmed but have been detected by ultrasonic inspection). This figure gives the impression that alarm activity tends to become greater in amplitude and more extended in time as the size of the crack increases. Because of the way in which the computer organizes the data, the amplitude of the alarm plot does not represent any intensity of alarm activity itself but indicates the number of acoustic emission events being detected during the time that the alarm flag is set high. Because of this, the separation between the end of one alarm episode and the beginning of the next may not be readily apparent in an alarm vs. time plot of a weld with a high rate of indications. To arrive at a more accurate count of the number of alarms as a function of flaw size, tabulations of the weld acoustic events (such as shown in Figure 4-23) are examined to count the number of periods where the alarm was set. Such a tabulation gives the scatter plot shown in Figure 4-25 where the straight line is a best fit between the averages of the vertical scatter. A tendency for larger cracks

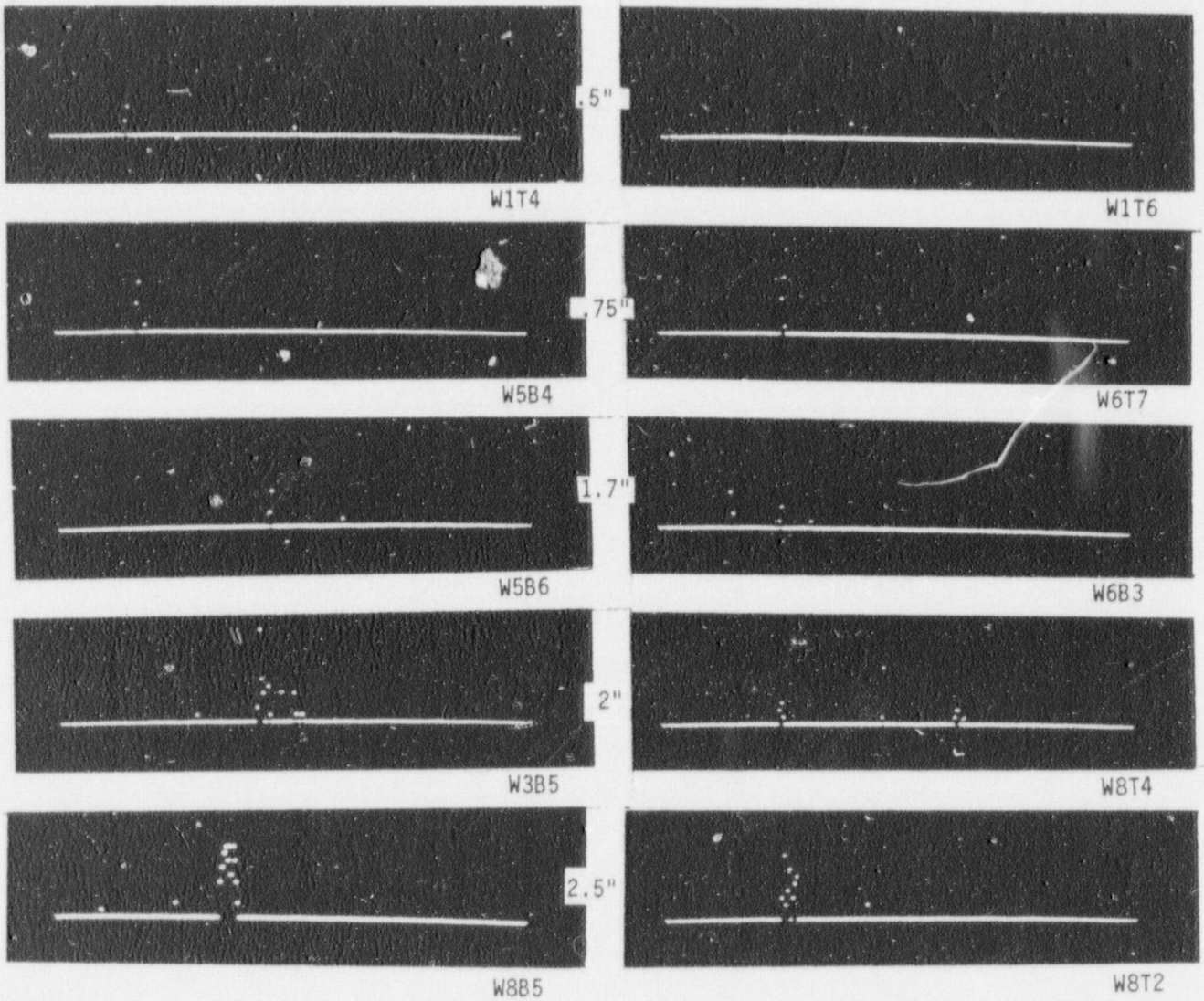

Figure 4-21. PREPROCESSOR ALARM ACTIVITY VS. RADIOGRAPHICALLY-MEASURED CRACK LENGTH

05 W8BCP4, 65 DB, 2.0"C- 7.0" OUT 00683

TIME	INTERVAL	COUNT	110	150	200	270	370	500	675	920	A-O-C-F
01250	00002	0002	1.00	1.90	1.50	0.67	0.75	1.18	1.05	1.27	0 0 0 1
01258	00008	0009	1.00	0.32	0.56	0.22	0.24	0.15	0.60	0.32	0 0 0 1
01262	00004	0011	1.00	0.40	0.53	0.14	0.23	0.49	0.61	0.41	0 0 0 1
01267	00005	0002	1.00	0.32	0.58	0.03	0.78	0.29	0.19	0.48	0 0 0 1
01274	00007	0001	1.00	0.40	0.85	0.44	0.54	0.54	0.97	0.60	0 0 0 1
01275	00001	0010	1.00	0.50	0.61	0.76	0.36	0.66	0.10	0.30	0 0 0 1
01281	00006	0001	1.00	0.55	0.89	0.42	0.42	0.51	0.19	0.46	0 0 0 1
01284	00003	0019	1.00	0.36	0.38	0.42	0.23	0.33	0.48	0.28	0 0 0 1
01286	00002	0012	1.00	0.76	0.62	0.56	0.34	0.45	0.59	0.54	0 0 0 1
01293	00007	0001	1.00	0.61	0.88	0.11	0.38	0.37	0.53	0.62	0 0 0 1
01300	00007	0003	1.00	0.26	0.47	0.10	0.43	0.32	0.63	0.34	0 0 0 1
01301	00001	0003	1.00	1.00	0.84	0.29	0.57	0.71	0.95	0.81	0 0 0 1
01303	00002	0063	1.00	0.28	0.34	0.37	0.19	0.13	0.12	0.22	0 0 0 1
01307	00004	0018	1.00	0.98	0.54	0.50	0.30	0.42	0.18	0.49	0 0 0 1
01311	00004	0002	1.00	0.56	0.54	0.47	0.32	0.25	0.66	0.47	0 0 0 1
01316	00005	0011	1.00	0.48	0.63	0.54	0.30	0.47	0.62	0.49	0 0 0 1
01318	00002	0009	1.00	0.53	0.40	0.30	0.26	0.35	0.19	0.53	0 0 0 1
01320	00002	0139	1.00	0.41	0.38	0.53	0.17	0.23	0.28	0.35	0 0 1 1
01323	00003	0003	1.00	0.89	0.91	0.77	0.32	0.62	1.00	0.74	0 0 0 1
01327	00004	0283	1.00	0.40	0.40	0.47	0.16	0.12	0.13	0.18	0 0 1 1
01330	00003	0002	1.00	0.40	0.54	0.65	0.26	0.54	0.76	0.60	0 0 0 1
01334	00004	0032	1.00	0.79	0.58	0.41	0.14	0.11	0.11	0.21	0 0 0 1
01335	00001	0138	1.00	0.52	0.47	0.31	0.27	0.58	0.73	0.68	0 0 1 1
01340	00005	0029	1.00	0.27	0.52	0.29	0.50	0.10	0.06	0.28	1 0 0 1
01344	00004	0795	1.00	0.80	0.56	0.43	0.18	0.18	0.16	0.13	1 0 1 1
01347	00003	0093	1.00	0.46	0.71	0.31	0.17	0.18	0.14	0.09	1 0 0 1
01354	00007	0448	1.00	0.83	1.00	0.77	0.30	0.13	0.22	0.28	1 0 1 1
01355	00001	0190	1.00	0.40	0.48	0.39	0.21	0.31	0.55	0.39	1 0 1 1
01358	00003	0015	1.00	0.39	0.29	0.55	0.15	0.22	0.42	0.32	1 0 0 1
01361	00003	0034	1.00	0.41	0.91	0.41	0.20	0.28	0.17	0.38	1 0 0 1
01363	00002	0008	1.00	0.42	0.69	0.18	0.28	0.45	0.55	0.60	1 0 0 1
01366	00003	0024	1.00	0.30	0.51	0.36	0.22	0.30	0.13	0.38	1 0 0 1
01371	00005	0001	1.00	0.47	0.43	0.35	0.23	0.24	0.09	0.42	1 0 0 1
01374	00003	0015	1.00	0.61	0.60	0.32	0.15	0.18	0.26	0.21	1 0 0 1
01376	00002	0384	1.00	0.55	0.94	1.03	0.59	0.66	1.37	0.75	1 0 1 1
01378	00002	0200	1.00	0.37	0.32	0.52	0.28	0.22	0.27	0.29	1 0 1 1
01381	00003	0001	1.00	0.64	0.95	0.80	0.46	0.47	0.62	0.59	1 0 0 1
01384	00003	0001	1.00	0.54	0.72	0.47	0.34	0.66	0.40	0.76	1 0 0 1
01391	00007	0004	1.00	0.35	0.54	0.24	0.23	0.19	0.72	0.33	1 0 0 1
01393	00002	0259	1.00	0.58	0.72	0.53	0.52	0.38	0.43	0.41	1 0 1 1
01399	00006	0836	1.00	0.89	1.00	0.48	0.18	0.10	0.25	0.16	1 0 1 1

Figure 4-22. ANALYZER COPY OF AN ACOUSTIC EMISSION EVENT TABULATION FOR THE FOURTH BACK COVER PASS OF WELD 8

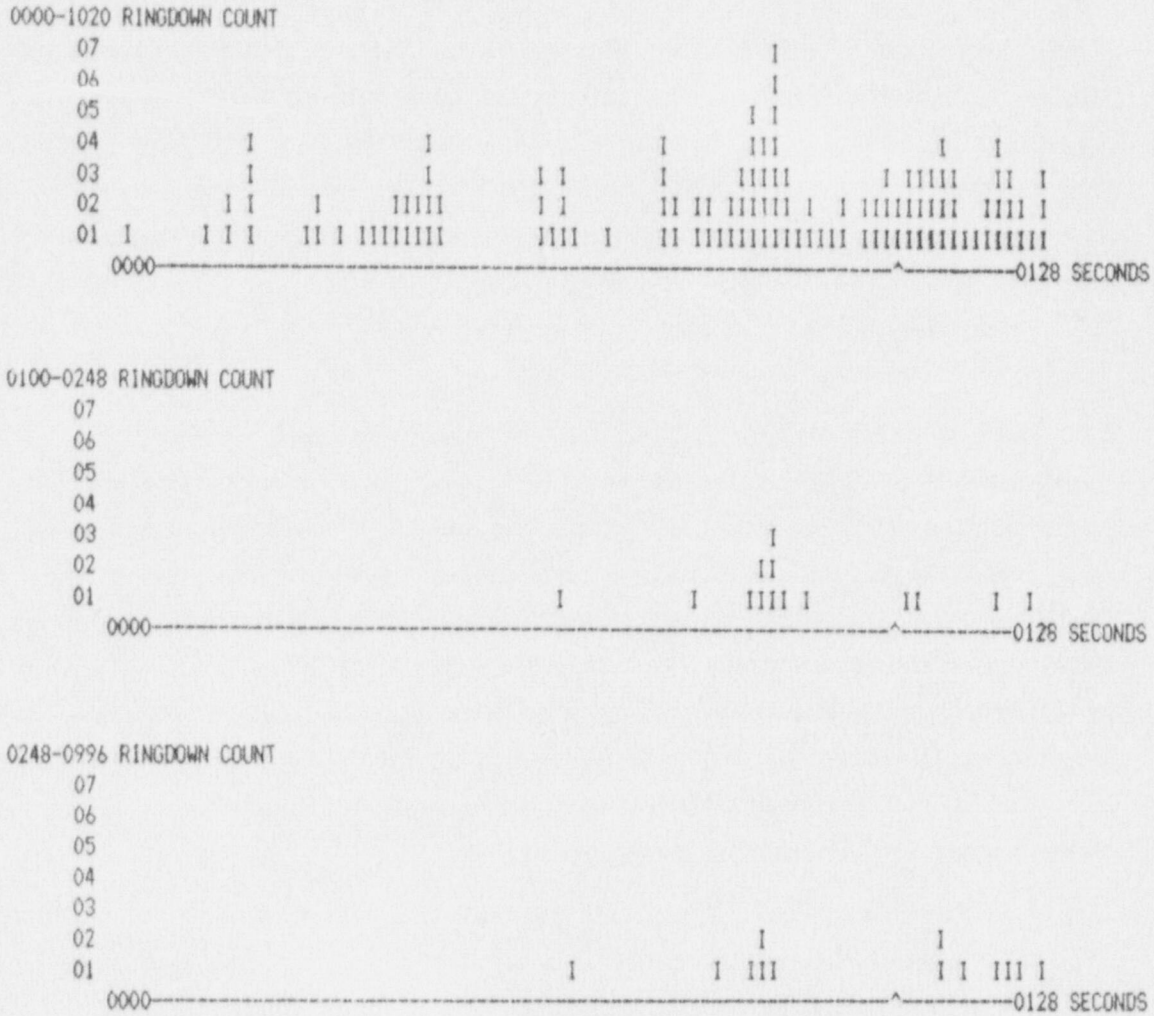

Figure 4-23. TIME - BASE RECORD OF EVENTS WITH SELECTED RINGDOWN COUNT LIMITS OCCURRING DURING WELDING

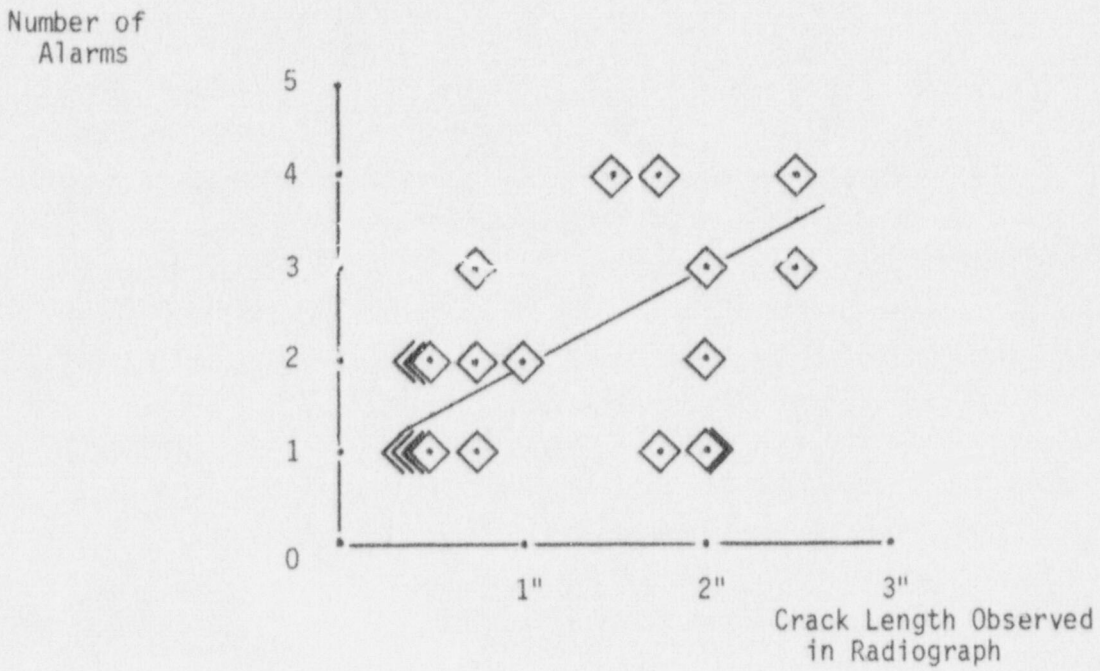

Figure 4-24. NUMBER OF ALARMS VS. SIZE FOR CRACKS IN SUBMERGED ARC WELDS

to yield more alarms per detection is evident, but the scatter of the data is very high. This may result from the number of alarms being more a result of the preprocessor's timing and logic decisions than a direct reflection of the activity occurring in the flaw. For example, it is possible with current alarm generating logic to have a number of potential alarms masked by the presence of an already active alarm, especially if these potential alarm events occur less than one second after initiation of the first alarm. It is also possible with the current computer interface to miss alarms in welds with quiet backgrounds and little post-alarm activity. In the preprocessor, each alarm is set after all its precursor events have occurred, and if no acoustic emission of any type occurs within one second after the alarm, that alarm does not become part of the event record. These effects may be removed by altering the nature of the computer interface or by processing alarm indications in the software.

The next sizing candidate parameter to be examined is that of the number of acoustic events detected with ringdown count limits of 100-250, 250-1000, and 100-1000. The computer presents the information rapidly in the format shown in Figure 4-23. Based on this information, plots of acoustic activity for selected energies can be plotted as a function of size (Figure 4-25). The scatter of the data seems to have been reduced somewhat and, in the case of total events with ringdown count between 100 and 1000, a linear size-activity relation can be seen for cracks less than 2½ inches of length. Cracks with an apparent length of 2½ inches seem to be more active than expected. This may be due to the size of larger cracks not being tracable by simple radiography. As the size of a crack or crack network increases, the number of potential branch points also increases and given the proper combinations of stress and material composition, increasingly larger portions of the crack may develop with orientation disadvantageous to radiography.

If crack extension is due to cooling stresses exceeding the local critical stress intensity factor around the crack edge, the energy stored at that point will be released and a major portion of it will serve to advance the flaw.

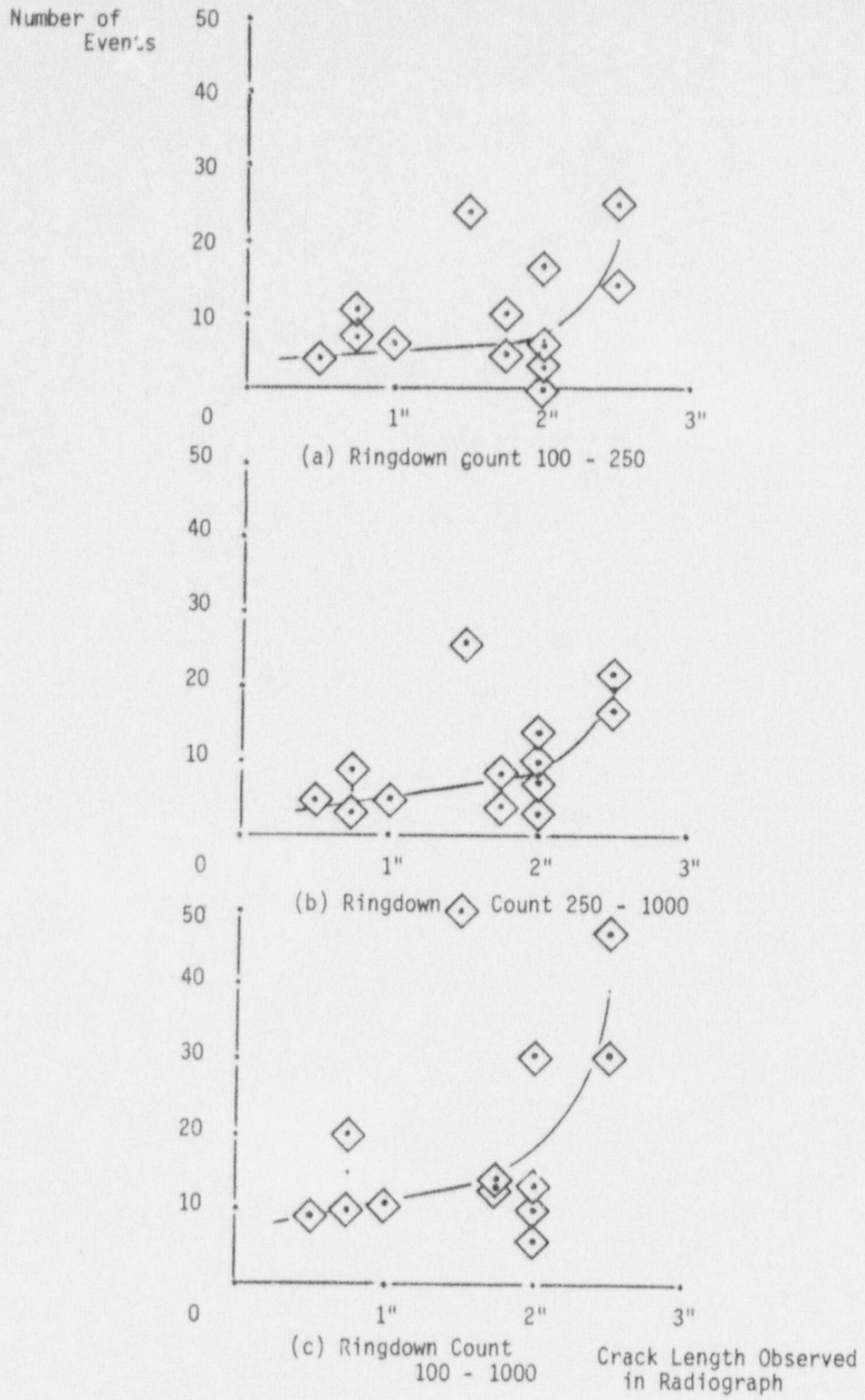

Figure 4-25. NUMBER OF EVENTS OF SELECTED ENERGY VS. SIZE FOR CRACKS IN SUBMERGED ARC WELDS

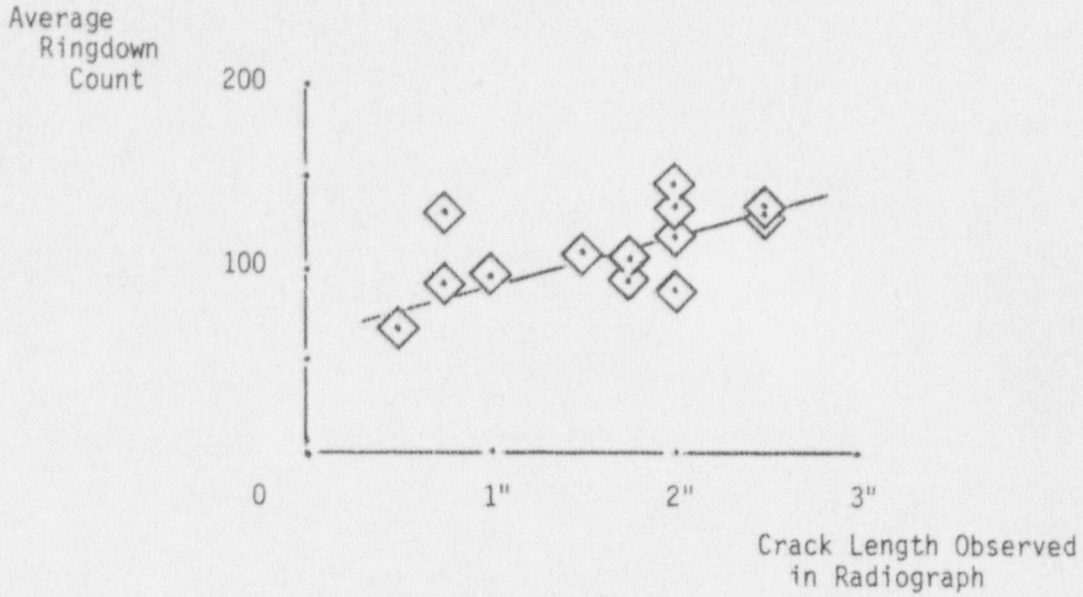

Figure 4-26. AVERAGE RINGDOWN COUNT VS. CRACK SIZE IN SUBMERGED ARC WELDS

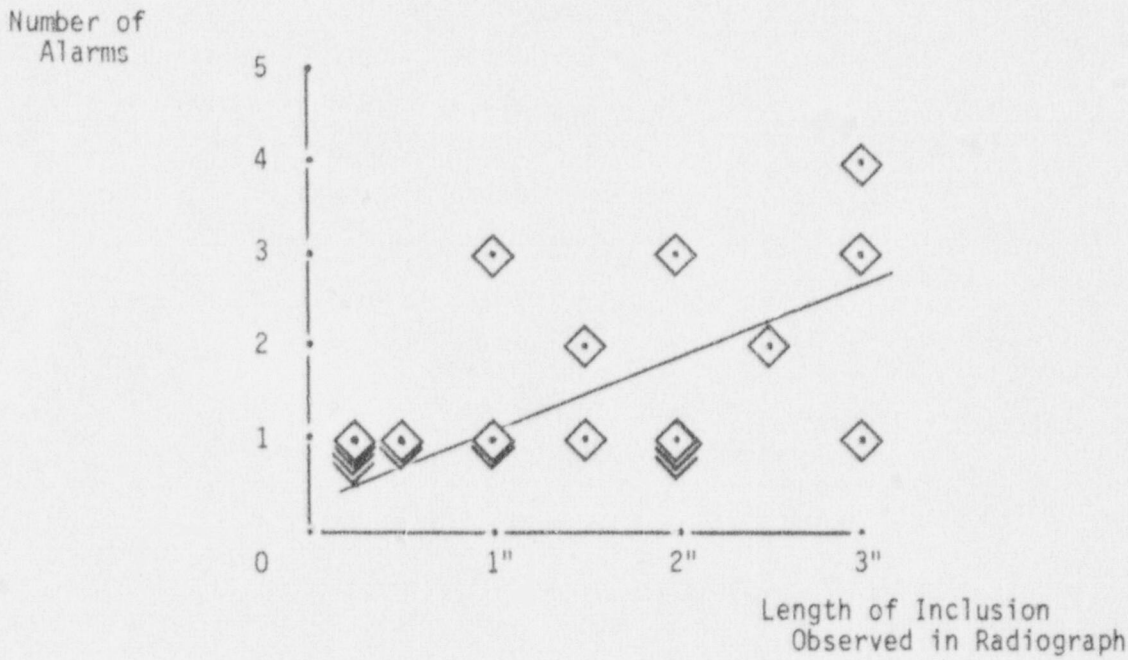

Figure 4-27. NUMBER OF ALARMS VS. SIZE FOR SLAG INCLUSIONS IN SUBMERGED ARC WELDS

It may be expected that the greater this stored energy, the greater will be the amount that does into propagating the crack when it advances and the greater will be the residual energy that goes into the acoustic emission wave. Ringdown count is a measure of this latter energy and may be related to crack size. Averages of ringdown counts were computed at the time of greatest activity for a flaw and plotted as a function of the apparent size of the flaw. The resulting plot (Figure 4-26) is another relation tending to be linear between average ringdown count and flaw size.

Except for three points (one above the trend line at 3/4" crack length, two above that line at 2" crack length), the scatter is very low. In fact, the two deviant data points at 2" crack length came from a weld in which procedure differed substantially from what is found in production welding. Most of the A533B submerged arc welds discussed in this report were fabricated by filling in one-half of a double-vee cross section before commencing the fill of the second half. Weld 3, in which three 2" cracks were successfully attempted, was the exception. In this weld, three passes were laid to partially fill one-half of the cross-section and then the other half was completely filled with 12 passes. After that, the first half of the cross-section was then finished with the laying in of 4 passes. If the cooling stresses act to bend the neighboring plate around the axis of the weld, the presence of the first three passes in the partially-filled half of the cross section can be seen to reinforce the neighboring plate against the buildups of stress induced during welding of the other half. Thus, it would take longer for the stresses around a flaw edge to build to the point where flaw propagation could occur. When flaw propagation did occur, the surrounding material would have cooled to the point where a given stress energy released to advance the flaw edge would be bucked by a greater binding energy of material through which the flaw attempted to propagate. Under these conditions, an acoustic emission of large energy (or ringdown count) would be associated with a flaw of smaller-than-expected size. As is shown in Figure 4-26, this was the case for the two 2" cracks exhibiting higher-than-trend ringdown counts

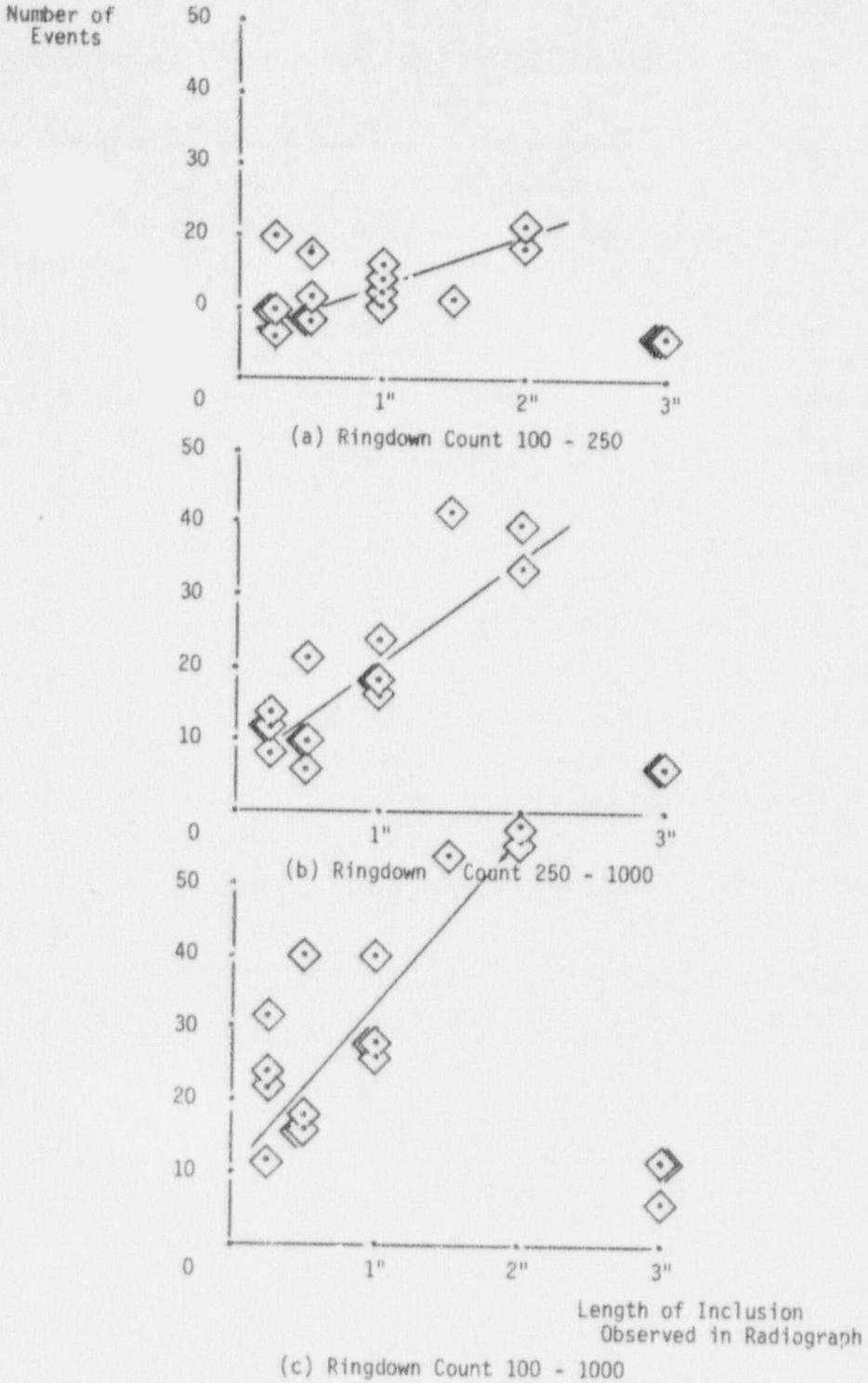

Figure 4-28. NUMBER OF EVENTS OF SELECTED ENERGY VS. SIZE FOR SLAG INCLUSIONS IN SUBMERGED ARC WELDS

induced on the first completely-filled half of weld 3. This hypothesized mechanism is reasonable in view of the fact that time records of the delay between flaw generations and the resultant acoustic emission showed that weld 3 passes had an average delay of 25 seconds, almost double that associated with cracks in the other submerged arc welds.

The third deviant point in Figure 4-26 associated with a 3/4" crack length came from a lower pass in Weld 5 in which incomplete penetration was also being detected by acoustic emission. The absence of a "pure" flaw type in this pass possibly qualifies this as a discardable data point. In summary, it appears that the radiographically apparent size of cracks can be linearly related to acoustic emission by either ringdown count average or the number of energetic events associated with the cracks.

Slag Inclusions

By procedures similar to those described above, a scatter plot of alarm occurrence as a function of inclusion length can be derived (Figure 4-27). The relation tends to be linear with a great deal of scatter. A plot of event number and size (Figure 4-28) reduces the variability while retaining a linear relation which appears to hold best for events with ringdown counts between 250 and 1000. A major deviation from this relation is apparent for inclusion sizes greater than 2 inches when the activity rate becomes unusually low. The activity is still energetic and does allow flaw detection, although that also becomes marginal. There may be a critical inclusion size between 2" and 3" above which acoustic activity drops dramatically. The underlying mechanism apparently involves the volume of space in which the trapped inclusion can or cannot find a means of relieving stress transmitted from the steel walls before cracking. Similar to the events associated with age hardening, stress buildup is apparently a maximum with a critical inclusion size. Over critical or large inclusions might therefore be expected, upon stress relief, to yield less AE than critical sizes.

A scatter plot of average ringdown count as a function of inclusion length was attempted (Figure 4-29) but does not show any apparent tendency. A major

problem with constructing this plot is that, although the average ringdown count is taken at or just before the time the weld head is at the site of the flaw, the activity at the time the weld head is at any flaw cannot always be assumed to be coming from that flaw alone if there exists more than one flaw in that weld or if spatially extensive flaws exist. Therefore, the existence of a size-ringdown count relation cannot be ruled out. The resolution of the present analysis may merely be insufficient to extract it.

During these experiments, the acoustic emission locator was used as an aid in determining what activity was coming from what flaw. However, the communications link was verbal and, while it worked for very localized flaws, the high density, activity, and interactions of the slag inclusions caused an unmanagable information overload. The next development in this type of data acquisition will be to link the locator and the computer electronically so that location can be added as part of the analyzer's data input.

Incomplete Penetration

Using procedures outlined above, a data plot of number of alarms as a function of radiographic assessment of incomplete penetration severity was made (Figure 4-30). The relation tends to be linear and shows the usual scatter. All degrees of incomplete penetration except "slight" could trip the pre-processor alarm at the normal recording gains. A plot of event number and flaw severity (Figure 4-31) still has a good deal of scatter but the central tendency is linear only for the slight to moderate degrees of flaw severity.

When a plot of average ringdown count if made against flaw severity (Figure 4-32) a very linear relationship with minimal scatter is observed. Even though the number of acoustic events increases remarkably for severe incomplete penetration (as seen in Figure 4-31), the associated energy follows a linear relation. In this analysis, specimen 17 does not quite fit. Radiographically it appears as moderate incomplete penetration and this interpretation was backed by dye penetrant tests. However, its acoustic

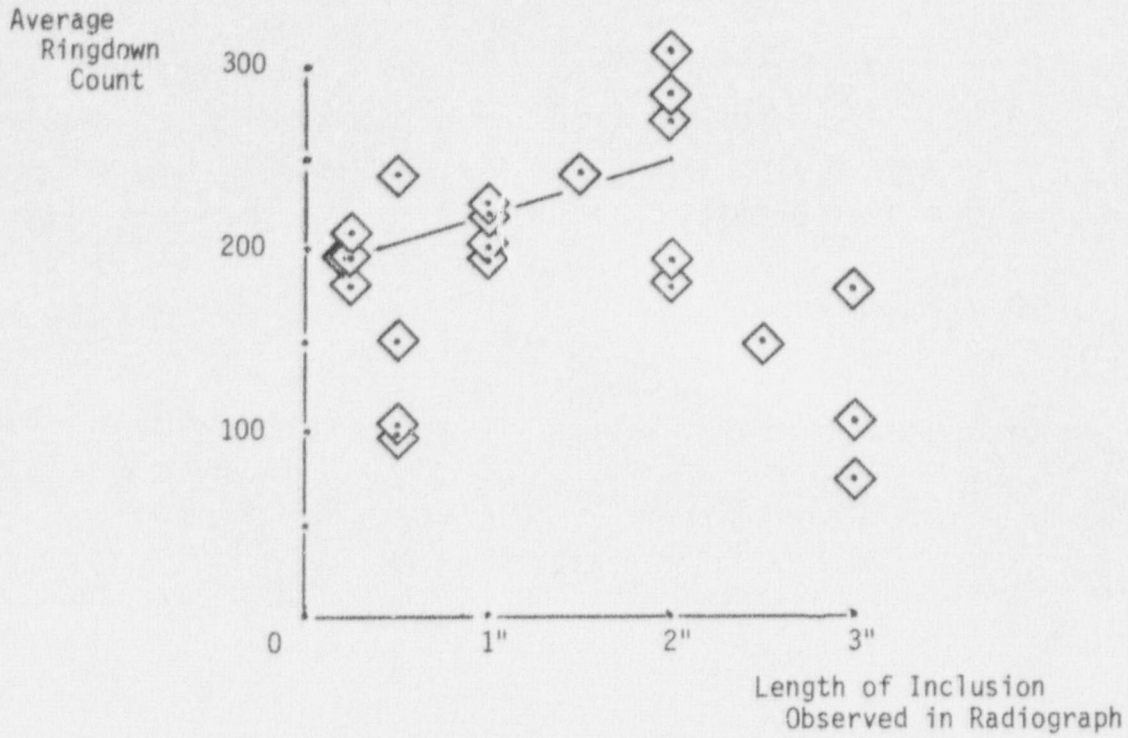

Figure 4-29. AVERAGE RINGDOWN COUNT VS. SIZE FOR SLAG INCLUSIONS ◇ IN SUBMERGED ARC WELDS

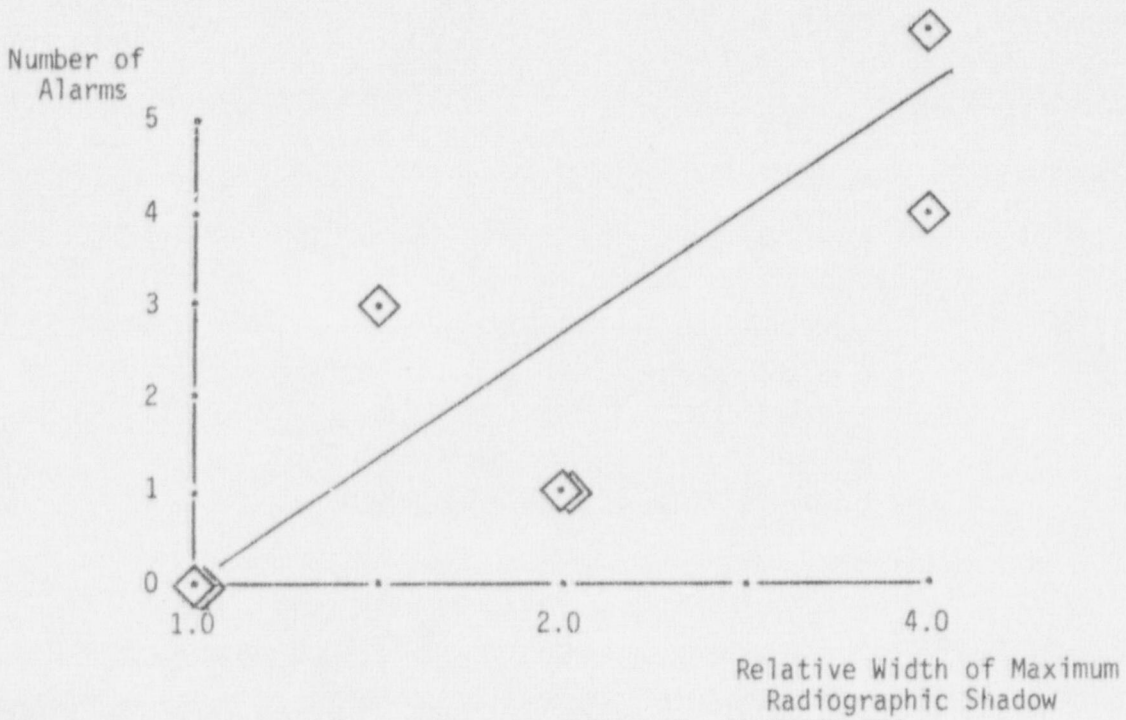

Figure 4-30. NUMBER OF ALARMS VS. SEVERITY FOR INCOMPLETE PENETRATION IN GMA WELDS

activity in all three of the given criteria is greater than expected for a flaw of moderate severity. Sectioning of this and other specimens will help resolve those anomalies.

4.4 Flaw Type Characteristics

The last type of information to be extracted from the analysis is that resulting from a search for a group of acoustic emission parameters which can be used to distinguish flaw type. Again, the discussions will be confined to those flaw types which have been found to be reliably detectable by acoustic emission (i.e., cracks, slag inclusions, and incomplete penetration). The search for a flaw characterization included examinations of ringdown count averages for the weld as a whole (lumped averaging) and during periods of each weld when the flaw was being generated and when the flaw was acoustically active (distributed averaging). In addition, both lumped and distributed average relative frequency response was charted and absolute frequency behavior was studied. In addition, time delays between flaw generation and detection were compared and the duration of detection activity was measured. It was found that flaw types can possibly be discriminated in submerged arc and GMA weld processes. The results will be discussed by the acoustic emission parameter examined.

Average Ringdown Count

As shown above, variations in average ringdown count can be used as a flaw size indicator for cracks and incomplete penetration. To determine if its behavior is stable enough to reflect flaw type also, the mean of the ringdown count averages was computed for cracks in GMA and in submerged arc welds, for incomplete penetration in GMA and in submerged arc welds, and for slag inclusions in submerged arc welds. The standard deviation of this computed mean varied from 1% to 60% of the value of the mean as compared to the standard deviation of the ringdown count average for each flaw, which varied from 80% to more than 100% of the associated average ringdown count. Thus, the variations of average ringdown counts from flaw to flaw of the same type is less than the variations of ringdown counts associated with any given flaw. This

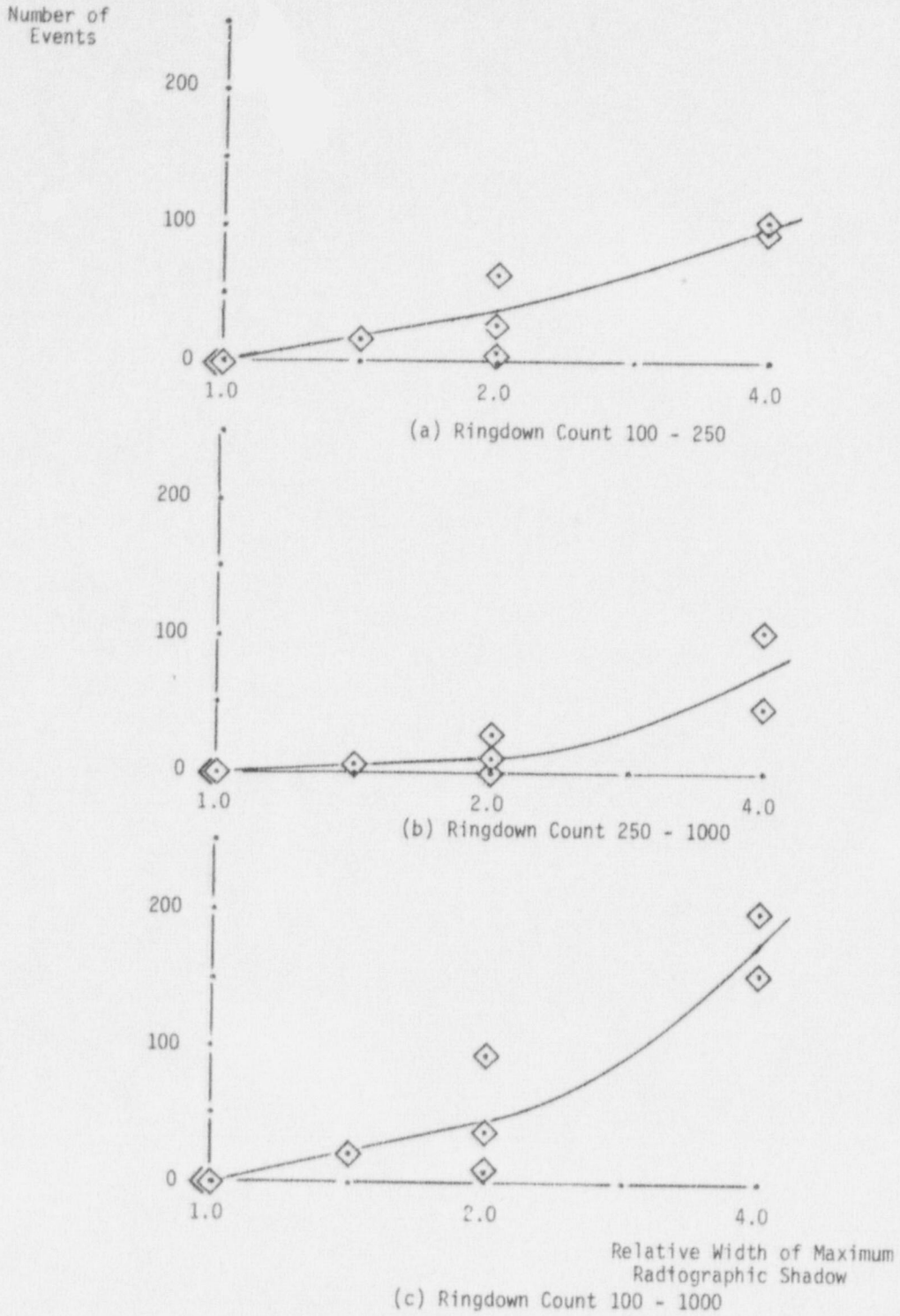

Figure 4-31. NUMBER OF EVENTS OF SELECTED ENERGY VS. SEVERITY OF INCOMPLETE PENETRATION IN GMA WELDS

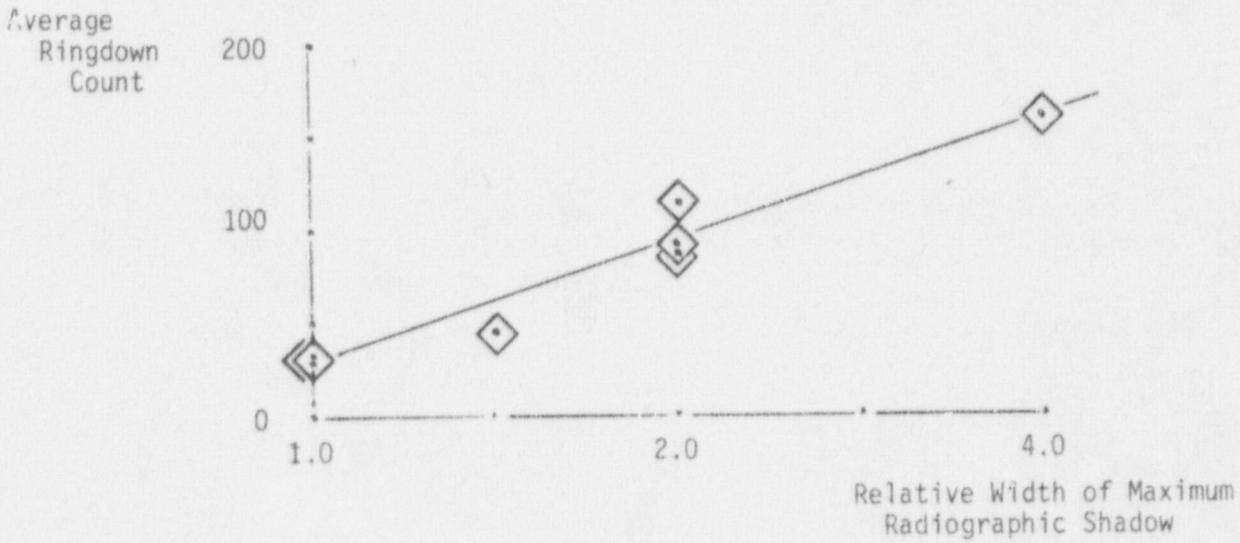

Figure 4-32. AVERAGE RINGDOWN COUNT VS. SEVERITY OF INCOMPLETE PENETRATION IN GMA WELDS

implies that the average ringdown counts can be a stable indication for examination of flaw type characteristics.

For GMA welds of ½" A106 piping-type steel, the average ringdown count was computed for the period the flaw was acoustically active. In the welds in which cracking was intended and confirmed, the average ringdown count equalled 154 with a deviation of 25% of the average value. In the welds in which incomplete penetration was intended and confirmed, the average RDC equalled 79 with a deviation of 57% of the average value. The average ringdown count for incomplete penetration was computed from the entire activity of the weld since this type of flaw is of an extended nature. The conclusion reached is that a distinction between cracking and incomplete penetration in GMA welds can be made using average ringdown count as a parameter.

For submerged arc welds of 2" A533B vessel-type steel, the average ringdown count was again computed for those periods in which the flaw was acoustically active. In the welds in which cracking was intended and confirmed, the average ringdown count equalled 113 with a deviation of 27% of the average value. In the welds in which slag inclusions were intended and confirmed, the average RDC equalled 205 with a deviation of 28% of the average value. In the weld in which incomplete penetration was intended and confirmed, the average RDC equalled 259 with a deviation of 1% of the average ringdown value. Although it appears an average ringdown count-based distinction can be made between cracks, slag inclusions, and incomplete penetrations in submerged arc welds, the distinction may be unrealistic due to the different methods of flaw generation used. The submerged arc welds were cracked in upper passes where background noise from the root was minimal, whereas slag inclusions and incomplete penetration were generated in passes near the root amid a high noise badkground. The ringdown count variation does not overlap between cracks and slag inclusions, but the ringdown count average for incomplete penetration lies exactly at the high limit of the slag inclusion range. Since incomplete penetration can represent an extreme form of slag inclusion in submerged arc welds, this result argues that no distinction based on average ringdown count can

really be made between slag inclusions and incomplete penetration in submerged arc welds. Most likely this is because there actually is no difference between these flaw types in this weld process. They are the same flaw type.

The difference in average ringdown count between cracks and slag inclusions in submerged arc welds may be due to the higher noise level present in the root passes where the inclusions were placed. This hypothesis is tested by observing some results from weld 14 in which porosity was attempted. In a number of pores, it was found by acoustic emission and confirmed by metallographic sectioning that slag was trapped during pore formation in upper weld passes. Therefore, a distinction based on average ringdown count can be made between cracks and slag inclusions in submerged arc welds. Weld 14 will be discussed further after the following introduction to flaw-associated frequency behavior.

Frequency Behavior

This parameter is derived from a collection of the outputs of eight tuned preprocessor filters monitored for each acoustic emission event. To determine if the activity in any one or a collection of these frequency bands can be used to discriminate flaw type, an average of each band activity was computed for cracks in GMA and in submerged arc welds, for incomplete penetration in GMA and in submerged arc welds, and for slag inclusions in submerged arc welds. This average could be presented as computed (absolute frequency response) for illustrating the activity within each band, or it could be presented as a proportion of activity of a selected band (relative frequency response) for illustrating the averaged spectrum associated with flaw-related activity. The selected band chosen for this analysis was 110 KHz.

For generation of cracks in GMA welds of A106 piping-type steel, the relative and absolute frequency responses are plotted in Figure 4-33. In general, the absolute response shows a relatively high level of high frequency activity for these welds. Major fluctuations in all bands can be observed in

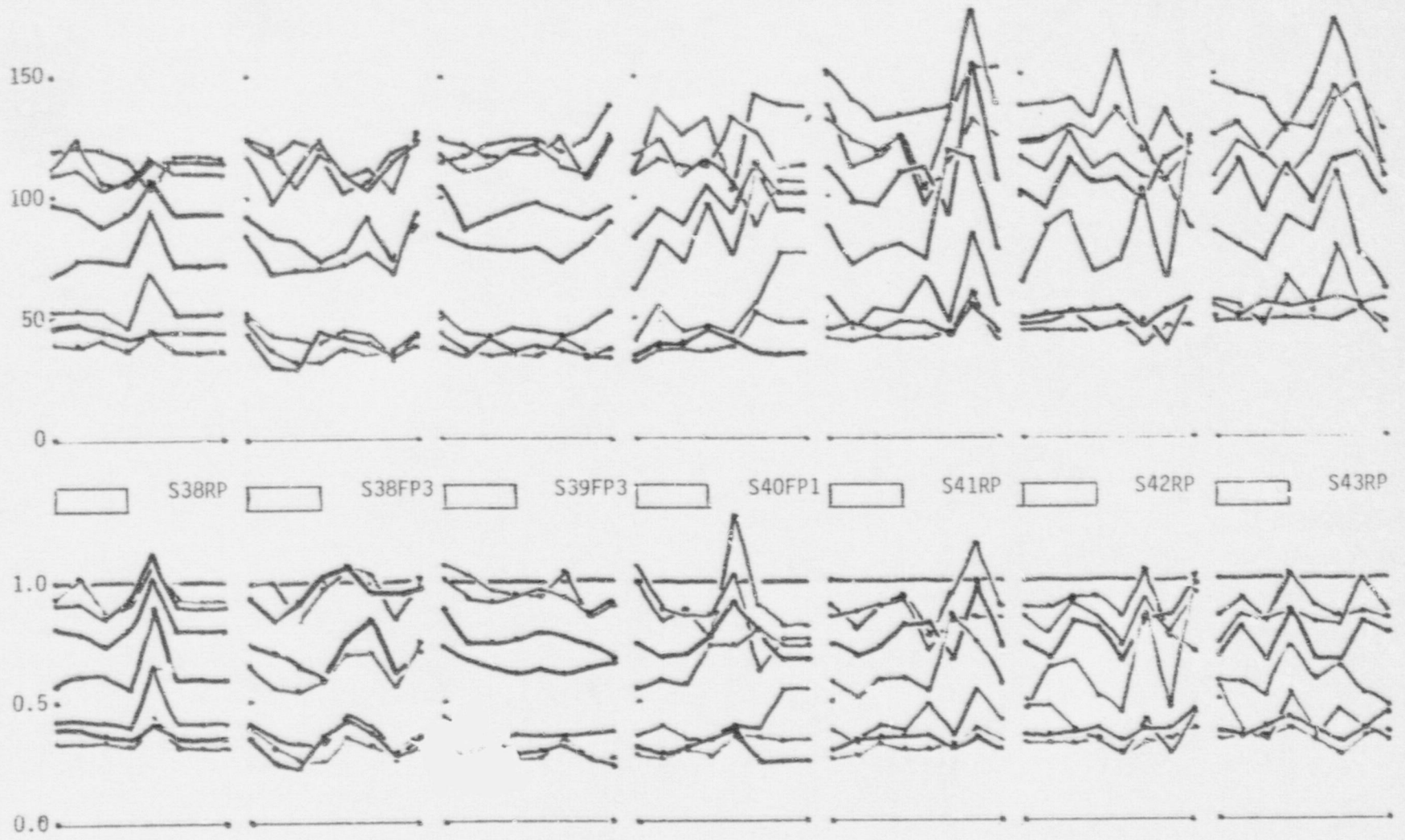

Figure 4-33. DISTRIBUTED AVERAGE FREQUENCY RESPONSES DURING GENERATION OF CRACKS IN GMA WELDS

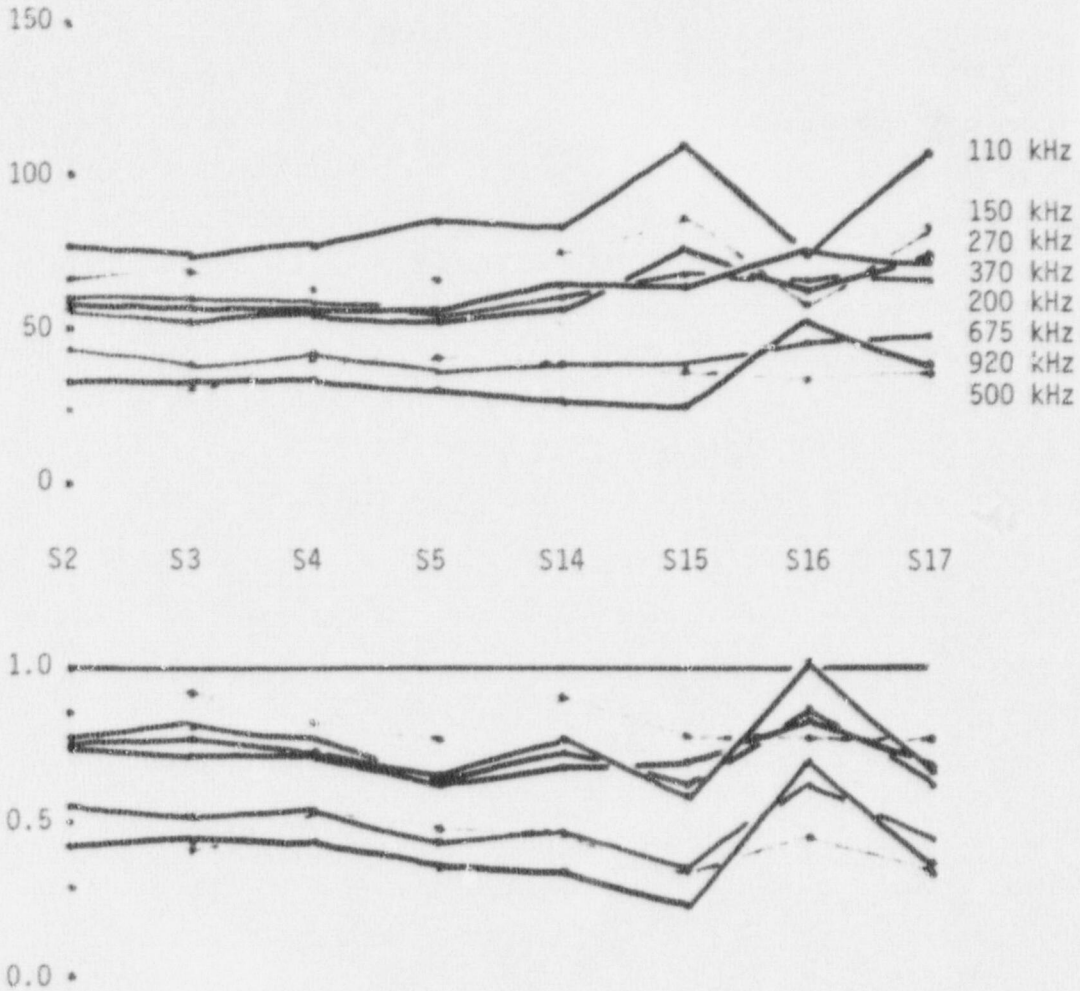

Figure 4-34. LUMPED AVERAGE FREQUENCY RESPONSES DURING GENERATION OF INCOMPLETE PENETRATION IN GMA WELDS

response to crack generation and the relative frequency response shows that during such responses, the lower frequency tends to become less active, thus enhancing the normalized spectral activity. Generations of incomplete penetration in these welds yields comparable high frequency absolute activity, but displays a reduction in the level of low frequency activity. As the apparent severity of the incomplete penetration increases, the absolute response of the low frequencies rises. Nevertheless, the maximum response for incomplete penetration (that for specimen 15) never exceeds the smallest response to a crack. The relative frequency response shows a shift of frequencies for incomplete penetration similar to that for cracking. Therefore, monitoring of relative frequency behavior may not be able to discriminate between cracks and incomplete penetration in GMA welds, but monitoring of absolute frequency response may provide some information.

For generation of cracks in some submerged arc welds of A533B vessel type steel, the relative and absolute frequency responses are plotted in Figures 4-35 to 4-37. In all cases, increases in absolute activity for all frequencies are evident during generation and reactivation of cracks, and the relative frequency response shows a similar picture. Generation of slag inclusions in these welds yields a higher absolute level of all frequency activity as shown in Figures 4-38 to 4-41. This higher level is also apparent in the relative response. Note that in weld 9 (Figure 4-38) two inclusions were induced when half the weld was done and that the high frequency activity level was less than that of inclusions placed in starting roots. This implies that the increase in high frequency activity seen in most of our slag-flawed welds is due more to the root geometry surrounding the initial flawed areas than to any activity related to the slag itself. Comparison of the frequency responses between crack flaws and slag inclusions implies that a distinction can be made on the basis that the intermediate frequencies tend to be more uniformly responsive for slag inclusions than they do for cracks. That is, slag inclusions tend to have more of "white noise" behavior than cracks. Generation of incomplete penetration in these

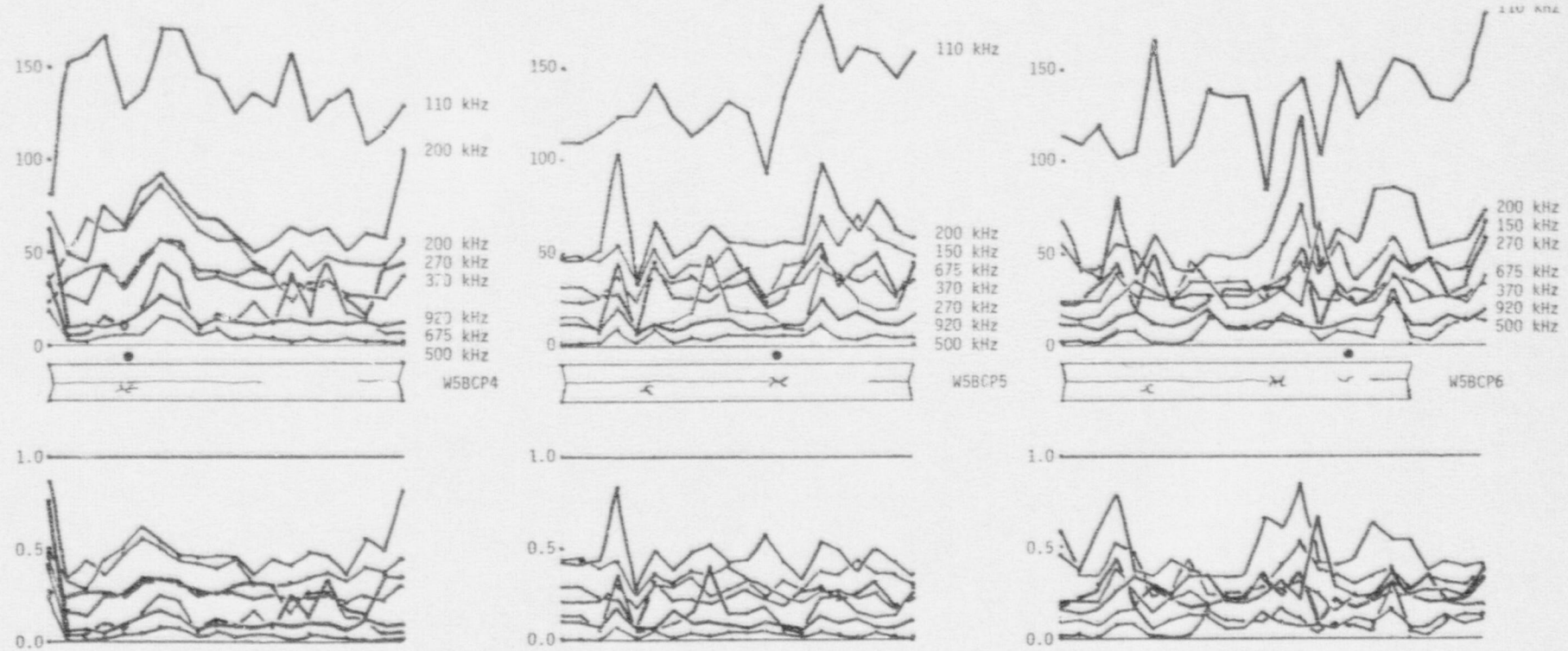

(a) Back cover pass 4 (b) Back cover pass 5 (c) Back cover pass 6

Figure 4-35. DISTRIBUTED AVERAGE FREQUENCY RESPONSES DURING GENERATION OF CRACKS IN SUBMERGED ARC WELD 5

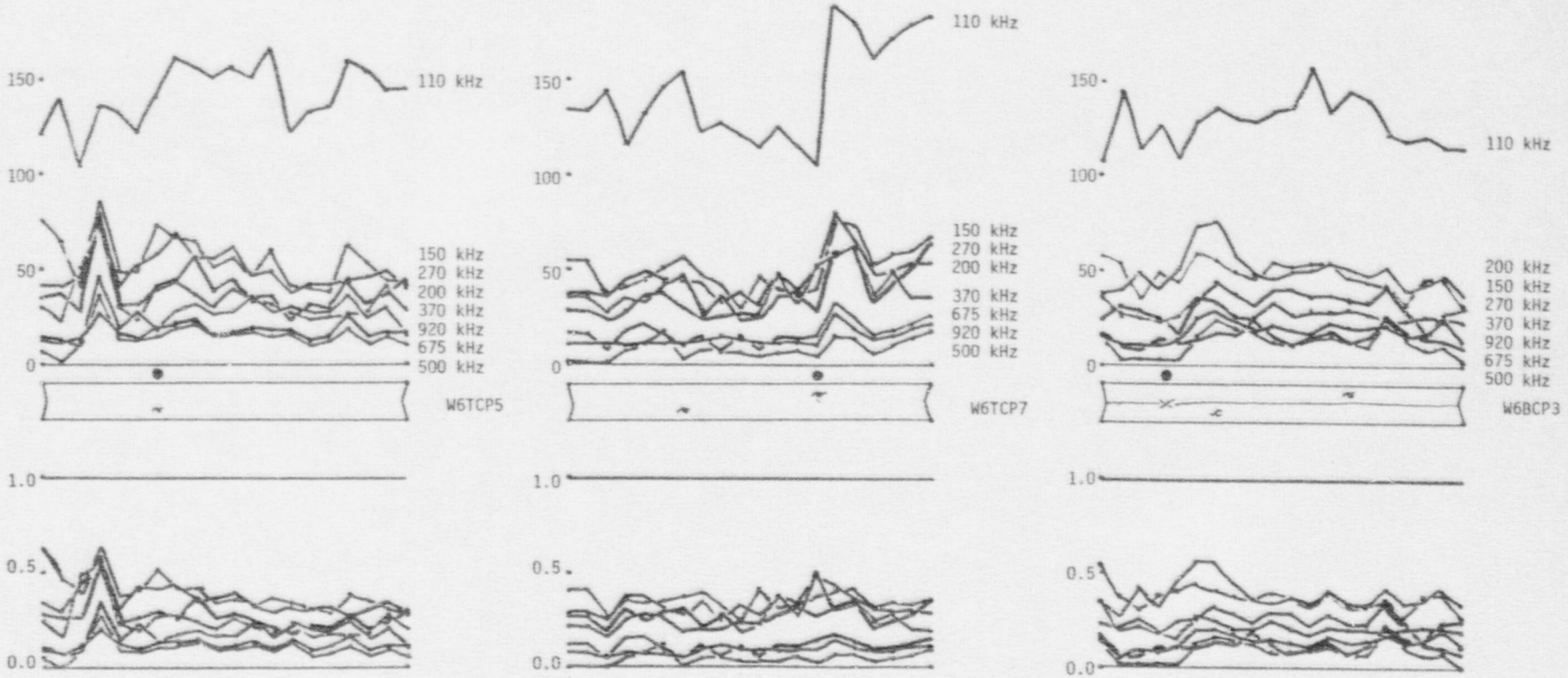

(a) Top cover pass 5 (b) Top cover pass 7 (c) Back cover pass 3

Figure 4-36. DISTRIBUTED AVERAGE FREQUENCY RESPONSES DURING GENERATION OF CRACKS IN SUBMERGED ARC WELD 6

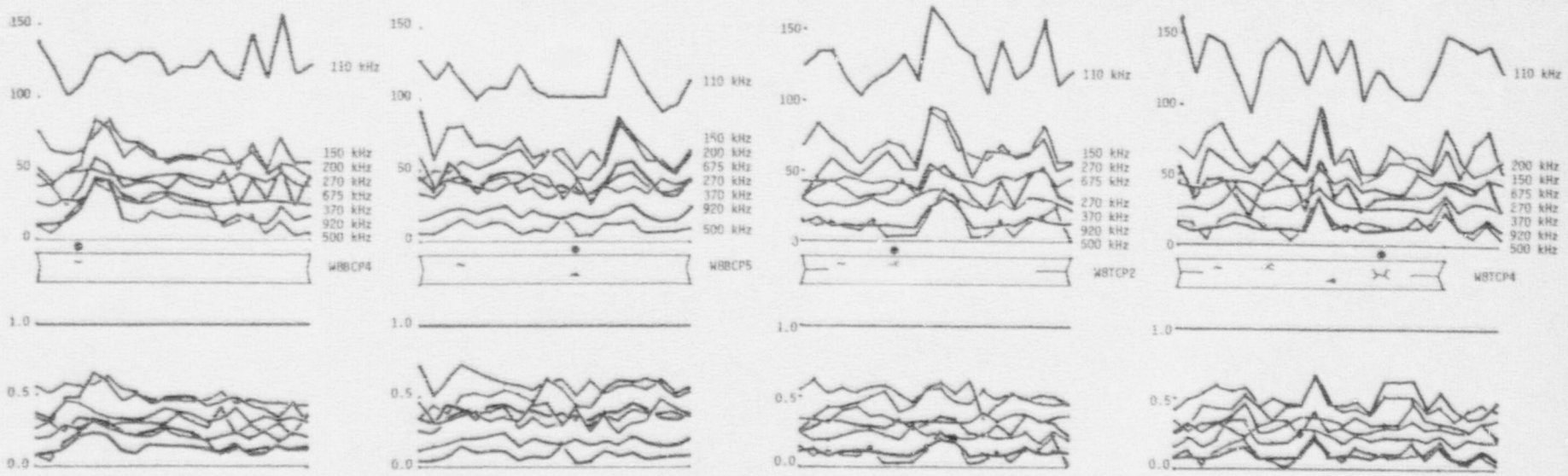

(a) Back cover pass 4 (b) Back cover pass 5 (c) Top cover pass 2 (d) Top cover pass 4

Figure 4-37. DISTRIBUTED AVERAGE FREQUENCY RESPONSES DURING GENERATION OF CRACKS IN SUBMERGED ARC WELD 8

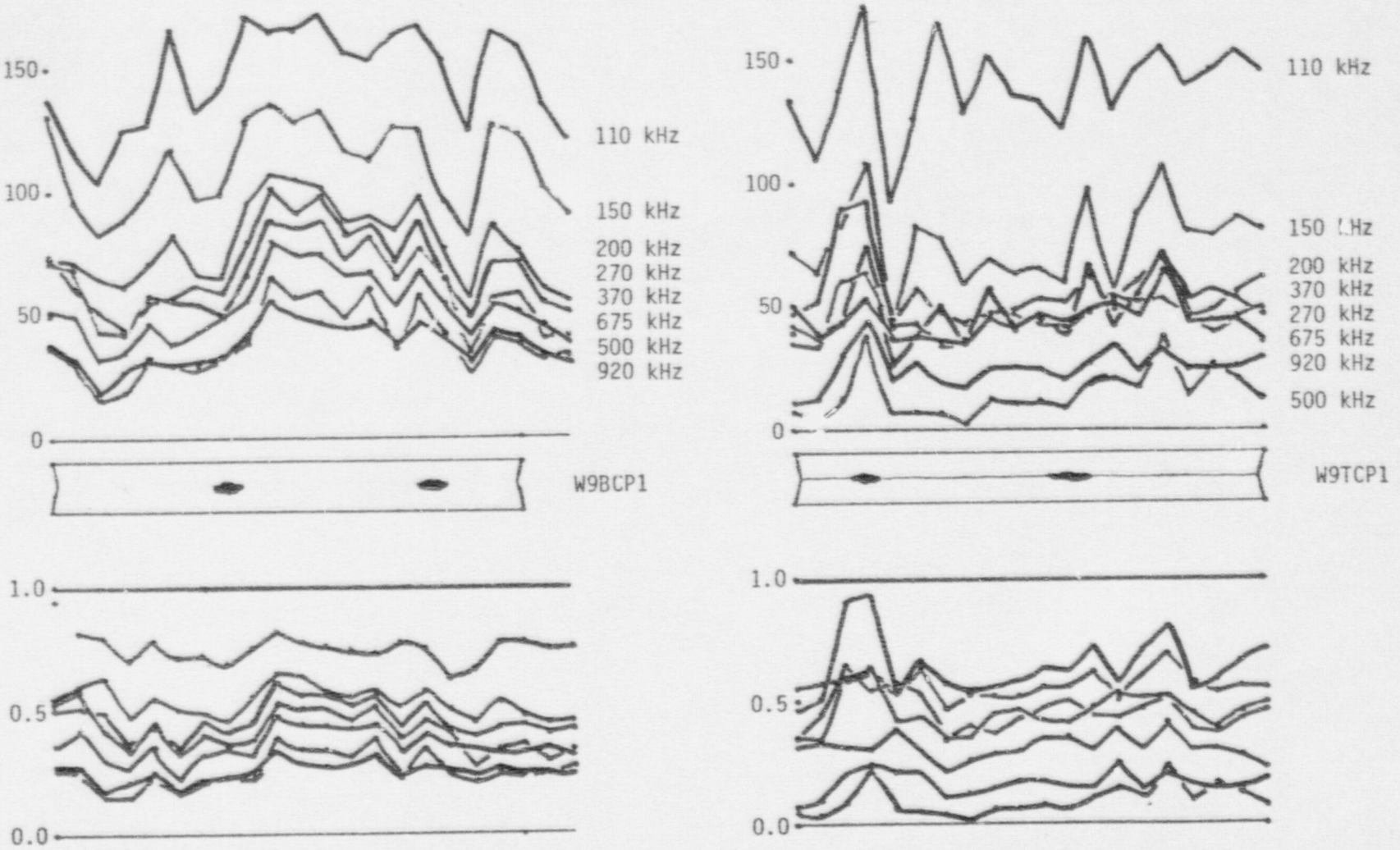

(a) Back cover pass 1

(b) Top cover pass 1

Figure 4-38. DISTRIBUTED AVERAGE FREQUENCY RESPONSES DURING GENERATION OF SLAG INCLUSIONS IN SUBMERGED ARC WELD 9

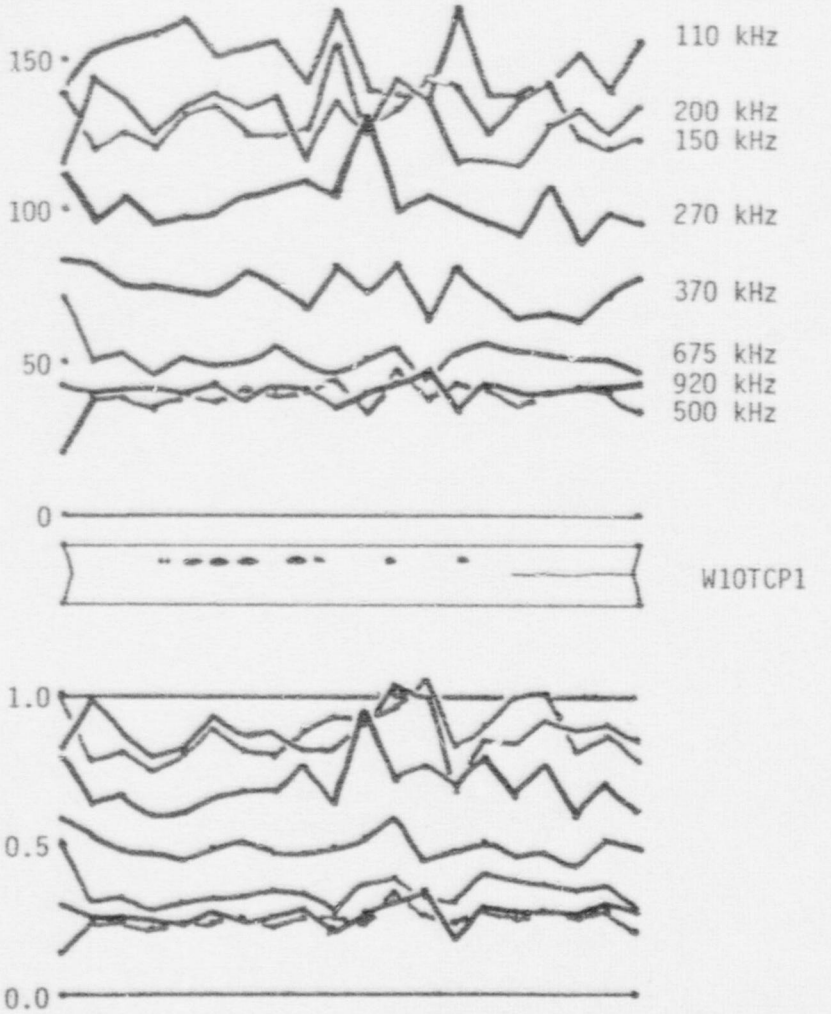

Figure 4-39. DISTRIBUTED AVERAGE FREQUENCY RESPONSES DURING GENERATION OF SLAG INCLUSIONS IN SUBMERGED ARC WELD 10

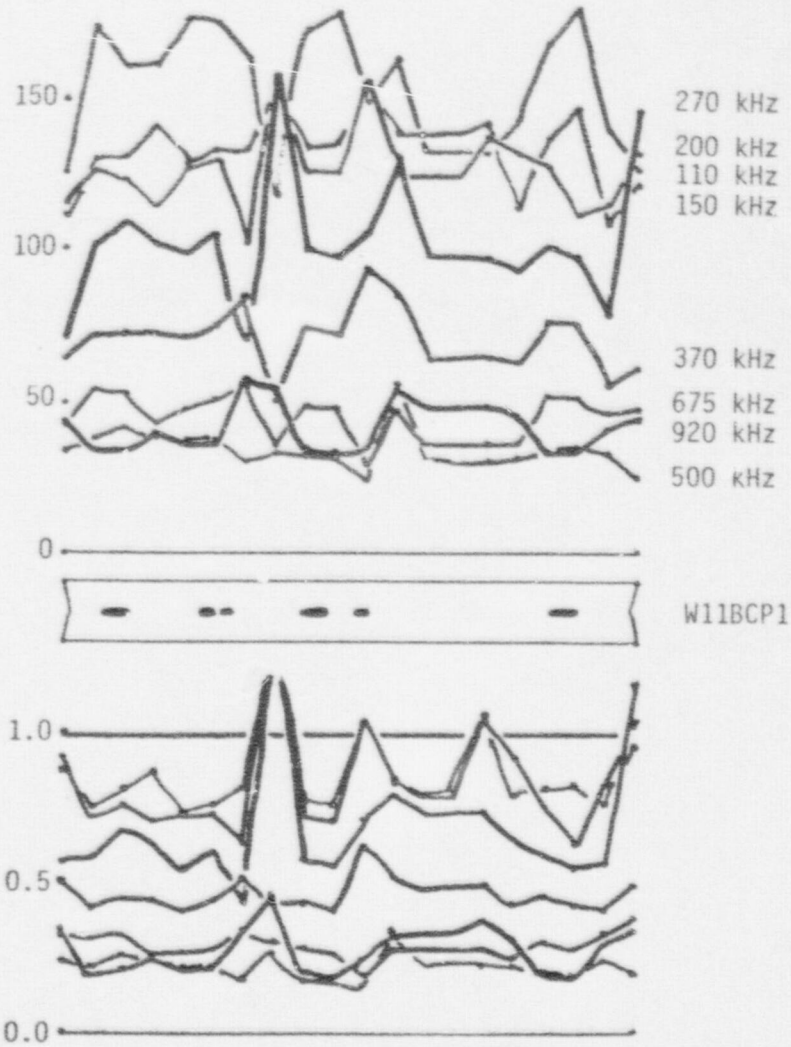

Figure 4-40. DISTRIBUTED AVERAGE FREQUENCY RESPONSES DURING GENERATION OF SLAG INCLUSIONS IN SUBMERGED ARC WELD 11

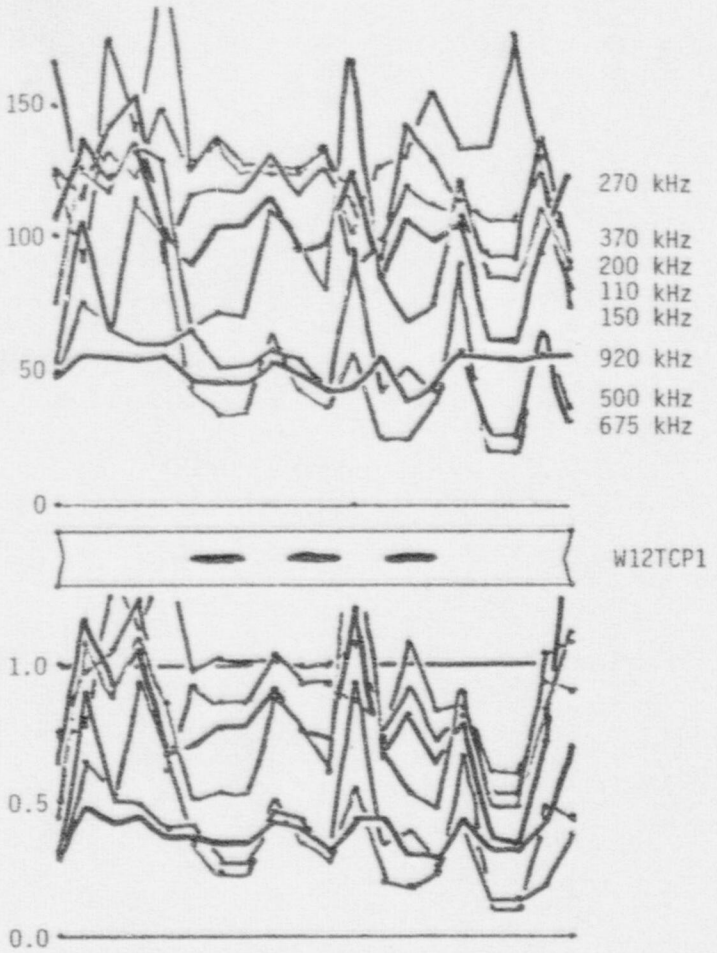

Figure 4-41. DISTRIBUTED AVERAGE FREQUENCY RESPONSES DURING GENERATION OF SLAG INCLUSIONS IN SUBMERGED ARC WELD 12

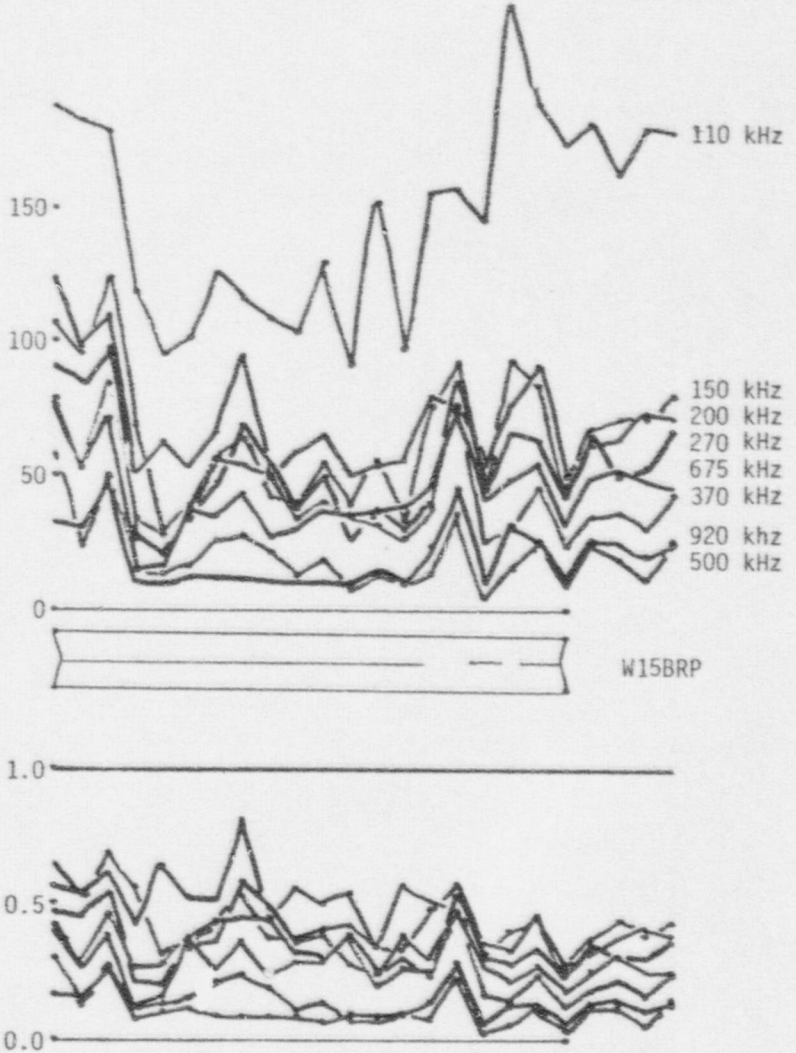

Figure 4-42. DISTRIBUTED AVERAGE FREQUENCY RESPONSES DURING GENERATION OF INTENTIONAL INCOMPLETE PENETRATION IN SUBMERGED ARC WELD 15

welds yields frequency responses that are similar to those accompanying the generation of cracks (Figure 4-40).This is not to be expected if an incomplete penetration in a submerged arc weld is wholly similar to an extreme form of slag inclusion. It suggests that some form of crack propagation may also be present.

The acoustic emission from weld 14 provides an interesting case of acoustic emission flaw detection and characterization. This weld was intended to be flawed with high density porosity generated by lessening the flux load at the flaw site. Radiography confirmed the presence of high density porosity at the intended sites (Figure A1)* and also indicated (1) the presence of incomplete penetration 18" to 24" from the start end and (2) the presence of a slag inclusion left in a repair of a root pass burn-through at 9" from the start. The repair inclusion shows as a light shadow on the radiograph and was missed in the first film reading. However, the acoustic emission preprocessor alarm record (Figure 4-20a) and the ringdown count record and the relative frequency response records (Figure A1) indicated the presence of a very active slag-like flaw. Subsequent ultrasonic inspection pinpointed the flaw's location and sectioning identified it as a slag inclusion (Figure A1). Re-examination of the radiograph yielded the associated indication.

Acoustic activity from the incomplete penetration clouded the record in the near-root passes (Figure 4-20a), but was at an acceptably low level by the time the flaws were generated.

Based on acoustic emission ringdown count activity, alarm records, and relative frequency response records, the porosity in Weld 14 appears to fall into three groups. One group exhibits heavy activity involving changes of relative response for all the frequencies. Flaws at 6" and 24" in the 3rd top cover pass, at 15" in the 7th back cover pass, and at 29" in the 5th back cover pass fall into this group (Figure A4). Another group exhibits moderate activity involving changes in the lower frequencies. The porosity at 21" in the sixth back cover represents this group (Figure A3). The third group exhibits no activity and no significant changes in relative frequency response. The flaw at 18" in the fourth top cover pass falls into this group (Figure A2).

---

* In Appendix

Sectioning of the weld at two flaws of the first, most active group, revealed entrapment of relatively large volumes of glassy-appearing slag in many of the pores. In addition, the slag was cracked. Sectioning at the flaw of the second group showed entrapment of smaller volumes of slag, mostly in granular form and surrounding pores rather than in them. Sectioning the weld at the flaw of the third, least active group, revealed clear porosity with no sign of slag entrapment.

The acoustic behavior of this weld confirms some of our previously held views about sound generation by flaws. Because the creation of porosity is not associated with discontinuous stress relief, no acoustic emission is expected. However, entrapment of flux may be expected to create sound colored to the higher frequencies due to cracks forming in the cooling slag.

Frequencies detected in this analysis were those present when ringdown count levels exceeded the preprocessor threshold. Averaging tabulations which compare activity associated with different levels of ringdown counts (such as shown in Figure 4-43) imply that much of the fluctuations in higher frequencies may be linked to events with low ringdown counts. A search through event-by-event tabulations show that high frequency activity associated with events of low energy invariably preceed flaw-associated acoustic emission. It may be that these events are precursors to the flaw activation and that a future reanalysis of this data base may yield better information about flaw generation by concentrating on these events.

Time Delay

It has been observed from our earliest work on acoustic emission monitoring of welds that the detection of crack-type flaws occurred a variable length of time after the flaw was generated. The data from these "laboratory" welds was searched to compute average delay-to-alarm times for the most reliably detectable flaws. The results obtained suggest that delay time used in conjunction with a flaw location can provide an additional parameter for flaw discrimination.

06 W8BCP5, 65 DB, 2.0"C-21.0" OUT 00756

	COUNT	110	150	200	270	370	500	675	920
NORM. AVG.		1.00	0.57	0.52	0.38	0.38	0.08	0.38	0.19
AVERAGE	00014	101	058	053	039	039	009	039	020
ST. DEV.	00020	038	027	024	023	018	010	021	012

(N = 00658) RDC: 00000 - 00100 TIME: 00000 - 60000

06 W8BCP5, 65 DB, 2.0"C-21.0" OUT 00756

	COUNT	110	150	200	270	370	500	675	920
NORM. AVG.		1.00	0.63	0.57	0.42	0.26	0.09	0.22	0.13
AVERAGE	00275	197	125	113	084	052	018	045	027
ST. DEV.	00196	047	051	053	041	026	019	034	022

(N = 00096) RDC: 00100 - 01000 TIME: 00000 - 60000

Figure 4-43. LUMPED AVERAGE TABULATION FOR SUBMERGED ARC WELD 8 BACK COVER PASS 5 IN WHICH A CONFIRMED CRACK WAS GENERATED. ILLUSTRATES HOW SPECTRAL ACTIVITY APPEARS TO SHIFT TO HIGHER FREQUENCIES (675 & 920 KHz) AMONG LOWER ENERGY ACOUSTIC EMISSION EVENTS

Cracks generated in ½" A106 piping-type welds were found to have detection delay times from 5 to 20 seconds whereas detection of incomplete penetration in these welds occurred within 0 to 10 seconds of flaw initiation. The principal ambiguity in this result is that whereas a crack is a well-defined, localized flaw, the acoustic site of an extended flaw like incomplete penetration is hard to pinpoint. The delay time given above for incomplete penetration is based largely on the time elapsed between noticable differences observed in the radiograph and the onset of alarm.

Cracks generated in 2" A533B vessel-type welds were found to have detection delay times from 10 to 30 seconds with two groups of data clustering about 12 and 25 seconds. The larger delay times were observed in two welds in which one side of the weld was partially filled before beginning to fill up the opposite side. This apparently caused a reduction in cooling stress. Delay times for detection of slag inclusions and incomplete penetration in these welds was found to be 0 seconds. In fact, detection of inclusions would often precede the site of the flaw by up to 5 seconds, presumably caused by the flux or slag melting and being drawn back into the molten pool under the weld head.

Alarm Duration

Observation of flaw activity as detected by the preprocessor and the acoustic emission locator indicated that the length of time the defect indication was set could also be used to discriminate among those flaw types being considered. Tabulated data from the "laboratory" welds was organized by the computer to provide accurate times during which the alarm flag was set in association with a flaw. The results indicate that duration of detection activity can also be used to discriminate flaw type.

In the piping-type welds, crack detection lasted for an average of 0.6 seconds compared to an average of 0.7 to 4.4 seconds for the detection duration of incomplete penetration. This implies that smaller incomplete penetrations may not be resolvable from cracks on this basis, but larger incomplete pene-

FLAW TYPE	ACOUSTIC EMISSION PARAMETER			
	Time between Flaw Induction and Detection	Potential Frequency Utilization	Duration of Detection Activity	Average Ringdown Count
CRACK				
Piping Weld	5 - 20 sec.	all	0.6 sec.	154 ± 39
Vessel Weld	10 - 30 sec.	all	1.3 sec.	113 ± 30
INCOMPLETE PENETRATION				
Piping Weld	0 - 10 sec.	low	0.7 - 4.4 sec.	79 ± 45
Vessel Weld	0 sec.	all	0.8 sec.	259 ± 4
SLAG INCLUSION				
Vessel Weld	0 sec.	all	2.5 sec.	205 ± 57
CONTROL				
Piping Weld	--	--	--	38 ± 8
Vessel Weld	--	--	--	18 ± 13

Table 4-10 CANDIDATE PARAMETERS FOR FLAW DISCRIMINATION

trations are. In vessel-type welds, crack detection lasted for an average of 1.3 seconds, slag inclusions lasted 2.5 seconds, and incomplete penetrations lasted 0.8 seconds. Although the variability of these times is great, there is a difference in the central tendency from flaw type to flaw type that can be used as a starting point for searching for factors that can reduce the variability. Thus, in the examination of these parameters, it appears that more than one factor can be used to characterize flaw type. More refined analysis of this and more data will be needed to reduce variations and tighten up the correspondence. The results of these discussions are summarized in Table 4-10.

4.5 Previous Laboratory Testing

The laboratory tests that were run prior to the latest series of tests served primarily as calibration tests. The on-line computer analysis system was not available and the magnetic tape recorder had a maximum upper frequency cut off of about 400 KHz. Hence the detailed information available in the current welds was not present in this series of welds. The piping series of welds consisted of twenty test welds in two sizes each of carbon and stainless steel nuclear grade piping. The data from one series (large diameter stainless) was not usable due to extremely high level slag cracking noise due to tightly clinging flux. The usable data covered fifteen welds and included the GMAW, GTAW, and SAW methods. A total of ten cracks were planned and 9 were actually generated. Eight of these were detected radiographically and one required metallographic sectioning for confirmation. All nine were detected by AE. In addition, five porosity flaws were generated by providing insufficient shield gas in the GMAW and GTAW welds. None of these flaws were AE detected.

One area of incomplete or lack of fusion was closely associated with a crack network and hence, was not AE separable. One area of excessive penetration was indicated by radiography and was not AE detected. These results are summarized in Table 4-11.

TABLE 4-11

PIPING CALIBRATION TEST SUMMARY

Weld	Material	Weld Method	Intended Flaws	Confirmation	AE Detection
1	6" A106	GTA/GMA	None	Radiography - No Flaws	None
2	6" A106	GTA/GMA	None	Radiography - No Flaws	None
3	6" A106	GTA/GMA	1 Crack	Radiography - 1 Crack	1 Crack
4	6" A106	GTA/GMA	1 Crack 2 Porosity	Radiography - 1 Crack 2 Porosity	1 Crack
5	6" A106	GTA/GMA	2 Porosity	Radiography - 2 Porosity	None
6	6" 304	GTA/GMA	None	Radiography - No Flaws	None
7	6" 304	GTA/GMA	None	Radiography - No Flaws	None
8	6" 304	GTA/GMA	1 Crack	Metalography - 1 Crack Radiography - No Flaws	1 Crack
9	6" 304	GTA/GMA	1 Crack	Metalography - No Flaws Radiography - No Flaws	None
10	6" 304	GTA/GMA	1 Crack 1 Porosity	Radiography - 1 Crack - 1 Porosity	1 Crack
11	14" A106	GTA/SA	3 Cracks	Radiography - 3 Cracks	3 Cracks
12	14" A106	GTA/SA	1 Crack	Radiography - 1 Crack	1 Crack
13	14" A106	GTA/SA	1 Crack	Radiography - 1 Crack - Incl. Fusion	1 Crack
14	14" A106	GTA/SA	None	Radiography - No Flaws	None
15	14" A106	GTA/SA	None	Radiography - 1 Excessive Pen.	None

The pressure vessel calibration test consisted of two multipass submerged arc welds in six inch thick pressure vessel steel. One was fabricated in A508 forging steel and one in A533 plate. Standard pressure vessel welding procedure was followed which included preheat and maintenance of interpass temperature between 300^{o}F and 500^{o}F. Two channel AE source location was utilized with these welds along with high temperature transducers and couplant. Flaws included both slag inclusions and cracks. A total of six intended flaws were placed in each specimen. The first specimen's intended flaws were two slag inclusions, two undercuts, one void, and a plate with an ELOX slot to simulate a crack. The specimen was intended to be an ultrasonic test block. AE detected all of the intended flaws plus several other areas. Radiography and ultrasonics confirmed all of the AE indications and the radiographic data indicated slag inclusions associated with all of the indicated flaw areas. The second specimen contained six planned flaws, four cracks and two slag inclusions. All six were easily detected by AE and later confirmed by ultrasonic testing.

Section V

SHOP CONFIRMATION OF IN-PROCESS AE WELD MONITORING

5.1 Introduction

This series of experiments includes six tests in both nuclear pipe fabrication facilities and nuclear pressure vessel shops. Four of the six tests were run using the GARD laboratory test system, two in pipe fabrication shops and two in pressure vessel shops. The remaining two tests utilized the production AE monitors in a pipe shop and a pressure vessel shop respectively.

The primary purpose of these experiments is to gain experience and gather data under actual nuclear production conditions that confirm the practicality of using in process AE monitoring as a production NDE method in the fabrication of nuclear component welds. The piping and pressure vessel phases of this work were conducted in two steps for both cases. First, the laboratory monitor system was utilized under GARD personnel supervision in nuclear fabrication shops on actual production pieces. These tests confirmed the validity of the sensitivity and signal processing parameters arrived at in the calibration tests and allowed necessary refinements to be made on the production monitors prior to their placement in the shops for long term evaluation.

The AE data gathered in these tests was compared to production ASME code NDE results, which is essentially radiography, and the results of this comparison provided confirmation of the methods ability to detect typical production flaws under real shop conditions.

Original plans were that the production monitor would be subjected to long term evaluation in piping and pressure vessel shops with actual production personnel operating the equipment. This approach proved unsatisfactory because production priority pressures on the personnel involved prevented sufficient utilization of the equipment to provide a satisfactory data gathering rate. Thus, a compromise approach was decided on in which GARD personnel would conduct the tests.

Due to the increased costs of this approach the duration of the tests was reduced somewhat, however, even under the reduced duration a sufficiently large body of data was gathered to indicate positively that in-process acoustic emission monitoring is a practical and effective NDE method for both nuclear pipe fabrication welding and nuclear pressure vessel welding. This AE data is again, as in the first series of tests correlated with production ASME code radiography.

The shop test, in addition to providing a comparison of in-process AE Weld monitoring to conventional NDE techniques(primarily radiography) also has shown that:

1. The AE equipment can perform reliably under typical shop environmental conditions.
2. In-process AE weld monitoring does not in any way hinder or impede normal production flow.

5.2 Equipment

Three AE monitoring systems were used in this series of tests. The first two, the GARD laboratory monitor and the production piping monitor have been described in previous NRC reports.[1] The production pressure vessel monitor was evaluated at Westinghouse-Tampa on production nuclear steam generator welds during this report period. A photograph of the system is shown in Figure F-1. The system utilizes signal processing and alarm circuitry identical to that used in the previously discussed monitors. The pressure vessel monitor utilizes a two channel time of arrival measurement system to allow for location of AE sources judged by the alarm circuitry to be flaws. The location, data handling and storage, and display and hard copy printout functions are all controlled by an internal custom microprocessor computer which utilizes the latest LSI microprocessor technology. This design approach was chosen not only for its greater reliability in data handling, storage, and retrieval, but also

1. "Inspection of Nuclear Reactor Welding by Acoustic Emission" D. Prine et al, NUREG 0035-1, Feb. 1976; NUREG 0035-2, Sept. 1976, NUREG 0035-3, June 1977.

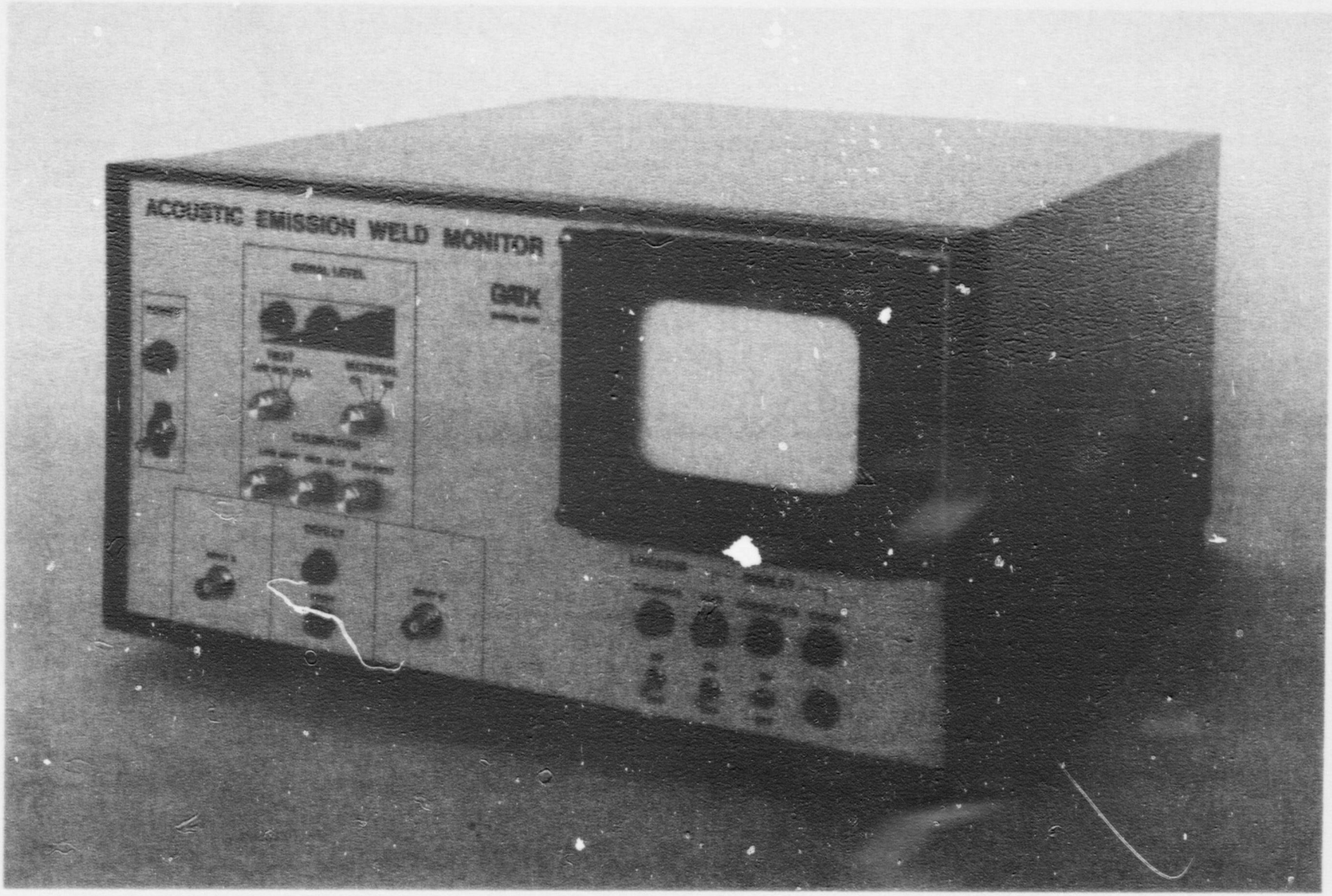

Figure 5-1 Acoustic Emission Weld Monitor

for the tremendous flexibility inherent in a programmable computer controlled system. The type and manner of display and readout is dependent on the computer program which is stored in solid state erasable read only memory. A photograph of the memory chip is shown in Figure 5-2. The computer's program is permanently stored in this single IC chip and if a radical change in system operation is desired, the previous program stored in the chip can be erased with a UV light source and a new modified program stored in its place. Program software development and testing is accomplished on the GARD microprocessor programming development facility.

Currently, the system program in the monitor provides the following features.

1. Real time display and storage of AE alarm locations on a built-in CRT display.
2. Manual dump of location data to X-Y recorder.
3. Automatic operation in which weld current and alarms vs time is plotted on a strip chart recorder along with automatic plotting of location data on the same chart.
4. Automatic calibration of locator.

In addition to these software controlled functions, a fail safe power supply keeps the computer operational in case of momentary loss of power from power lines. Function 3 allows the monitor to run essentially unattended. The weld current is monitored by means of a magnetic pickup attached to one of the welding cables. A plot of weld current vs time gives a record of weld passes. If during a pass an AE alarm occurs, this data is stored in computer memory and at a pre-set time after weld current stoppage the strip chart is automatically shifted to a higher speed and a plot of AE alarm locations for that pass is produced. Upon completion of the plot the speed of the strip chart is reset to a low setting to conserve paper and the locator memory is cleared. An example of a typical record is shown in Figure 5-3. The track labled I is the weld current vs time plot, II is the locator read out track and III is AE alarm. A good pass is shown

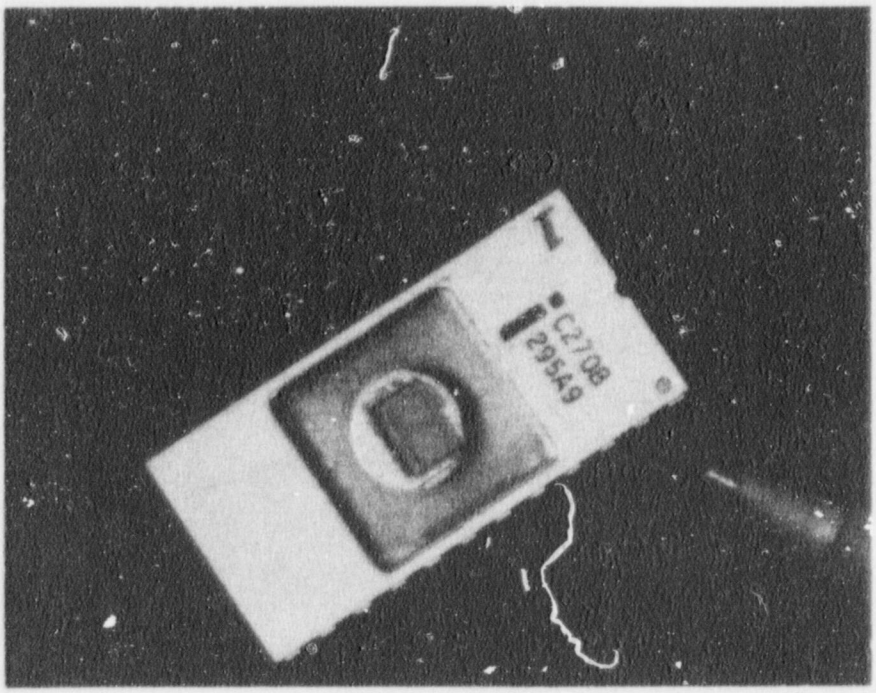

Figure 5-2 U-V Erasable Programmable Read Only Memory

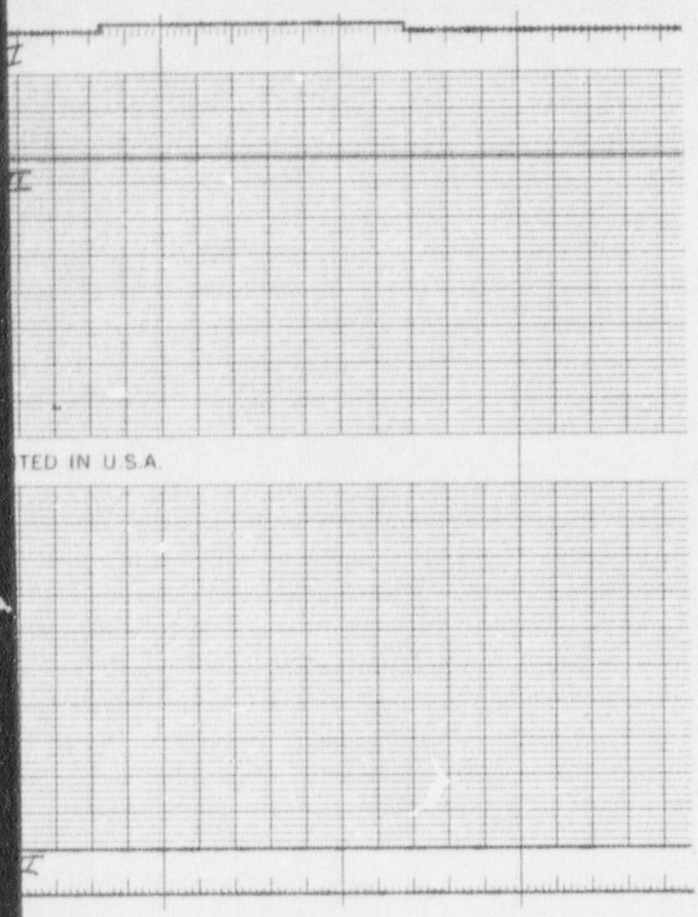

Weld Current

Location

Alarm

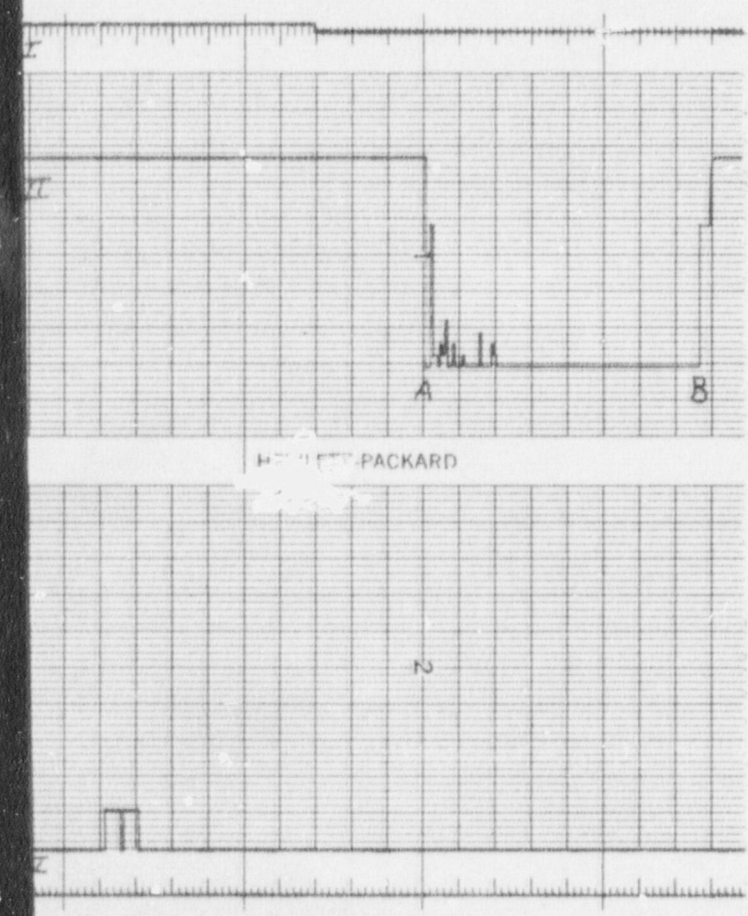

Figure 5-3
Locator Printout showing
Typical Good Weld above
and Flawed Weld below

in the top Figure. The lower Figure shows a pass with AE alarms as indicated on the III track. After a preset delay to allow any delayed AE activity to be recorded a plot is shown of the location of the AE alarms. The left end of the plot represents one end of the weld and the right end, the other. Location of alarms is shown ranging from A to about A +25%. The height of the location indication is proportional to the number of alarms at that location.

The automatic calibrate feature is another important function that is controlled by the microprocessor. The locator measures the difference in arrival time for an AE burst arriving at two transducers attached at opposite ends of the weld. The time difference is translated into a number corresponding to one of 128 location memory cells by counting a clock signal with an electronic up-down counter. For any given transducer spacing there is one uniquely correct clock frequency that will give correct location data. In most commonly used locator equipment the clock is manually adjusted by a trial and error process consisting of rapping or tapping on the structure under test at predetermined locations and adjusting the clock until correct locations are indicated by the locator. The automatic calibrate function turns one of the two transducers into a transmitter and sends pulses to the other channel. The computer measures elapsed time and sets the clock automatically to produce correct location results.

A front panel light goes on when the switch is set to calibrate then the light goes off when the calibration is complete. If for any reason the computer is unable to achieve a satisfactory calibration the calibration light flashes periodically. The automatic calibrate mode is particularly useful when monitoring pre-heated welds such as are common to most nuclear pressure vessel welds. The automatic mode eliminates the need for a technician to walk around on the hot vessel to calibrate the system. The calibration mode also checks for proper transducer-couplant and cable operation in both channels.

5.3 Shop Evaluation of Production Pressure Vessel Monitor

A total of three longitudinal welds in nuclear steam generator shells were monitored at Westinghouse, Tampa, Fla. All of the welds were in A533 pressure vessel steel utilizing the submerged arc process. Length of weld in all cases is 9.5 feet. Two of the shells were 4 inches thick and the third was 3 inches thick. The four inch thick welds took 65 and 59 passes respectively to complete while the three inch thickness took 42 passes to complete. Interpass temperature was maintained at approximately 400°F throughout welding by means of gas heaters. Figure 5.4 shows an overall view of the welding set-up. A completed shell is seen in the foreground. The welds are fabricated with a backing bar tacked to the back of the weld root. The major portion of the weld is completed by welding from the OD of the cylinder. After completion of the OD portion, the backing bar is removed and the back six passes of the weld are ground out to sound weld metal. Following this operation, the weld is completed by welding from the ID. Thus, the bottom passes and the cap or crown passes of the weld are removed prior to final inspection.

In an effort to maximize, within a given time period, the amount of welding AE monitored, monitoring was restricted to the OD weld. The production pressure vessel monitor was used in the automatic recording mode as discussed previously in Section 5.2. A photograph of the monitor and the strip chart recorder in position on the welding scaffold is shown in Figure 5.5.

The first weld monitored had only three significant acoustic emission indications. All three indications occurred at the same extreme end of the weld. They were associated with visually confirmed slag entrapments in the run off pad at that end. Radiography on this weld showed it to be free of flaws. The acoustic emission records for these three indications in passes 35, 59, and 66 are shown in Figures 5-6, 5-7, 5-8, respectively. In Figure 5-6 the AE record is shown for pass 35 of weld number one. The top track is a plot of weld current vs time. The chart speed during welding is 25mm/min. so each major division is one minute of welding. The weld was 9 feet 6 inches

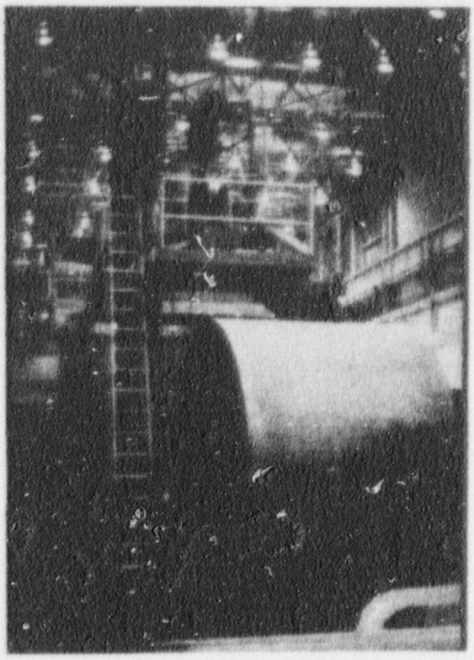

Figure 5-4
Overall View of Nuclear
Steam Generator Shell
Fabrication Facility

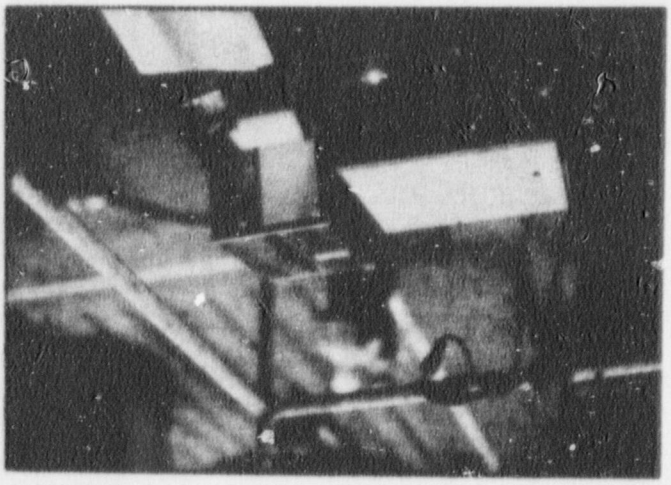

Figure 5-5
AE Weld Monitor in Place
in Nuclear Steam Generator
Fabrication Facility

Figure 5-6 AE Record for Weld 1 Pass 35

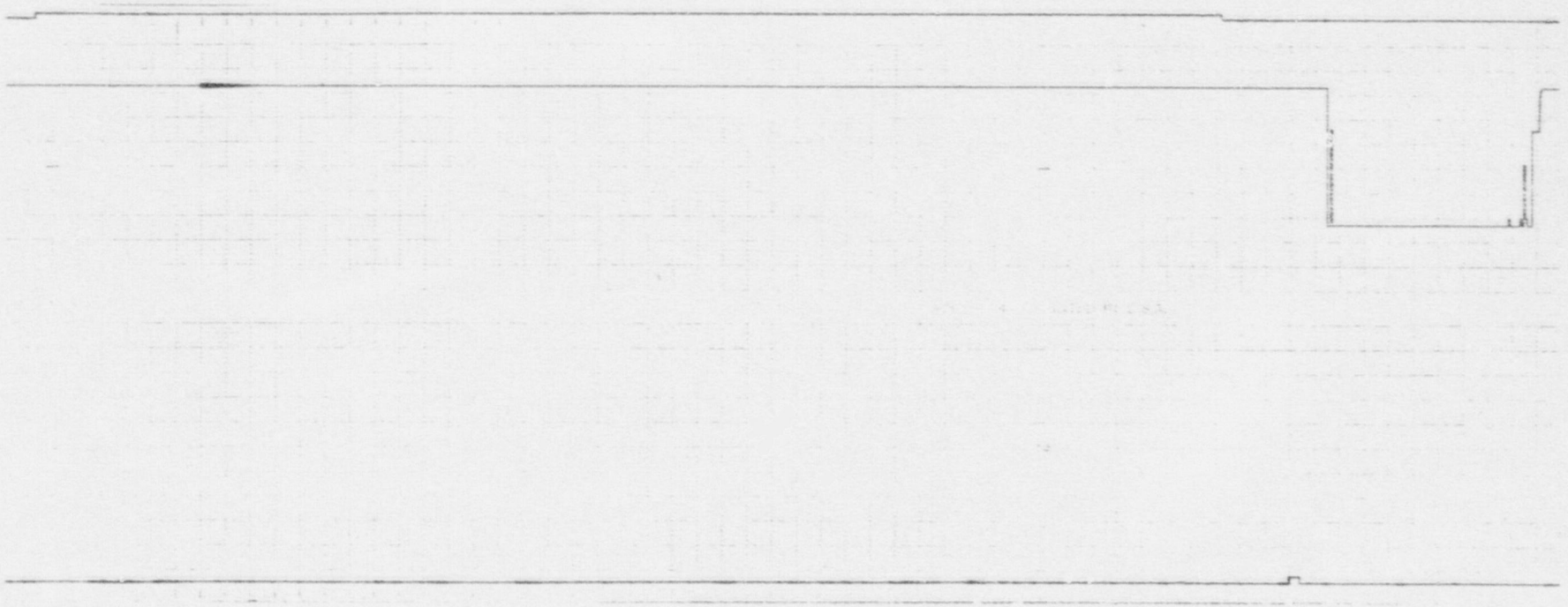

Figure 5-7 AE Record for Weld 1 Pass 59

Figure 5-8 AE Record for Weld 1 Pass 66

long not counting the runoff pads and the welding speed was approximately 12 inches per minute. Approximately thirty seconds after welding is complete two AE alarms occur and can be seen on the bottom track of the chart. The second track on the chart shows an AE location plot of the signals that produced the alarms. The plot starts approximately 45 seconds afterwelding is completed. Chart speed is increased to 25 mm per second. The 3/4 scale spike at the extreme left end of the plot indicates the end of the weld arbitrarily lapled "A". This 3/4 scale step at the right end indicates the "B" end of the weld. The height of the location indication is proportional to the number of AE events located at that position. The AE indications all seem to be very near the "B" end of the weld. (Transducers are actually 6 inches away from the weld). The small indications correspond to one event while the large one is approximately 8 events. Because of the history of very low frequency of code-rejectable flaws in this type of welding we ran the sensitivity of the monitor at a somewhat higher than normal level in an attempt to pick up any possible AE activity that would demonstrate the system's capabilities.

AE events that produced multiple or tightly bunched locations and or that reactivated within two succeeding passes in the same location were judged significant. This indication is one of three such indications for this weld. The delay time for the alarm, the location indications and visual inspection of the runoff pad at the "B" end of the weld tend to indicate that the detected activity was probably due to slag entrapment in the runoff pad. Two additional indications of this type occurred and are shown in Figures 5-7 and 5-8. The multiple indication at approximately "A" plus 25% in Figure 5-8 is a location artifact that troubled us during this test. Subsequent modifications have removed this problem.

The second weld monitored had three AE indications that were judged significant. All of these indications were correlated with visually confirmed weld discontinuities. All indications were in the lower passes of the weld which are removed by grinding prior to completion and inspection and so will not be available for radiographic confirmation. Two of the

three indications were visible slag inclusions and in one case the backup bar broke loose from the weld during the root pass and the AE monitor alarmed and located at the position where the break occurred. Radiography has not been completed on this weld as of the date of this writing. Figure 5-9 shows the AE record for the root pass of this weld. The two adjacent AE locations and the AE alarm are caused by the backup bar breaking loose during the welding. The bar broke loose approximately one foot ahead of the weld head near the "B" end of the weld. The alarms shown during the location plot period are from clean-up and are ignored by the plotter since they occur after the preset delay period.

Figure 5-10 shows the AE record for pass number two of the second weld. Several alarms are seen during welding. Alignment problem caused the weld to climb up on one wall of the bevel and the resulting under cut on the opposite wall trapped some slag. The locator properly located the visually confirmed slag with a multiple locations. The scattered single locations are associated with the alarms after weld stoppage and were the result of an overly anxious welder applying the chipping hammer prior to the end of the prescribed waiting period. Normally, this type of activity will not activate the monitor, however, in this case light taps with the hammer instead of the normal solid whacks fooled the monitors noise rejection circuits.

Figure 5-11 shows the AE record for pass 4 of this same weld (weld #2). The single alarm and the tightly bunched single level location indications were caused by another visually confirmed slag entrapment.

The third weld monitored was free of significant AE indications. Radiography is not yet completed on this weld.

In summary, this test provided confirmation of the practicality of using in-process AE monitoring to provide on line NDE of nuclear welds. A total of six indications were obtained which correlated 100% with visual discontinuities. None of these discontinuities constitute a code required repair due to their location in the weld, however, if they had been located

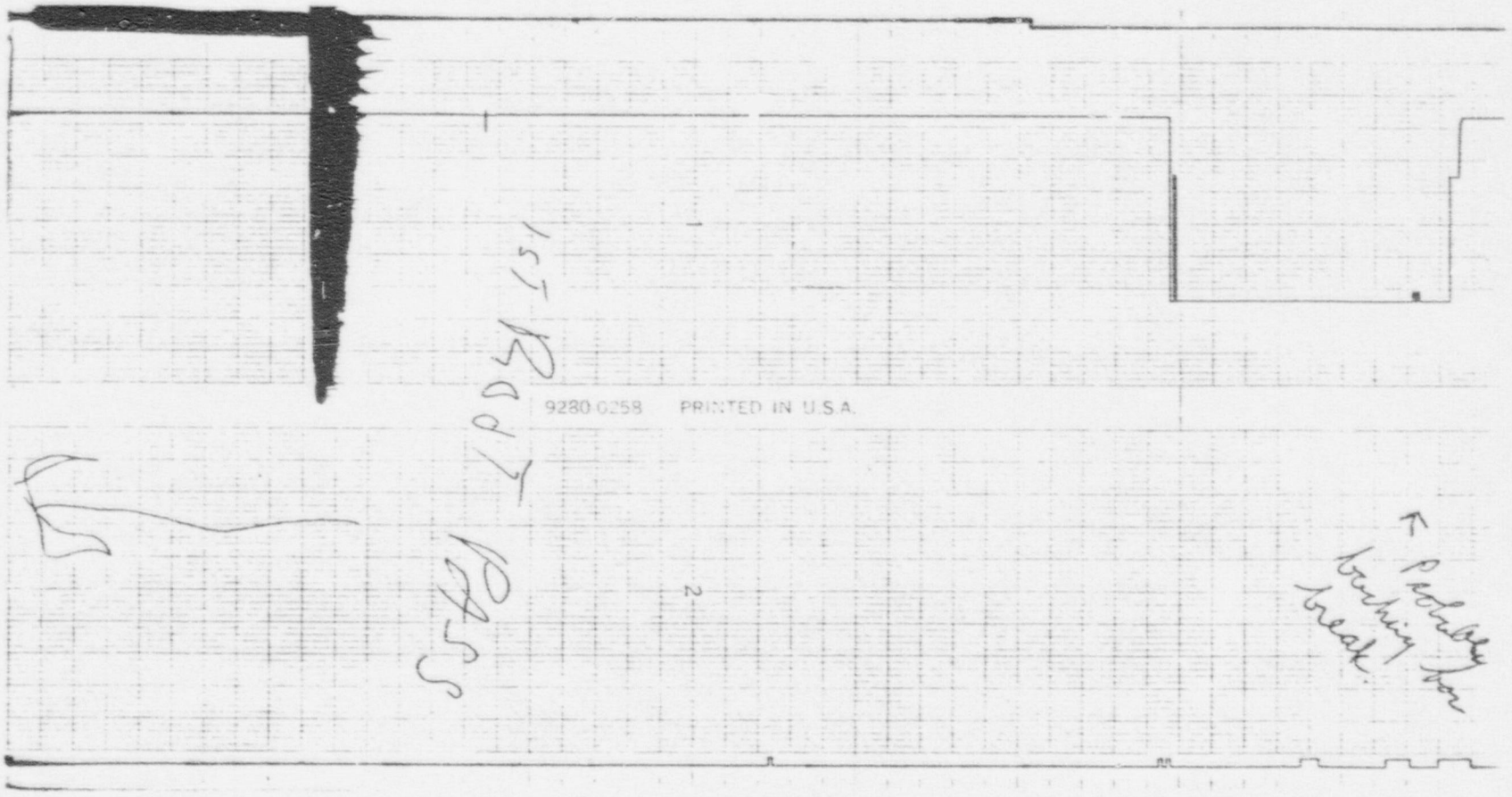

Figure 5-9 AE Record of Root Pass Weld 2

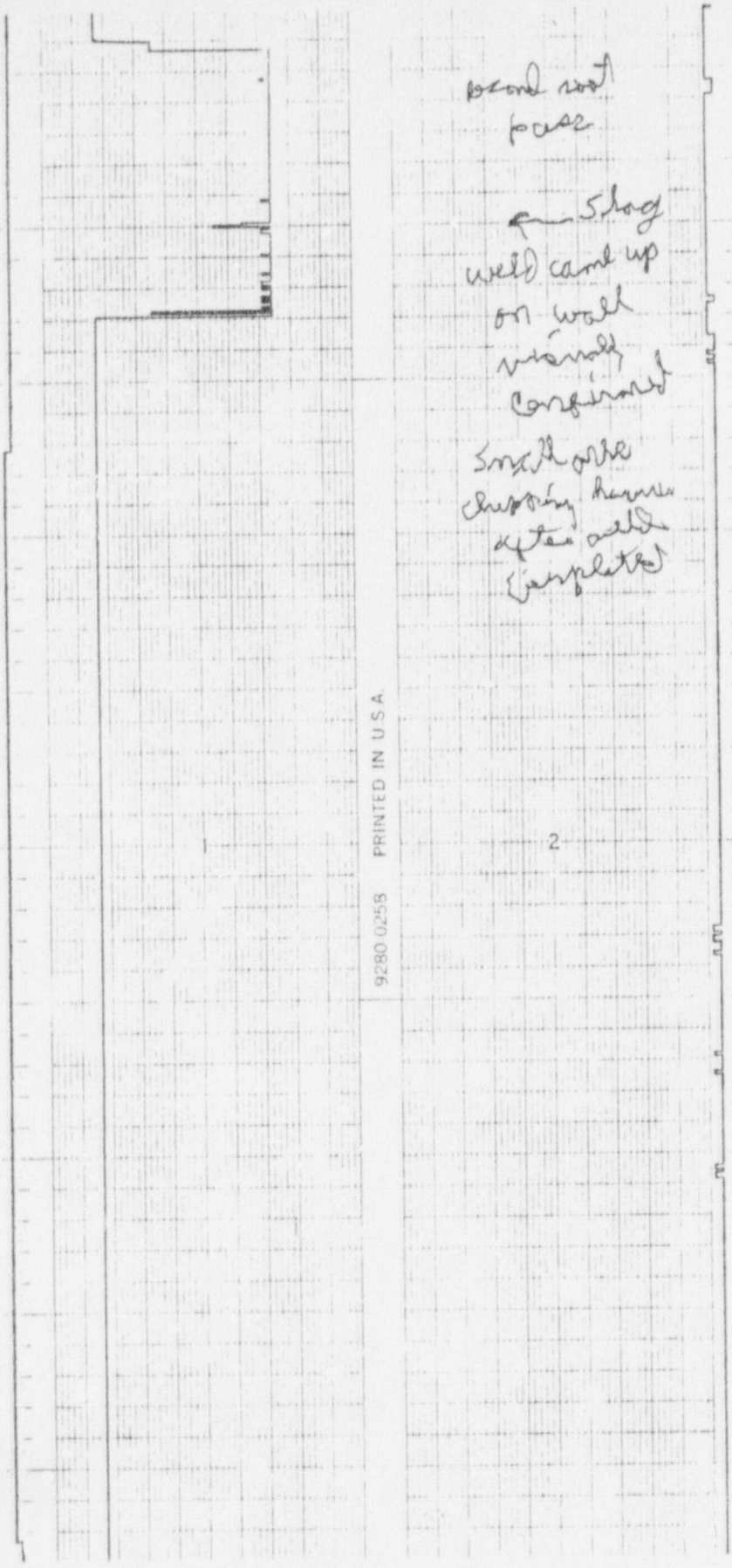

Figure 5-10 AE Record for Pass 2 Weld 2

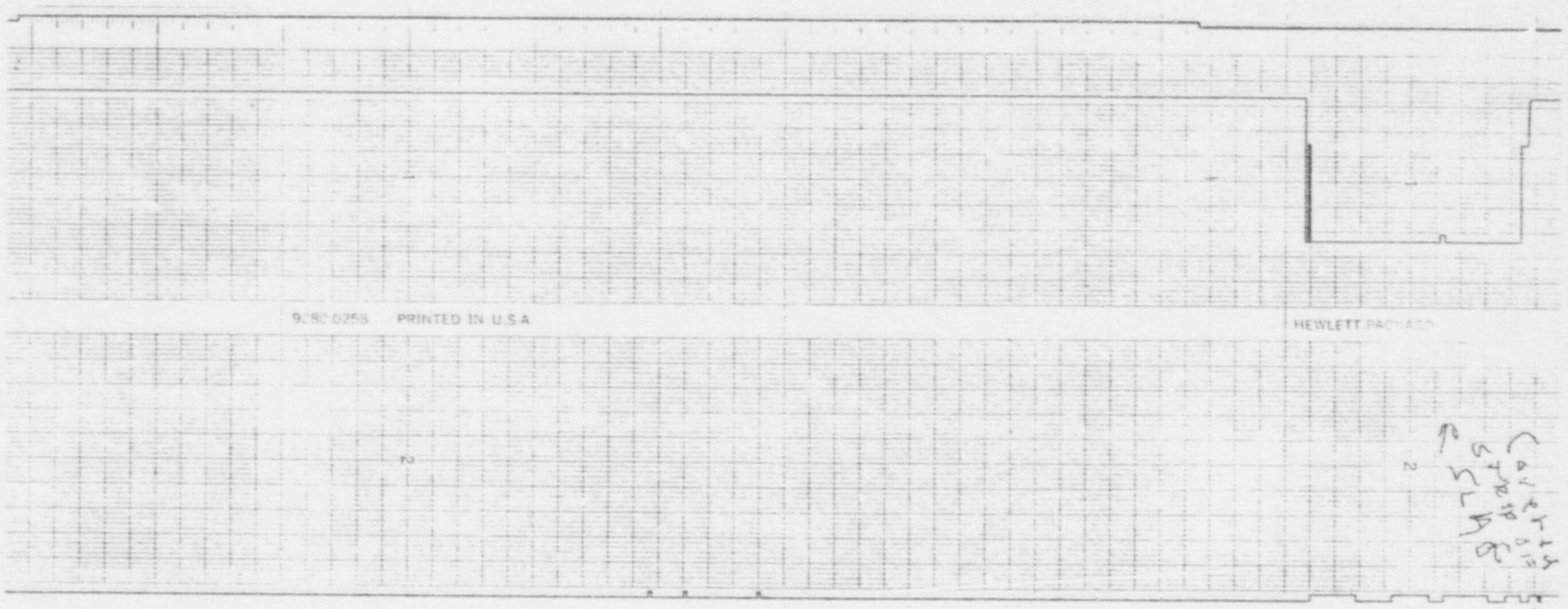

Figure 5-11 AE Record for Weld 2 Pass 4

Figure 5-12 SHOWING AE STRIP CHART RECORD FOR B&W NOZZLE WELD CHART SPEED, 1 MM/SEC.

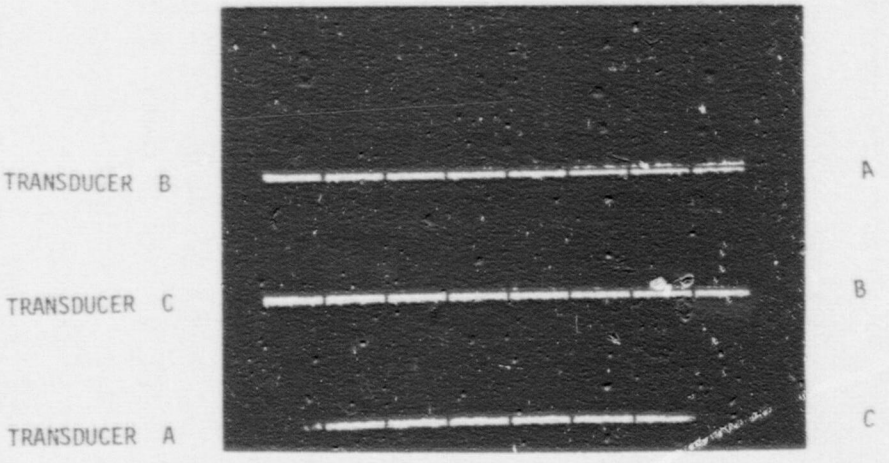

Figure 5-13 SHOWING LOCATION OF AE INDICATION SHOWN IN FIGURE 5-12

in the main body of the weld in-process AE would have allowed the repair to be made at a time when delay and expense would have been greatly reduced as compared to normal procedures.

The AE monitor, the first of its type to incorporate a microprocessor performed very well under typical production conditions which included high temperature and humidity. In-process AE monitoring in no way interferred with normal production procedures. The automatic hard copy feature provided by the microcomputer allowed welding which proceeded on a 24 hour a day basis to be monitored 100% without a full time technician present.

5.4 Pressure Vessel Shop Tests with Laboratory AE Monitor

Prior to the experiment discussed in Section 5.3 that was conducted with the "production" pressure vessel monitor a series of two experiments in two different unclear pressure vessel fabrication facilities was conducted using the GARD laboratory system. The primary purpose of these experiments was to provide additional confirmation on equipment sensitivity and signal processing parameters which were arrived at as a result of the pressure vessel lab tests discussed in Nu Reg. 0035-2, In addition, these experiments would provide data on background noise and other problems which might be inherent in a real nuclear pressure vessel fabrication production environment.

A further purpose of these experiments was to provide a demonstration of in-process acoustic emission weld monitoring to nuclear production personnel which would not only show the practicality of AE weld monitoring but also show that the method could be utilized without undue interference to the normal production process.

These experiments fulfilled all of the above mentioned requirements and are reported in detail in previously published data (NUREG 0035-2). For purposes of continuity and completeness they will be presented in summary form in this document.

The first was run at Babcock and Wilcox's Mount Vernon, Indiana Nuclear facility. The outside weld on a reactor vessel inlet nozzle was monitored

using a three channel version of the GARD laboratory AE monitor to provide AE location data around the circumference of the weld. The weld consisted of 100 complete circumferential passes plus two shortened portions of 83 passes each to fill in the saddle shape of the weld. Only one AE indication was obtained from this weld. A portion of the AE strip chart record and location display photograph is shown in Figure 5-12 and 5-13. The AE ring-down count activity is seen in the lower track on the chart recording and the resulting alarms on the upper track. The location record is divided into three segments representing the three 120° segments of weld between each of the three AE transducers. The single location pip approximately 1/3 of the way from transducer A to transducer C matched the location of a visually confirmed slag inclusion.

The slag was entrapped in one of the final cap passes of the weld as the result of a "roll over" of the weld bead. This portion of the weld is removed by final machining prior to radiography and so would not constitute a code-rejectable flaw.

Due to production delays, radiography has not been performed on this weld as of yet.

The second test of this type was performed at Westinghouse, Tampa Florida. The weld was a Bead Temper Repair weld of a cavity in test vessel V7B done in the vertical position. The V7B vessel is a special test vessel with 6" thick walls made of A533B pressure vessel steel and the repair weld was performed as part of the ORNL/NRC HSST program. The welding method used was manual stick electrode. The weld was extremely quiet acoustically. A few scattered AE indications were found during welding. One such area in the 56th layer of the weld was particularly active and subsequent grinding exposed small scattered porosity in the area indicated by AE.

The post weld heat treat and cool down was also AE monitored and was found to be acoustically inactive. Radiography and UT performed on the vessel detected some scattered porosity in two areas and in both cases the

indications were judged to be code-acceptable. Some AE activity was present in these areas, however, it was not as severe as that obtained for layer 56. In addition to the code-acceptable indications found by RT and UT an area of visual porosity was detected and repaired during the grinding away of the backing bar. Again some AE activity was detected in this area, however, it too was not as severe as the previously mentioned area in layer 56.

An example of the AE indications associated with the typical small scattered porosity encountered in layer 56 is shown in Figure 5-14. The figure shows three tracks per chart containing respectively, ring down counts, weld current, and AE alarms. The ringdown counts represent unprocessed AE signals. The weld current was monitored by using an induction pick-up wrapped around the weld cable. The reason for monitoring weld current is that occasionally clean-up procedures would produce an AE alarm. To eliminate these false alarms from consideration we decided from empirical observations that any event occurring more than 5 seconds after end of welding was not due to flaws generated in that weld. This is valid because of the very rapid cool down of the very low heat input weld. The high ringdown count signals after the end of welding are caused by clean up. The false alarms due to clean up were generally produced by very light wire brushing on the weld surface.

In the two examples shown in Figure 5-14, chart speed is 25 mm per min, or 12 seconds per major horizontal division. The recording on the left is typical of most of the weld while the one on the right shows unusual ring down count activity near the middle of the pass and two alarms associated with it. This activity was caused by small porosity being generated in the weld. Figure 5-15 shows some of this porosity which was exposed by grinding and has been circled by a marker to show location in the photograph.

None of the AE indications in this weld were judged to be severe enough to be a code-rejectable repair. In general, this agreed with NDE findings on this weld. The one exception was the "visual" porosity uncovered by the grinding away of the back-up bar. The scattered AE indications found in this

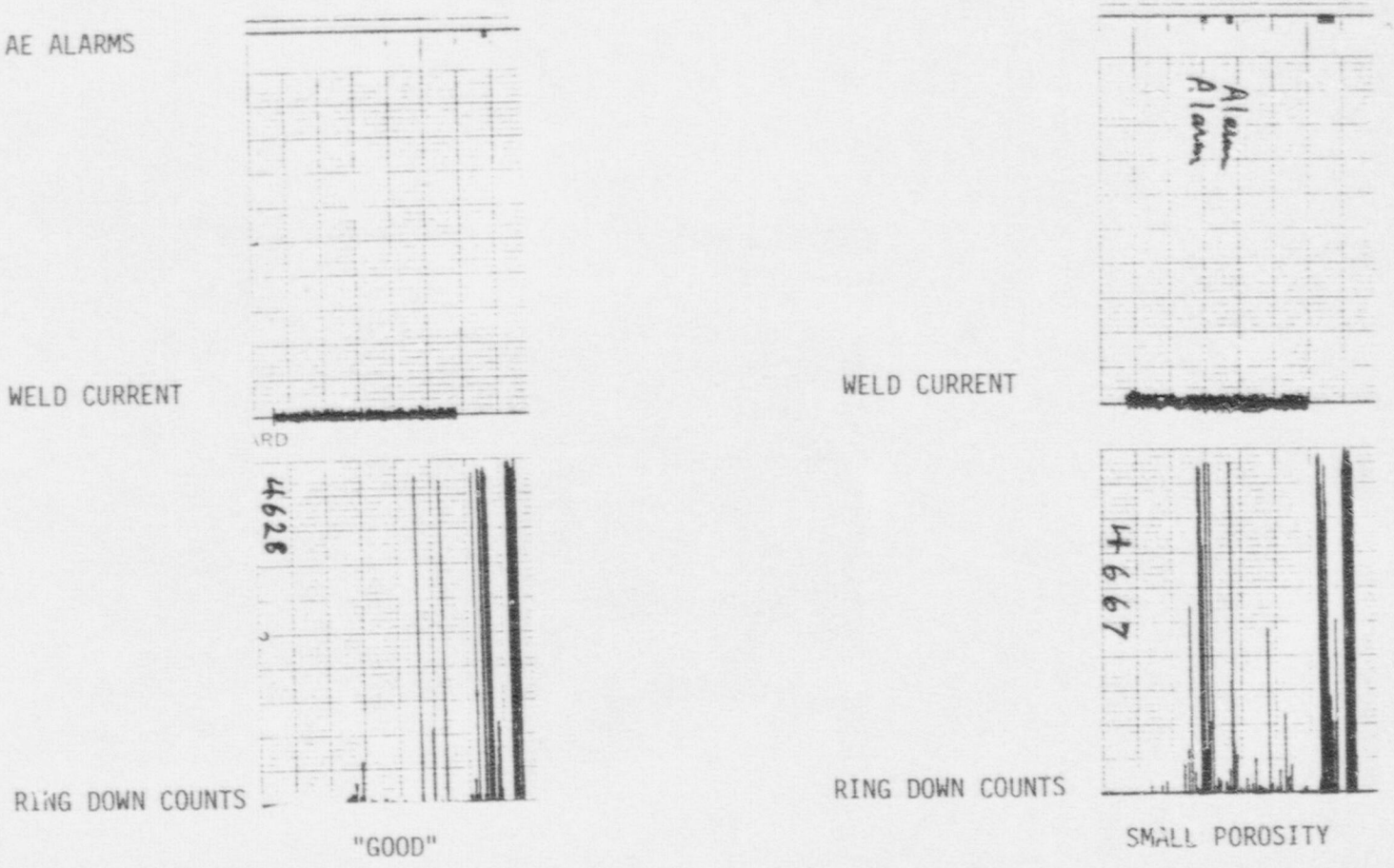

Figure 5-14 SHOWING AE STRIP CHART RECORDS FOR TWO STICK PASSES ON V7 REPAIR. CHART SPEED 25 MM/MIN.

Figure 5-15

SHOWING SMALL SCATTERED POROSITY IN V7 REPAIR WELD WHICH WAS DETECTED BY ACOUSTIC EMISSION. THE PORES EXPOSED BY GRINDING ARE ENCIRCLED TO ENHANCE VISIBILITY.

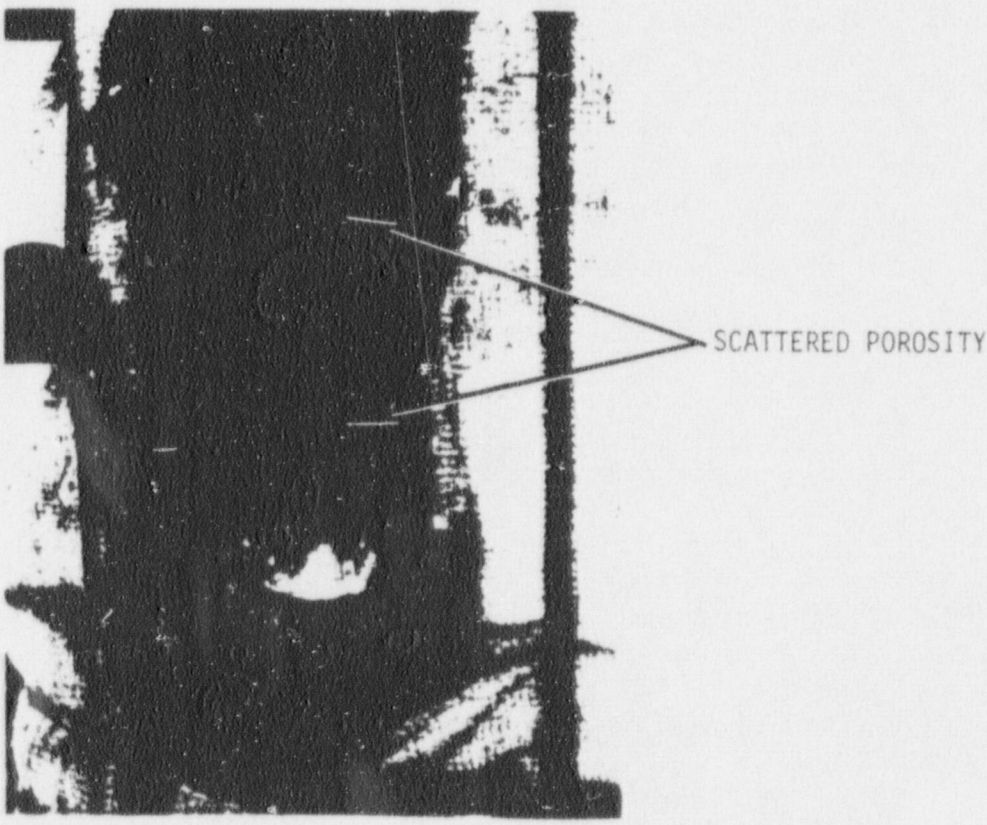

area were not nearly as severe at the layer 56 indications discussed above. Subsequent laboratory testing has shown that AE is not a good detector of porosity and in general AE only detects porosity when slag is associated with it.

5.5 Pipe Shop AE Monitoring Tests

A series of three tests of this type were conducted in this program. The first two were performed at Southwest Fabricating and Welding, Houston, Texas, and ITT Grinnel, Kernersville, North Carolina and utilized the GARD laboratory monitor. Both tests were reported in detail in NUREG 0035-1. The first series of welds consisted of 18 welds in both stainless steel and carbon steel piping. A total of seven AE indications were obtained in this batch of welds which totaled approximately 400 feet of weld passes. Six of the indications were cracks in repair welds on a stainless steel specimen and were confirmed by dye penetrant. The seventh indication correlated with a slag inclusion in a carbon steel pipe that was judged to be ASME code acceptable by radiographic testing.

The second series of welds consisted of 10 welds in carbon steel pipe similar to the Southwest series. These welds corresponded to about 340 feet of weld pass AE monitored. A total of four AE indications were detected. Three of these correlated with non-code rejectable slag inclusions that were radiographically detected while one was visually confirmed as a crater crack in a root weld which was repaired on the spot.

These tests further showed the practicality of in-process AE. All of the AE indications were correlated with either visual of NDE results.

The third piping production test was conducted at Gulf & Western's Energy Product Group, Plant # 1 Cicero, Illinois. The piping production monitor was utilized for these tests. A detailed description of this experiment and the results are presented in NUREG-0035-3. Tables I and II below summarize these test results.

Considering the problems inherent in correlating AE with production radiography without supportive metallographic sectioning the correlation

TABLE I

PIPE SHOP EVALUATION/GULF + WESTERN'S PLANT 1

- Total of 80 longitudinal pipe seams monitored and X-ray confirmed in carbon steel nuclear grade pipe to date.
- Wall thickness 3/8 inches to 2½ inches, diameter from 19 inches to 42 inches.
- 1482 feet of multipass weld monitored (total of approximately 5800 feet of weld).
- X-ray detected a total of 223 AE comparable indications.
- AE detected 137 of these indications (61%).
- AE found a total of 58 indications that did not correlate with X-ray. (3.9% over inspection - 58/1482).
- AE was correct in indicating a X-ray detectable flaw $\frac{137}{(137 + 58)}$ or 70% of the time.

TABLE II

FLAW-TYPE CORRELATION FROM PIPE SHOP EVALUATION

	AE	X-Ray	Correlation (AE with X-Ray)
Cracks	9	9	100%
Porosity	88	151	58%
Slag	40	63	63%

is surprisingly good for this large bank of data. The high "hit" rate for AE or cracks has prompted Gulf & Western personnel to consider using the AE monitor on the spot for detection and repair of end cracks in this type of welding.

APPENDIX

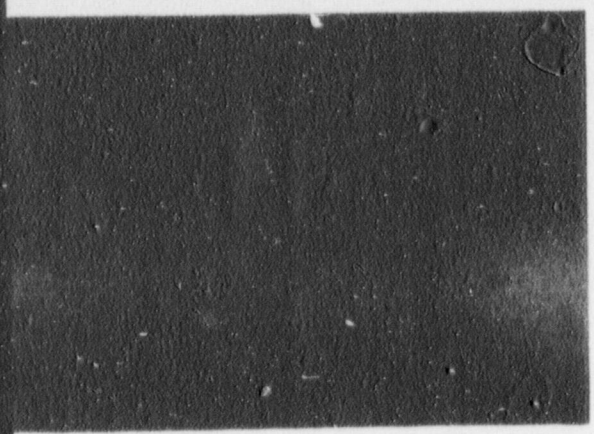

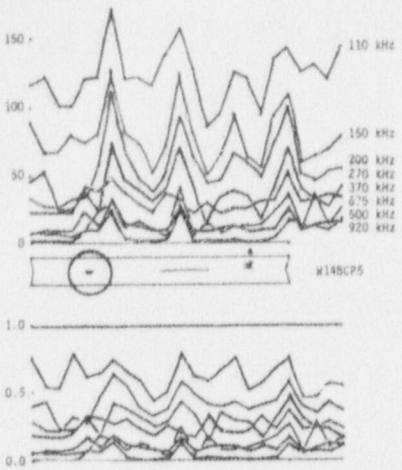

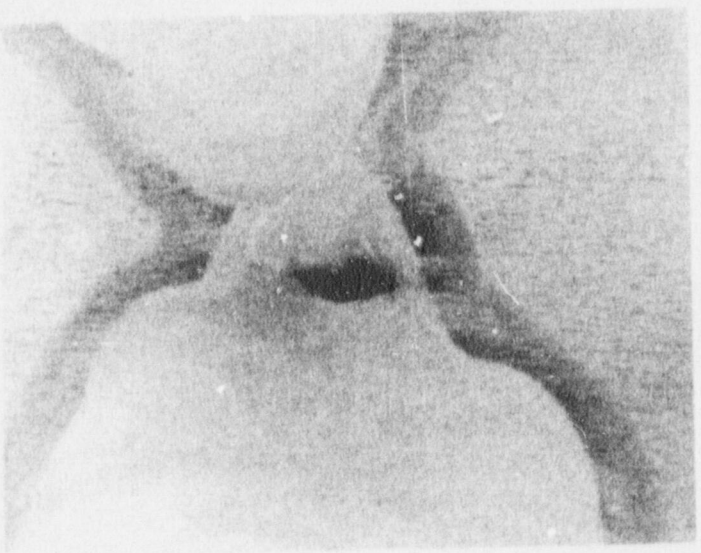

FIGURE A1. Unintended Slag Inclusion in Repair of Root Burn-Through 9 Inches from Start of Weld 14. Illustration Shows Closeup Radiograph of Flawed Area, Absolute Frequency Response, Tracing of Weld, Relative Frequency Response, Metallographic Section of Flawed Area

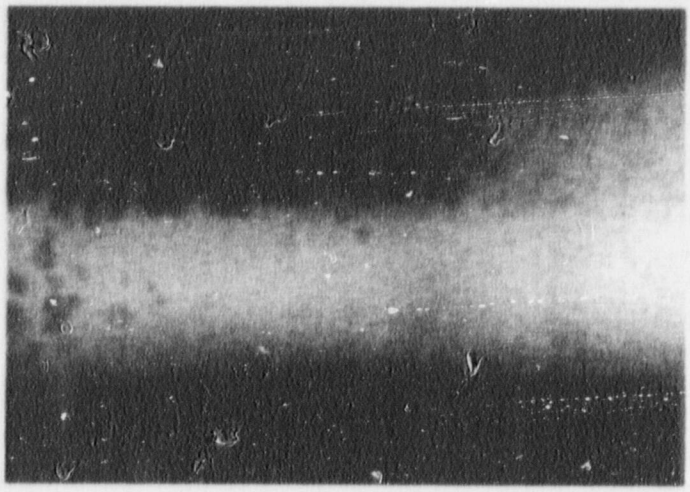

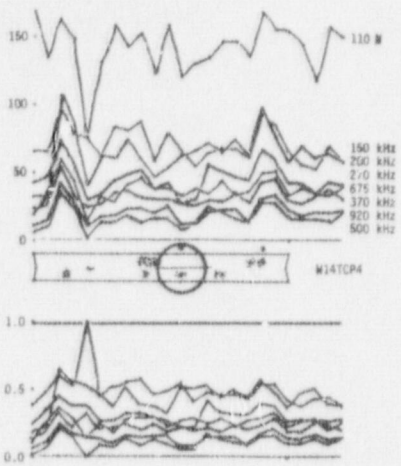

FIGURE A2. Pure Porosity Generated at 19 Inches in Top Cover Pass 4 of Weld 14. Illustration Shows Closeup Radiograph of Flawed Area, Absolute Frequency Response, Tracing of Weld, Relative Frequency Response, Metallographic Section of Flawed Area

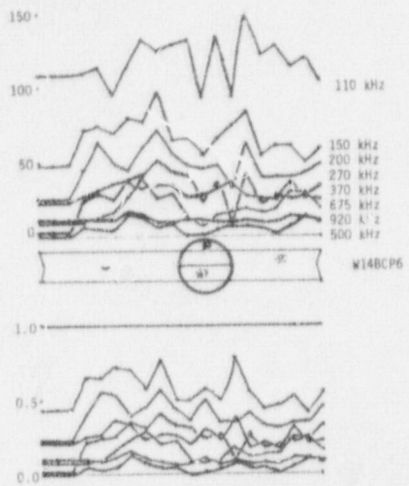

FIGURE A3. Porosity with Moderate Slag Entrapment at 21 Inches in Back Cover Pass 6 of Weld 14. Illustration Shows Closeup Radiograph of Flawed Area, Absolute Frequency Response, Tracing of Weld, Relative Frequency Response, Metallographic Section of Flawed Area

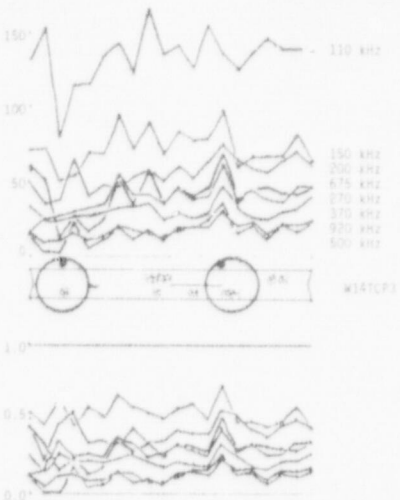

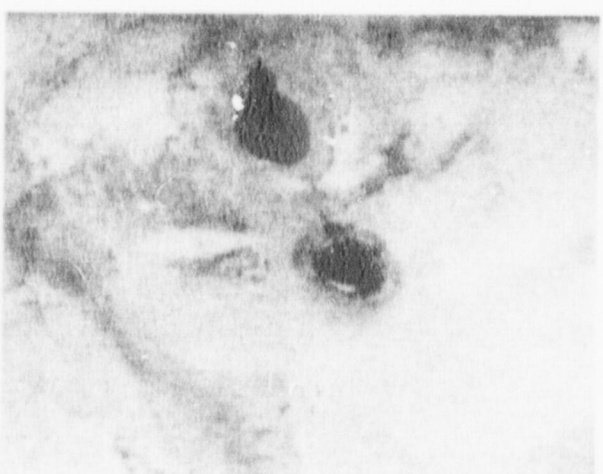

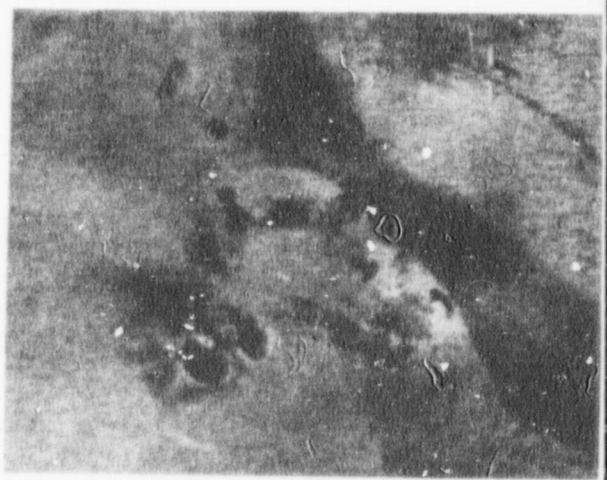

FIGURE A4. Porosity with Heavy Slag Entrapment at 6 Inches and at 24 Inches in Top Cover Pass 3 of Weld 14. Illustration Shows Closeup Radiograph of Flawed Area, Absolute Frequency Response, Tracing of Weld, Relative Frequency Response, Metallographic Section of Flawed Area

NRC FORM 335 (7-77)

U.S. NUCLEAR REGULATORY COMMISSION

BIBLIOGRAPHIC DATA SHEET

1. REPORT NUMBER (Assigned by DDC)
NUREG/CR-0461

4. TITLE AND SUBTITLE (Add Volume No., if appropriate)
Inspection of Nuclear Reactor Welding by Acoustic Emission

2. (Leave blank)

3. RECIPIENT'S ACCESSION NO.

7. AUTHOR(S)
D. Prine, T. A. Mathieson

5. DATE REPORT COMPLETED
MONTH: November YEAR: 1977

9. PERFORMING ORGANIZATION NAME AND MAILING ADDRESS (Include Zip Code)
GARD, Inc.
7449 Natchez Avenue
Niles, IL 60648

DATE REPORT ISSUED
MONTH: October YEAR: 1978

6. (Leave blank)

8. (Leave blank)

12. SPONSORING ORGANIZATION NAME AND MAILING ADDRESS (Include Zip Code)
Meatllurgy & Materials Research Branch
Division of Reactor Safety Research
U.S. Nuclear Regulatory Commission
Washington, DC 20555

10. PROJECT/TASK/WORK UNIT NO.

11. CONTRACT NO.
AT(49-24)-0187

13. TYPE OF REPORT
Final Report

PERIOD COVERED (Inclusive dates)
11/74 - 10/77

15. SUPPLEMENTARY NOTES

14. (Leave blank)

16. ABSTRACT (200 words or less)

This report presents results for the first three years of a program aimed at proving feasibility and applying the in-process acoustic emission (AE) monitoring of welds to the NDE of Nuclear power component welds. The method has been tested under both controlled laboratory conditions and in nuclear fabrication shops. Prototype single and two channel monitors have been built and production tested. Over 13,000 feet of weld passes have been monitored with excellent correlation of AE to conventional NDE and metallography. AE has been proven to be a reliable and practical NDE tool for detection and location of weld flaws. Current efforts are aimed at improving the method to provide flaw characterization as to type and size.

This report presents in detail the analysis of a large bank of laboratory controlled weld data. This work is providing flaw detection probabilities for various flaw types, AE flaw detection mechanisms, and candidate AE signals parameters for flaw size and type discrimination.

17. KEY WORDS AND DOCUMENT ANALYSIS

17a. DESCRIPTORS

17b. IDENTIFIERS/OPEN-ENDED TERMS

18. AVAILABILITY STATEMENT
Unlimited

19. SECURITY CLASS (This report)
Unclassified

21. NO. OF PAGES

20. SECURITY CLASS (This page)
Unclassified

22. PRICE
$

NRC FORM 335 (7-77)

UNITED STATES
NUCLEAR REGULATORY COMMISSION
WASHINGTON, D. C. 20555

OFFICIAL BUSINESS
PENALTY FOR PRIVATE USE, $300

POSTAGE AND FEES PAID
U.S. NUCLEAR REGULATORY
COMMISSION

U.S. MAIL

120555028651 1 RSAN
US NRC
ADM TIDC DSB
MIKE ATSALINOS
C16
WASHINGTON DC 20555